STUDY REPORT SYSTEMS TOXICOLOGICAL EVALUATION OF THS2.2 MENTHOL 90 DAY INHALATION STUDY OECD 413 – OECD PLUS PHASE

(STUDY NUMBER **176500**)

Table of Contents

Table of Contents 2

Table of Figures 6

Table of Tables 7

1 Approval 9

1.1 Study Director's Statement of Compliance 9

1.2 Quality Assurance Statement 10

2 General Information 10

2.1 Names and Addresses 10

2.2 Study Schedule 12

2.3 Test Guidelines 12

3 Study Plan Deviations/Amendments 13

4 Abstract/Executive Summary 15

4.1 Introduction 15

4.2 Study Objective 16

4.3 Experimental Design 17

4.4 Results and Main Conclusions 17

5 Introduction 21

6 Objectives – Plus part 24

7 Experimental Design 25

7.1 Test and Reference Items 25

7.2 Test System 25

7.3 Identification, Description, and Storage Conditions 25

7.4 Experimental Groups and Dosing 26

7.5 Sample Generation 26

7.6 Scope of Reporting 27

7.7 Lung Sample Cryoslicing 28
7.8 Lung Samples Processing (RNA and Protein Isolation) 28
7.9 Nasal Epithelium Processing (RNA and Protein Isolation) 28
7.10 Liver Processing (RNA and Protein Isolation) 29
7.11 Quantity Determination of Isolated RNA and Proteins 29
7.12 Quality Control of the Isolated RNA and Protein 30
7.12.1 Affymetrix Gene Chips Processing 30
7.12.2 Data Processing for Transcriptomics Analysis 30
7.12.3 Number of Replicates Per Group 31
7.13 iTRAQ LC-MS/MS Procedure 33
7.13.1 Sample Lysis and Labeling for Quantitative Proteomics 33
7.13.2 Definition of iTRAQ Analysis Sets 33
7.13.3 Mass-Spectrometry for Identification and Quantification 34
7.13.4 Number of Replicates Per Group and Protein Identification 34
7.14 Lipidomics 39
7.14.1 Samples and Platforms 39
7.14.2 Sample Preparation and Lipid Extraction 42
7.14.3 Mass Spectrometric Analyses 42
7.14.4 Acceptance Criteria for the Results 43
8 Statistical Methods and Computational Methods 44
8.1 Sample Randomization Protocol 44
8.2 Computational Methods 44
8.2.1 Gene/Protein-Set Analysis 44
8.2.2 Network Perturbation Amplitude 44
8.2.3 Biological Impact Factor 46
8.3 Statistical analysis of Lipidomics data 47

9 Results 49

9.1 Body Weight 49

9.2 Respiratory Nasal Epithelium Transcriptome after 90 Days of Exposure and after a 42-day Recovery Period in Male and Female Rats 49

9.2.1 Differentially Expressed Genes in Respiratory Nasal Epithelium after 90 Days of Exposure to Reference Cigarettes and THS2.2M, or after a 42-day Recovery Period 49

9.2.2 Biological Network Perturbation Amplitude Analysis in Nasal Epithelium Tissue after 90 Days of Exposure to Reference Cigarettes and THS2.2M, or after a 42-day Recovery Period 57

9.3 Lung Transcriptome after 90 Days of Exposure and after a 42-day Recovery Period in Male and Female rats 63

9.3.1 Differentially Expressed Genes in Lung Tissue after 90 Days of Exposure to 3R4F or THS2.2M, or after a 42-day Recovery Period 63

9.3.2 Biological Network Perturbation Amplitude Analysis in Lung Tissue after 90 Days of Exposure to Reference Cigarettes and THS2.2M, or after a 42-day Recovery Period 69

9.4 Liver Transcriptome after 90 Days of Exposure and after a 42-day Recovery Period in Male and Female rats 74

9.4.1 Differentially Expressed Genes in Liver Tissue after 90 Days of Exposure to 3R4F or THS2.2, or after a 42-day Recovery Period 74

9.4.2 Biological Network Perturbation Amplitude Analysis in Liver Tissue after 90 Days of Exposure to Reference Cigarettes and THS2.2M, or after a 42-day Recovery Period 82

9.5 Respiratory Nasal Epithelium Proteome after 90 Days of Exposure and after a 42-day Recovery Period in Male and Female Rats 82

9.5.1 Differentially Expressed Proteins in Respiratory Nasal Epithelium 82

9.5.2 Effects of Exposure Conditions on Functional Groups (Set Enrichment Analyses) 89

9.6 Lung Proteome after 90 Days Exposure and after a 42-day Recovery Period in Male and Female Rats 92

9.6.1 Differentially Expressed Proteins in Lung Tissue 92

9.6.2 Effects of Exposure Conditions on Functional Groups (Set Enrichment Analyses) 98

9.7 Liver Proteome after 90 Days Exposure and after a 42-day Recovery Period in Male and Female Rats 101

9.7.1 Differentially Expressed Proteins in Liver Tissue 101

9.7.2 Effects of Exposure Conditions on Functional Groups (Set Enrichment Analyses) 107

9.8 Lung Lipidome after 90 days of Exposure and after a 42-day Recovery Period in Male and Female Rats 111

9.9 Liver Lipidome after 90 days of Exposure and after a 42-day Recovery Period in Male and Female Rats 113

10 Discussion and Conclusion 115

11 Archiving 118

12 References 118

12.1 Literature 118

12.2 Philip Morris International's List of Standard Operating Procedures (SOP) and Work Instructions (WKI) 125

12.3 Philip Morris International's Internal Documents. 126

13 Abbreviations 127

14 Supplementary Tables and Figures 128

14.1 Tables 128

14.2 Figures 128

Table of Figures

Figure 1: Concept of the OECD study Plus design. 21

Figure 2: Principal component analysis. 35

Figure 3: Volcano plots representing the systems response profiles in respiratory nasal epithelium. 50

Figure 4: Number of significant differentially expressed genes in RNE tissue. 52

Figure 5: Heat map of gene expression in respiratory nasal epithelium. 54

Figure 6: Biological impact calculated from respiratory nasal epithelium tissue. 58

Figure 7: Heat map of network perturbation in nasal respiratory epithelium. 61

Figure 8: Volcano plots representing the systems response profiles in lung tissue. 64

Figure 9: Number of significant differentially expressed genes in lung tissue. 65

Figure 10: Heat map of gene expression in lung tissue. 67

Figure 11: Biological impact calculated from lung tissue. 70

Figure 12: Heat map of network perturbation in lung tissue. 73

Figure 13: Volcano plots representing the systems response profiles in liver tissue 75

Figure 14: Number of significant differentially expressed genes in liver tissue. 77

Figure 15: Heat map of gene expression in liver tissue. 79

Figure 16: Volcano plots representing the proteome response profiles in RNE (comparisons for 90 days, Set 1). 83

Figure 17: Volcano plots representing the proteome response profiles in RNE (comparison between 90 days and 90+42 days, Set 2). 84

Figure 18: Numbers of differentially expressed proteins in RNE. 85

Figure 19: Fold change and significance in protein profiles across the exposure conditions. 86

Figure 20: Set enrichment results for KEGG pathway collection. 92

Figure 21: Volcano plots representing the proteome response profiles in lung (comparisons for 90 days, Set 1). A) Male, B) female. 93

Figure 22: Volcano plots representing the proteome response profiles in lung (comparison between 90 days and 90+42 days, Set 2). 94

Figure 23: Numbers of differentially expressed proteins in lung. 95

Figure 24: Fold change and significance in protein profiles across the exposure conditions. 97

Figure 25: Set enrichment results for 90 days of exposure (Set 1). 99

Figure 26: Set enrichment results for 90 days and 90+42-days of exposure (Set 2). 100

Figure 27: Volcano plots representing the proteome response profiles in liver (comparisons for 90 days, Set 1). A) Male, B) female. 102

Figure 28: Volcano plots representing the proteome response profiles in liver (comparison between 90 days and 90+42 days, Set 2). 103

Figure 29: Numbers of differentially expressed proteins in liver. 104

Figure 30: Fold change and significance in protein profiles across the exposure conditions in liver. 105

Figure 31: Set enrichment results for 90 days of exposure in liver (Set 1). 108

Figure 32: Set enrichment results for 90 days and 90+42-days of exposure in liver (Set 2). 109

Figure 33: Effects on the lung lipidome. 112

Figure 34: Effects on the liver lipidome. 114

Table of Tables

Table 1: Study Plan Deviations. 13

Table 2: Exposure groups designated for exploratory ‘Plus’ groups. 26

Table 3: Collected tissues or fluids and intended use. 27

Table 4: Sample size per group used for data transcriptomics data evaluation. 31

Table 5: Number of valid replicates for proteomics analysis. 36

Table 6: Number of proteins for differential expression analysis. 38

Table 7: Number of samples processed by Zora. 40

Table 8: Lipidomics platforms and lipid classes measured in the lung and liver. 41

Table 9: Unique genes that were differentially expressed only in RNE of female rats after THS2.2M exposure. 56

Table 10: Unique expressed genes after THS2.2M treatment found in the lung tissue.....68

Table 11: Unique expressed genes found in the liver tissue after THS2.2M treatment. ...80

Table 12: Unique MRTP proteins. 88

Table 13: Unique differentially expressed proteins after THS2.2M treatment. 98

Table 14: Unique differentially expressed proteins after THS2.2M treatment. 106

Table 15: Overarching summary of results.....117

1 Approval

1.1 Study Director's Statement of Compliance

The accountability of this study lies with the study director.

The study director takes accountability for the study having been executed as defined in the study plan. The laboratory heads take responsibility for the data generated in their labs.

Name	Justification	Date / Signature
Julia Hoeng	Approved by Program Leader, Systems Toxicology	19th April 2016 Julia Hoeng
Nikolai Ivanov	Approved by Manager, Research Technology / Approved as Business Owner / Test Facility Manager	19 April 2016
Keyur Trivedi	Approved by Supervisor, Tissue Research Laboratories	19th APRIL 2016
Emmanuel Guedj	Approved by Supervisor, Gene Expression	19 APR 2016
Ashraf Elamin	Approved by Supervisor, MS-based Proteomics	19 Apr 2016
Ulrike Kogel	Approved by Work Package Leader, OECDplus Part / Study Director	13. April 2016 U. Kogel

1.2 Quality Assurance Statement

Not Applicable

2 General Information

2.1 Names and Addresses

Sponsor	Manuel Peitsch Philip Morris Products S.A. Quai Jeanrenaud 5 2000 Neuchâtel Switzerland
Program Leader	Julia Hoeng Quai Jeanrenaud 5 2000 Neuchâtel Switzerland
Test Facility	Philip Morris Products S.A. Research & Development PMI Product Testing Quai Jeanrenaud 5 2000 Neuchâtel Switzerland

Test Facility Management	Nikolai Ivanov Genomics Research and Technology Laboratories Philip Morris Products S.A. Research & Development Quai Jeanrenaud 5 2000 Neuchâtel Switzerland
Test Site for Lipidomics analysis	Zora Biosciences Oy Biologinkuja 1 02150 Espoo Finland
Principal Investigator for Lipidomics	Mika Hilvo, PhD Senior Scientist Zora Biosciences Oy Biologinkuja 1 02150 Espoo Finland

2.2 Study Schedule

Experiment start date:	2 November 2014
Experiment completion date:	8 July 2015

2.3 Test Guidelines

Not Applicable

3 Study Plan Deviations/Amendments

During the execution of study 176500, deviations from the study plan occurred. These deviations are summarized below:

Table 1: Study Plan Deviations.

Number	Description	Impact on study data and integrity
1	Because of tissue size, the transcriptomics lab had to change the elution volume in the RNA generation step: Lungs: elution from 20 µL to 50 µL Liver: elution from 170 µL to 570 µL	No impact on study data.
2	The slicing of the left lung was done to the end of the tissue sample and not to the main bronchus (see 15025 THS SP chapter 5.4.4).	This change may have an impact on the composition of the lung tissue used for analysis.
3	In the study plan in 5.4.12 the sentence: "The concentration needs to amount to at least 50 ng/µl"was stated. The correct amount is 33.3 ng/µL.	No impact on study data.
4	PMI_RD_WKI_000813 (Affymetrix-IVT2-Express BioMek) was replaced by PMI_RD_WKI_001109 Affymetrix IVT PLUS Protocol.	No impact on study data
5	We added the liver for proteomics analysis. For proteomics**,** no liver samples had been planned. However, a large liver piece, "liver B" (see 15025 THS SP part 10.2.7), was frozen for later use, such as Oil Red O staining.	This deviation had an increased value for the study data. We collected proteomic data from the liver for the first time.

(Table continues)

Number	Description	Impact on study data and integrity
	A piece of B was used for proteomics analysis. Piece B was cut in half; half was used for the LC-MS/MS analysis, and the other half was stored in the freezer. The liver slice was homogenized and processed for protein extraction, followed by acetone precipitation according to the WKI: PMI_RD_WKI_001211.	
6	In the study plan the scientific question was stated: "Can we detect a gender effect in the different exposure groups after 90 days of exposure?" In the report we did not tackle that question, specifically. We have analyzed the two genders separately and the data can be compared for differences. However, to address the question in full detail, we will use e.g. an "interaction model" for calculating the differences.	To not address all questions which are stated in the study plan do not impact the quality of the results stated in the report.
7	In the study plan the scientific question was stated: "Can we detect a difference on the biological impact between 3R4F and 3R4F-like menthol smoke?" We have not concretely analysed the difference between 3R4F and DDA3s for the reporting. This also may require to use an interaction model.	To not address all questions which are stated in the study plan do not impact the quality of the results stated in the report.
8	In the study plan we mentioned a verification experiment for proteomics (see 15025 THS SP" part 5.5.18); this experiment was not performed.	To not perform that experiment do not impact the quality of the results stated in the report.
9	The Study Plan (15025_176500 THS SP) contains the wrong number in the header. It should be 176500.	No impact on data

These deviations are integrated into the description of the methods (Section 7).

4 Abstract/Executive Summary

4.1 Introduction

Patskan and Reininghaus hypothesized that the chemical composition of the aerosol generated by burning or heating tobacco, along with its toxicological effects, largely depend on temperature (Patskan 2003). The current version of the product (THS2.2), which is operated at a temperature below 350°C, generates largely reduced amounts of harmful and potentially harmful constituents (HPHCs) relative to the Kentucky Reference cigarette 3R4F, under smoking machine conditions.

Here, the mentholated version of this product (THS2.2M) was assessed. To characterize toxicity and assess the hazard of the THS2.2M product, we conducted a battery of chemical and toxicological assays. Among the studies performed, we included the 90-day inhalation study, as described in the Organisation for Economic Co-operation and Development (OECD) guideline 413 (OECD 2009), aimed to characterize the adverse effects caused by repeated daily inhalation exposure to THS2.2M for 90 days.

Ninety day inhalation studies have been widely used to assess the impact of cigarette modifications (Gaworski 2011a, Gaworski 2009, Gaworski 2011b, Renne 2006, Stavanja 2008, Theophilus 2007, Vanscheeuwijck 2002) or new cigarette designs, including designs in which tobacco is heated rather than burned (Moennikes 2008, Terpstra 2003, Werley 2008).

The standard study design has proven to be suitable for providing information on the hazard likely to arise from repeated exposure by the inhalation route, and has shown to be capable of distinguishing between categories of products for systemic toxicological parameters and detecting histopathological changes in the respiratory tract (e.g., Werley 2008).

However, to obtain additional insights into the molecular mechanisms underlying the toxicity, we have added an additional study arm to generate omics data as transcriptomics, proteomics, and lipidomics data. Experience demonstrated that toxicological markers are only detectable after substantial damage has already occurred, and therefore are considered to lack sensitivity (Ellinger-Ziegelbauer 2011). The combined approach of omics and conventional toxicology has been shown to be a useful tool for mechanistic investigation and for the identification of putative biomarkers (Cutler 1999, Ellinger-Ziegelbauer 2011).

4.2 Study Objective

A pre-clinical assessment program was performed on the second generation of tobacco heating systems, THS2.2M, flavored with menthol, to determine whether adult smokers participating in clinical studies are exposed to increased or new hazards compared with those presented by continued smoking of combustible cigarettes. The rationale for the pre-clinical program was based on the United States Food and Drug Administration (FDA)'s Center for Tobacco Products draft guidance (Food and Drug Administration 2012). It includes evaluation of the toxicological properties of the materials used to make the product, evaluation of the aerosol through non-targeted chemical screening, measurement of droplet size to characterize the aerosol to which smokers are exposed, measurement of the yield of HPHCs, assessment of the genotoxicity and cytotoxicity of the aerosol compared with 3R4F, and a 90-day inhalation study on rats according to the Organization for Economic Co-operation and Development (OECD) test guideline (TG) 413 (OECD 2009).

Here we report on the 90-day inhalation study arm, which aimed to complement basic OECD requirements with additional molecular biological endpoints to investigate the biological impact of the THS2.2M product in comparison with 3R4F and 3R4F-like menthol cigarettes, and to assess potential molecular differences in the biological effects evolving in a rat model.

In relation to chemical hazard/risk assessment, omics technology provides tools for improving our understanding of mechanisms of toxicity.

4.3 Experimental Design

Male and female Sprague–Dawley rats were exposed to three concentrations of aerosol from THS2.2M and mainstream smoke from 3R4F, along with DDA3 1x Menthol in Smoke (MIS) and DDA3 2xMIS generated under the Health Canada Intense (HCI) smoke protocol (Health Canada 1999); DDAs were designed as additional reference cigarettes which also contain menthol. A full assessment of the parameters listed in the OECD test guideline 413 was carried out (please refer to 15025 THS SR Part1).

To obtain an understanding of the toxicity pathways involved in the response to the exposure regimen, additional rats were exposed in parallel to the same conditions ("OECDplus" arm), and harvested for the analysis of systems toxicology endpoints. Groups of rats were necropsied either at the end of the 90-day inhalation period or after a 42-day post-inhalation period to assess the reversibility or delayed occurrence of findings. The overall health and well-being of the rats, together with smoke uptake and response, were tracked throughout the study. Here, we present the molecular endpoints that were investigated through transcriptomics and proteomics analysis of lung tissue, nasal epithelium and liver after 90 days, or after the 42-day recovery period. The lung and liver tissues were also investigated using a lipidomic approach.

4.4 Results and Main Conclusions

The aerosol was reproducibly generated and delivered to the animals. Exposure was confirmed by test atmosphere-concentration dependent amounts of nicotine metabolites recovered in the urine of the rats. The inhalation toxicity observed in animals exposed to THS2.2M was much lower than in the rats exposed to 3R4F or DDA3 1xMIS or DDA3 2xMIS (please refer to "15025 THS SR Part 1" for details).

The biological effects caused by the test item were limited mainly to hematological changes, blood chemistries, and changes in liver weights. Lung inflammation and changes in the histopathology of respiratory tract organs in THS2.2M-exposed rats were lower than those in reference cigarette-exposed rats (please refer to "15025 THS SR Part 1" for details).

In the respiratory nasal epithelium (RNE) of 3R4F-, DDA3 1xMIS-, DDA3 2xMIS- (all 23 µg/L nicotine) exposed male and female rats after 90 days of exposure, about and more than 7,000 genes were differentially expressed. After exposure to the double nicotine concentration of THS2.2M (high; 50 µg/L nicotine) for 90 days, only nine genes were

differentially expressed in the RNE of male rats. After exposure of female rats to the high dose of THS2.2M (50 µg/L nicotine) for 90 days, more than 2,100 genes were differentially expressed in the RNE. After 42 days of recovery from THS2.2M exposure, most genes resumed their regular expression rates, and only 120 genes were detected as differentially expressed in the RNE of female rats. In general, the fold change of the differentially expressed genes was much lower after THS2.2M exposure at all tested concentrations than the fold change found after 3R4F or DDA3 1x or 2x MIS exposure.

Biological network analysis found processes describing mechanisms for cell fate, tissue repair and angiogenesis, inflammatory processes, cell stress, and cellular proliferation impacted in the RNE of both male and female rats, which had been exposed to cigarette smoke from the three reference cigarettes (3R4F or DDA1xMIS or DDA2xMIS). In contrast, only RNE of female rats exposed to the highest THS2.2M concentration (50 µg/L) showed a well-detectable network perturbation – with a highly similar pattern as upon reference CS exposure, but with much lower perturbation amplitudes.

In the lung tissue of female rats after exposure to reference smoke, about 2,700 genes were differentially regulated and about 1,700 genes were differentially regulated in the lung tissue of male rats. In contrast, after THS2.2M exposure at the highest concentration (50 µg/L nicotine), only 45 genes were differentially expressed in the lung tissue of female rats, and only one gene was found in the corresponding male group. Of note, the overall reduced effect in the lung compared with the nose could be explained by the fact that rats are obligate nasal breathers.

The analysis of the lung transcriptomics data showed that cell fate, tissue repair and angiogenesis, inflammatory processes, cell stress, and cellular proliferation were impacted by the exposure to the three reference cigarettes. In male rats, a perturbation of cell stress and inflammatory processes was found after exposure to THS2.2M after 90 days with the highest dose (50 µg/L nicotine). In female rats, all five tested biological processes were impacted after THS2.2M exposure at the high dose. However, the amplitude of perturbation by THS2.2M aerosol exposure was much lower than found after exposure to smoke from the reference cigarettes in both male and female rats. The biology of those processes, separated into different contributing signaling pathways, showed that in the lung tissue of male rats after exposure to the highest THS2.2M concentration, the number of impacted signaling pathways was only half of what was found in the lungs of rats after exposure to the reference cigarette smoke. In the lung tissue of female rats, the majority of impacted signaling pathways were the same in THS2.2M and reference groups, but the quantitative impact of THS2.2M was lower. An exception was the signaling pathway representing the

biology of nuclear receptor signaling that was a subnetwork from the cell proliferation network; this signaling pathway was not found to be significantly activated by exposure to reference cigarettes.

Although with a lower impact compared to respiratory tissues, liver gene expression was also affected by reference smoke and THS2.2M aerosol inhalation. Similarly to the respiratory tissues, the analysis of differentially expressed genes showed lower effects of exposure to THS2.2M than to reference cigarettes.

In male rats, the differential expression of 156, 227, and 68 genes was observed upon exposure to 3R4F, DDA1X MIS, and DDA2X MIS respectively. THS2.2M exposure at matching nicotine concentration (23 µg/L) resulted in differential expression of only 1 gene. THS2.2M at double nicotine concentration (50 µg/L) increased the number of differentially expressed genes up to 57 and thus still remained well below to the minimum differentially expressed gene number for the reference cigarettes.

In female liver tissue, the overall number of differentially expressed genes was higher compared to the males. However, the reduced effects for THS2.2M vs. reference cigarette exposure was also found for females. Of note, only exposure to THS2.2M at 50 µg/L nicotine concentration resulted in an effect on the liver transcriptome that was comparable to the effect observed for reference cigarette exposure.

The quantitative proteomics results confirmed these overall trends. Consistently, the THS2.2M exposed groups showed a strong reduction in the number of differentially expressed proteins in RNE, lung tissue and liver, compared with the DDA3 1xMIS, DDA3 2xMIS, and 3R4F exposure groups. A clear effect of the highest dose of THS2.2M could be detected in the nasal epithelium but not in the lung tissue. Analysis of the KEGG compendium of biological pathways suggested a reduced biological activity of the differentially expressed proteins in the nose and lung tissue of rats exposed to THS2.2M.

In female rat liver tissues, the number of differentially expressed proteins was overall higher compared with male liver tissue. However, the differences between reference cigarettes and THS2.2M were kept, with the THS2.2M-induced differentially expressed protein number lower than for the reference cigarette exposures.

In general, the THS2.2M groups (23 and 50 µg/L nicotine) showed less pronounced lipid changes in lung than the reference groups when compared with the sham group. The difference was especially notable for ceramide lipid classes (ceramides, globotriaosylceramides, and glucosyl/galactosylceramides), showing an increase in the reference groups, but much more limited alterations in the THS2.2M groups. Only the

livers of male rats, but not from female rats, showed a few lipid species that were significantly affected by THS2.2M exposure, however, generally the same trends were also observed for the reference cigarettes.

In summary, we found through omics analyses that THS2.2M, even applied at a higher nicotine concentration (50 µg/L vs. 23 µg/L), caused a weaker effect, measured as differential fold changes for transcriptomics, proteomics, and lipidomics, and showed a reduced quantitative impact on pathways for transcriptomics and proteomics compared to the reference cigarette exposures (23 µg nicotine/L).

Therefore, and in combination with the OECD 90-day study data and in vitro toxicology data collected, human adults using THS2.2M will likely not be exposed to additional hazards beyond those presented by smoking conventional cigarettes.

5 Introduction

The OECD promotes the regulatory use of alternative test methods. To use alternative methods for complex endpoints, mechanisms and modes of toxicity need to be understood.

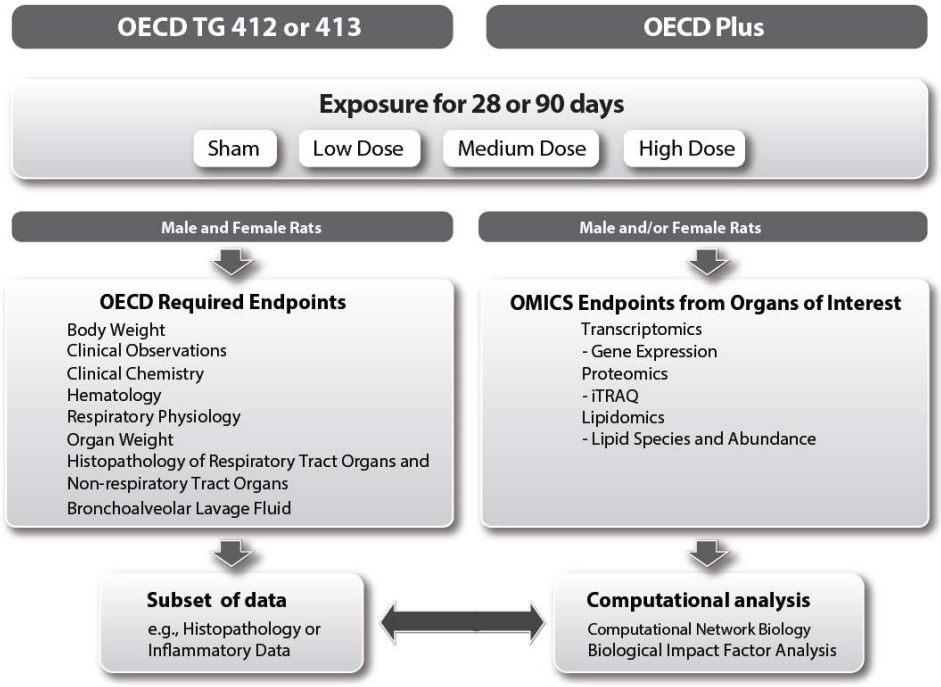


Figure 1: Concept of the OECD study Plus design.
Comparison of the endpoints in the classical and OECD Plus concept.

Figure 1 presents a concept of combining the conventional toxicological assessment approach with additional molecular biological endpoints. In brief, toxicity studies employ additional animals for the purpose of obtaining "omics" data. These animals undergo the same exposure conditions at the same time. Organs (e.g., lung,) of interest are collected from the exposed animals. Omics data are generated, computationally analyzed and subsequently correlated with the classical endpoints described in the OECD guidelines.

The objective of the present study was to characterize the toxicity of mainstream aerosol from THS2.2 menthol (THS2.2M) in a 90-day inhalation study of Sprague–Dawley rats by

analyzing molecular data from the OECDplus arm. In line with OECD test guideline 413, the mainstream aerosol from THS2.2M was generated and diluted to three target concentrations of 15, 23, and 50 µg/L nicotine. The observed effects following repeated daily inhalation exposure to THS2.2M mainstream aerosol were compared with those of 3R4F reference cigarettes and DDA3 1xMIS and DDA3 2xMIS mentholated combustible cigarettes that were included in the study to enable equal comparisons based on menthol content. DDA3 1xMIS and DDA3 2xMIS were designed to produce approximately 1.2 mg and 2.4 mg menthol in smoke (MIS), respectively, when smoked according to ISO standard 3308 (International Organization for Standardization 2000). The 3R4F, DDA3 1xMIS and DDA3 2xMIS cigarettes were used at a single target nicotine concentration of 23 µg/L.

Rats were nose-only exposed to mainstream aerosol/smoke or filtered and conditioned air (sham exposure group) for 6 h/day, 5 days/week for 13 weeks, followed by a 42-day post-inhalation (recovery) period. An exposure time adaptation phase was included during the first 7 days of exposure to acclimatize the rats to the target aerosol concentration (1.5-h exposure on days 1 and 2, 3-h exposure on days 3 and 4, and 4.5-h exposure on days 5–7). The 3R4F cigarettes, DDA3 1xMIS, DDA3 2xMIS, and THS2.2M sticks were smoked in conformity with Health Canada standards, with slight changes on 30-port smoking machines. The test aerosol was diluted to the target nicotine concentrations with filtered and conditioned air. The nicotine concentrations for 3R4F cigarettes were selected according to previous results from PMRL BVBA, Leuven (Belgium) (PMI Internal Report *12694* Part1, 2010), and results from PMI-RL Singapore (15006 THS SR Part 1), which demonstrated that a 23 µg/L nicotine concentration is suitable for detecting possible differences in effects throughout the respiratory tract. For THS2.2M, a 50 µg/L nicotine concentration was selected as the high dose, based on the results of the previous 15006 study (15006 THS SR Part 1). However, because high levels of added menthol are used in the test and reference item, a dose range-finding study was conducted before this study, that aimed to determine the maximal tolerable concentration (MTC) of mainstream aerosol generated from THS2.2M, and the MTC of mainstream smoke generated from DDA3 2xMIS (PMI Internal Report *15024*, 2014). The results of that study suggested using 50 µg/L nicotine as the maximal dose.

The inhalation study was conducted in compliance with the OECD Principles of Good Laboratory Practice (as revised in 1997). The study was run in an Agri-Food & Veterinary Authority of Singapore–licensed facility, where care and use of the rats was in accordance with the National Advisory Committee for Laboratory Animal Research (NACLAR) guidelines (2004).

General health conditions and aerosol uptake/exposure were monitored. The endpoints for analysis were analyzed as outlined in OECD TG 413 for subchronic inhalation studies. These include in-life observations during and following exposure, determination of the health status including ophthalmoscopy, body weight, and food consumption, pathology (post-mortem gross necropsy and histopathological assessment of both respiratory and non-respiratory organs and tissues), blood analysis (clinical chemistry, complete blood counts), and bronchoalveolar lavage fluid (BALF) analysis. To monitor aerosol exposure and carbon monoxide levels, four daily samples from the breathing zone of the exposure chambers were prepared for analysis and determination of nicotine concentration and total particulate matter (TPM). The aerosol intake was quantified through blood carboxyhemoglobin measurement and through the quantification of nicotine metabolites in urine and blood samples. Menthol levels were also quantified in blood samples. Rat breathing patterns during exposure were monitored using head-out plethysmography.

This report describes the work and analysis done post-dissection of the additional rats employed for performing the OECD Plus part, comprising additional molecular endpoints to complement the classical OECD approach with a systems toxicology approach.

The experimental part prior to dissection is described in the overall inhalation study plan under GLP "15025 THS SP" and reported in part 9 of the GLP report "15025 THS SR Part 9". For the report on the main study please refer to the GLP report "15025 THS SR Part 1".

6 Objectives – Plus part

The objective was to generate omics data and conduct a systems toxicology analysis from the tissues that were collected after the inhalation phases of the OECD study (please refer to GLP study plan "15025 THS SP").

The objectives were to compare as priority:

a) The effect of THS2.2 M vs. references

b) The effect of a recovery period

c) The dose effect of THS2.2 M concentrations

7 Experimental Design

7.1 Test and Reference Items

Test items and storage conditions were described in detail in the main study plan in section 4.1. See "15025 THS SP".

- Reference item 1: 3R4F.
- Reference item 2: DDA3 1xMIS and DDA3 2xMIS are combustible cigarettes designed to meet the tar, nicotine, carbon monoxide, and cigarette diameter specifications of the 3R4F conventional cigarette from the University of Kentucky (for specifications, analysis report A-0011876 and A-0011877), with added menthol (approximately 1.2 mg and 2.4 mg MIS respectively, when smoked according to the ISO 3308 standard).
- Test item: THS2.2M (for specifications, batch release B-11130).

7.2 Test System

Experiments were conducted on male and female Sprague–Dawley rats bred under specific pathogen-free conditions, and acquired from Charles River (USA) at 6–7 weeks of age. For more details, see the main study plan, section 4.2: "15025 THS SP".

7.3 Identification, Description, and Storage Conditions

The test item, THS2.2M, consists of a tobacco stick, a holder containing a battery, electronics, and a calibrated heating element designed to generate a temperature profile of 320–350°C to ensure constant delivery of nicotine. THS2.2M is produced by Philip Morris International, Neuchâtel, Switzerland. The reference cigarette, 3R4F, was obtained from the University of Kentucky and used as comparator in the present study.

THS2.2M and the references were conditioned according to ISO 3308 (International Organization for Standardization 2000) prior to use.

7.4 Experimental Groups and Dosing

All experimental groups included in the main study are described in the main study plan, section 4.5: "15025 THS SP"

Table 2 summarizes the animal number per group for the OECD plus omics study.

Table 2: Exposure groups designated for exploratory 'Plus' groups.

			90d	90+42d
Group Code	**Long Name**	**Target nicotine (µg/L)**	**M/F**	**M/F**
012	Sham PLUS	0	6/6	0/6
013	3R4F PLUS	23	6/5	0/6
014	DDA3 1xMIS PLUS	23	6/6	0/0
015	DDA3 2xMIS PLUS	23	6/6	0/6
016	THS2.2M Low PLUS	15	6/6	0/0
017	THS2.2M Medium PLUS	23	6/6	0/0
018	THS2.2M High PLUS	50	6/6	0/6
	Total		42/41	0/24

In total, the study included 108 animals, divided into 7 groups, 2 sexes, 2 time points for female rats, and 6 biological replicates. One female rat of the 3R4F group died during the blood collection process within the 90 days of exposure (Total animals = 107). F = female, M = male.

7.5 Sample Generation

The animal dissection and sample collection were described in detail in the study plan:

"15025 THS SP".

Table 3 summarizes the tissues that were collected for this study for the indicated purposes. Only the tissues in bold were further processed and are reported herein.

Table 3: **Collected tissues or fluids and intended use.**

Blood/ tissues	**Planned Endpoint**
Whole blood	Transcriptomics
White blood cells	Transcriptomics
Serum	Proteomics/lipidomics
Left lung	**Transcriptomics/proteomics**
Right lung	**Lipidomics**
Liver	**Transcriptomics/lipidomics/proteomics**
Kidneys	Transcriptomics
Left RNE	**Transcriptomics**
Right RNE	**Proteomics**
Trachea	Transcriptomics

Tissues and endpoints in bold letters are the scope of this report. The other tissues were collected but will not be reported here due to their exploratory nature.

7.6 Scope of Reporting

This report contains an evaluation of the transcriptomics and proteomics data gained from lung, respiratory nasal epithelia (RNE) tissue, and liver.
The lipidomics data generated from lung tissue and liver are also within the scope of this report.

The isolation of RNA from the trachea was an exploratory approach. The obtained number of replicates was not sufficient in all groups. We generated 38 CEL files from selected male samples. The data have not been processed yet, and will be reported separately because of their exploratory nature.

Whole blood was collected for transcriptomics analysis, as was serum for proteomics analysis; both are still stored frozen for future translational confirmation experiments.

RNA was isolated from the white blood cells, but could not be amplified, resulting in no generation of data (CEL files).

The kidneys were not analyzed in this study, and were kept frozen.

7.7 Lung Sample Cryoslicing

The Tissue Research Laboratory cryosectioned the left lung lobe into 40-µm slices. Serial sections were collected for transcriptomics, proteomics (iTRAQ analysis), and genomics analysis (stored frozen for a separate study plan).

7.8 Lung Samples Processing (RNA and Protein Isolation)

For **transcriptomics**, the cell lysate was further processed with the miRNeasy extraction kit (Qiagen, Valencia, CA, USA) according to the PMI_RD_WKI_001115 document. Purified RNA was eluted in 20-50 µL of RNase-free water.

For **proteomics**, the lung slices were homogenized in lysis buffer (BioRad, Hercules, CA, USA) with a bead-assisted procedure in Tissue Lyser II (Qiagen, Valencia, CA, USA) and split into two aliquots (one for iTRAQ LC-MS/MS and one for freezer storage). The iTRAQ aliquot was subjected to acetone precipitation by adding 4 × volume of pre-chilled acetone for 2 h at −20°C, followed by centrifugation at 16,000 × g at 4°C. The precipitates were resuspended in 200 µL of 0.5 M triethylammonium bicarbonate (TEAB) buffer (Sigma–Aldrich, St. Louis, MO, USA) containing 1 M urea and 0.1% SDS. The procedure is described in the WKI: PMI_RD_WKI_001043.

7.9 Nasal Epithelium Processing (RNA and Protein Isolation)

For **transcriptomics**, left RNE samples had been collected in 2-mL MagNA Lyser tubes and frozen at −80°C. Samples were thawed by adding 700 µL QIAzol buffer. The samples were vortexed for 30 s. Further RNA isolation was done with the miRNeasy extraction kit (Qiagen) according to the PMI_RD_WKI_001117 document. Purified RNA was eluted in 30 µL of RNase-free water.

For **proteomics**, the homogenized mixture was thawed and sonicated, then split into two aliquots (one for iTRAQ LC-MS/MS and one for freezer storage). The iTRAQ aliquot was subjected to acetone precipitation by adding 4 × volume of pre-chilled acetone for 2 h at −20°C, followed by centrifugation at 16,000 × g at 4°C. The precipitates were resuspended in 200 µL of 0.5 M TEAB buffer containing 1 M urea and 0.1% SDS. The procedure is described in the WKI: PMI_RD_WKI_001297.

7.10 Liver Processing (RNA and Protein Isolation)

For **transcriptomics**, liver piece A1 was thawed (tissue segment indicated with "A" was cut into two pieces for lipidomics and RNA isolation) (see: "15025 THS SP", part 10.2.7). Liver samples were ground in 700 µL of Qiazol buffer in 2.0-mL MagNa Lyser tubes. Further processing followed the miRNeasy extraction kit (Qiagen) handbook (miRNeasy Mini Handbook) following the PMI_RD_WKI_001117 document. Purified RNA was eluted in 170 to 570 µL of RNAse-free water, depending on the size of the tissue.

For **proteomics,** rat liver samples (part B) were cut into two parts using a scalpel. The first half was frozen at −80°C. The dedicated proteomics samples were homogenized with a bead-assisted procedure in Tissue Lyser II (Qiagen) in tissue lysis buffer (BioRad, Hercules, CA, USA). In random order, proteins were then precipitated with acetone. For all tissues, the precipitates were resuspended in 0.5 M TEAB, 1 M urea, and 0.1% SDS. The procedure is described in the WKI: PMI_RD_WKI_001211.

7.11 Quantity Determination of Isolated RNA and Proteins

The quantity of the isolated **RNA** was determined with the NanoDrop 1000 or 8000 spectrophotometer (Thermo Fisher Scientific, Waltham, MA, USA) or Spectramax Plus 384 (Molecular Devices, Sunnyvale, CA, USA). The subsequent RNA amplification protocol using the HT 3′ IVT kit requires 100 ng of RNA. The threshold concentration is 33 ng/µL. If the concentration was too low, the sample was further concentrated using vacuum centrifugation (Eppendorf, Hamburg, Germany). The RNA was dissolved in RNase-free water in an appropriate volume.

Protein concentrations of the samples were determined using the Bradford assay according to supplier's instructions. Procedure is described in the WKI: PMI_RD_WKI_001103.

7.12 Quality Control of the Isolated RNA and Protein

RNA quality was measured using an Agilent 2100 Bioanalyzer (Agilent Technologies, Santa Clara, CA). An RNA integrity number (RIN) score greater than 6.0 serves to qualify minimal acceptance criteria for the RNA samples, which were analyzed for gene expression.

The quality control procedure to check the sample **proteins**' stability before performing the experimental analyses consisted of two steps: (1) Determination of protein concentrations, and (2) determination of sample integrity using LabChip (PerkinElmer, Waltham, MA, USA) according to WKI: PMI_RD_WKI_001131.

7.12.1 Affymetrix Gene Chips Processing

For lung and nose, amplification and labeling of RNA was done with the High Throughput 3' In Vitro Transcription Plus (HT 3' IVTPLUS) kit (Affymetrix, Santa Clara, CA, USA). The procedure was carried out as described in the GeneChip® HT 3' IVT PLUS Kit User Manual.

See PMI_RD_WKI_001118, PMI_RD_FOR_000763, PMI_RD_WKI_001109, PMI_RD_WKI_000816, and PMI_RD_FOR_000761 .

Each sample was hybridized to an Affymetrix GeneChip® Rat Genome 230 2.0 Array. Hybridization, washing, and staining were done using the fluidics station 450 (Affymetrix) according to manufacturer's instructions. More details are in 15025_176500 THS SP.

7.12.2 Data Processing for Transcriptomics Analysis

Data were processed through the standard pipeline. Briefly, raw data files were read by the ReadAffy function of the affy package (Gautier 2004) in the Bioconductor suite of microarray analysis tools (Gentleman 2004b) available for the R statistical environment (R Development Core Team 2007). Quality was controlled by generating and examining RNA degradation plots (AffyRNAdeg function of the affy package), NUSE and RLE plots (affyPLM package) (Brettschneider 2008), calculating the MA (RLE) values.

Arrays that fell below a set of thresholds on the quality control checks were excluded from further analysis. Robust Multi-array Analysis (RMA) background correction and quantile

normalization were used to generate microarray expression values (Irizarry 2003) from all arrays passing quality control checks.

7.12.3 Number of Replicates Per Group

After QC analysis, the following sample group size was used for data analysis (Table 4).

Table 4: Sample size per group used for data transcriptomics data evaluation.

A) Respiratory nasal epithelium:

			90 d	90+42 d
Group Code	**Long Name**	**Target Nicotine (µg/L)**	**M/F**	**M/F**
012	Sham PLUS	0	6/5	0/6
013	3R4F PLUS	23	6/5	0/5
014	DDA3 1xMIS PLUS	23	5/6	0/0
015	DDA3 2xMIS PLUS	23	6/6	0/6
016	THS2.2M Low PLUS	15	6/6	0/0
017	THS2.2M Medium PLUS	23	6/5	0/0
018	THS2.2M High PLUS	50	6/6	0/5
	Total		41/40	0/22

(Table continues)

B) Lung tissue:

			90 d	90+42 d
Group Code	**Long Name**	**Target Nicotine (µg/L)**	**M/F**	**M/F**
012	Sham PLUS	0	5/6	0/6
013	3R4F PLUS	23	4/3	0/5
014	DDA3 1xMIS PLUS	23	5/6	0/0
015	DDA3 2xMIS PLUS	23	6/4	0/6
016	THS2.2M Low PLUS	15	6/5	0/0
017	THS2.2M Medium PLUS	23	4/4	0/0
018	THS2.2M High PLUS	50	5/5	0/5
	Total		35/33	0/22

C) Liver tissue:

			90 d	90+42 d
Group Code	**Long Name**	**Target Nicotine (µg/L)**	**M/F**	**M/F**
012	Sham PLUS	0	6/5	0/5
013	3R4F PLUS	23	5/4	0/5
014	DDA3 1xMIS PLUS	23	6/6	0/0
015	DDA3 2xMIS PLUS	23	6/6	0/6
016	THS2.2M Low PLUS	15	6/6	0/0
017	THS2.2M Medium PLUS	23	6/6	0/0
018	THS2.2M High PLUS	50	6/6	0/6
	Total		41/39	0/22

Sample size per group after QC. A) RNE, B) lung tissue, C) liver tissue.

An overall linear model was fitted to the contrasts of interest to generate raw *p*-values for each probe set on the expression array (Smyth 2004). The Benjamini–Hochberg false discovery rate (FDR) method was then used to correct for multiple testing effects.

7.13 iTRAQ LC-MS/MS Procedure

7.13.1 Sample Lysis and Labeling for Quantitative Proteomics

A 50-µg aliquot was processed for the iTRAQ 8-plex labeling procedure according to the manufacturer's instructions (AB Sciex, Framingham, MA, USA). Trypsin (Promega, Madison, WI, USA) was added in a 1:10 trypsin-to-protein ratio (w/w) to the samples, followed by overnight digestion at 37°C. The digested samples were labeled with reporter-ion tags for the different treatment groups for two separate iTRAQ analysis sets (see next section). For iTRAQ Set 1, a common reference mix containing 50 µg of all protein extracts from each treatment was prepared and labeled with an iTRAQ reporter-ion tag. All labeled samples belonging to one iTRAQ set were pooled and dried in a SpeedVac. Samples were desalted using 0.5 mL by volume detergent removal columns (Pierce Biotechnology, Rockford, IL, USA), followed by the use of 1-mL C18 reversed-phase Sep-Pak columns (Waters, Milford, MA, USA) according to the manufacturers' manuals. Samples were dried in a SpeedVac and resuspended in nanoLC buffer A (5% acetonitrile [Sigma–Aldrich] and 0.2% formic acid [Sigma–Aldrich]).

7.13.2 Definition of iTRAQ Analysis Sets

Two multiplexed iTRAQ analysis sets were prepared, to allow for full comparison of exposure, time, and sex effects.

iTRAQ Set 1 was focused on the exposure and sex effects after 90 days. Each 8-plex labeling set included one reference mix, i.e., the mixture of all samples, and one sample of each 90-day sample type (sham, 3R4F, DDA3 1xMIS, DDA3 2xMIS, THS2.2M Low, THS2.2M Medium, and THS2.2M High). For each replicate set and each 90-day sample type, either a male or a female sample was randomly selected (out of the total 2×6 replicates). Within each replicate labeling set, the sample for channel mapping was randomized.

iTRAQ Set 2 was focused on the exposure and 90+42-day recovery effect for female rats only. Each 8-plex labeling set included one sample of each 90+42-day sample type (sham, 3R4F, DDA3 2xMIS, and THS2.2M High; female only), and the corresponding female sample types after a 90-day exposure. Again, the biological replicates were randomly assigned to the (six) replicate labeling sets, and the channel-mapping sample for each set was randomized.

Missing samples were randomly replaced by a copy of the same sample type. These duplicated, placeholder samples were removed after data analysis and processing.

7.13.3 Mass-Spectrometry for Identification and Quantification

Samples were analyzed in random order using an EASY-nLC 1000 instrument (Thermo Fisher Scientific, Waltham, MA, USA) connected online to a Q Exactive mass analyzer (Thermo Fisher Scientific). Peptides were separated on a 50-cm long C18RP RSLC EASY-Spray column (2 µm particle size; Thermo Fisher Scientific) at a flow rate of 200 nL/min with a 200 min gradient from nanoLC buffer A (5% acetonitrile, 0.2% formic acid) to 40% acetonitrile, 0.2% formic acid. Each sample was injected twice with two different analysis methods: A fast method and a sensitive method, as described by Kelstrup et al. (Kelstrup 2012), on the same column. Both mass-spectrometry runs were searched together as merged mass-lists against the rat reference proteome set (UniProt, October 2013 version, canonical isoforms only), using Proteome Discoverer version 1.4.0.288 software (Thermo Fisher Scientific). Sequest HT (implemented in Proteome Discoverer) was used as the search tool, and iTRAQ-reporter ion intensities were determined from the Proteome Discoverer software. The Percolator node of the Proteome Discoverer software was used to estimate peptide-level adjusted *p*-values (q-values). iTRAQ peptide-level quantification data were exported and further processed in the R statistical environment (R Development Core Team 2007). The quantification data were filtered for a q-value < 0.01 and for "unique" quantification results, as defined by the Proteome Discoverer software. A global variance stabilizing normalization (VSN) was performed with the respective Bioconductor package in R (Huber 2002, Hultin-Rosenberg 2013). Each iTRAQ reporter ion set was normalized to its median, and protein expression values were calculated as the median of these normalized peptide-level quantification values (Herbrich 2013). For the detection of differentially expressed proteins, a linear model was fitted for each exposure condition and its respective sham group, and *p*-values from a moderated t-statistic were calculated with the empirical Bayes approach (Gentleman 2004a). The Benjamini–Hochberg FDR method was then used to correct for multiple testing effects. Proteins with an adjusted *p*-value < 0.05 were considered differentially expressed.

7.13.4 Number of Replicates Per Group and Protein Identification

After quality control, the following samples were excluded from the analysis:

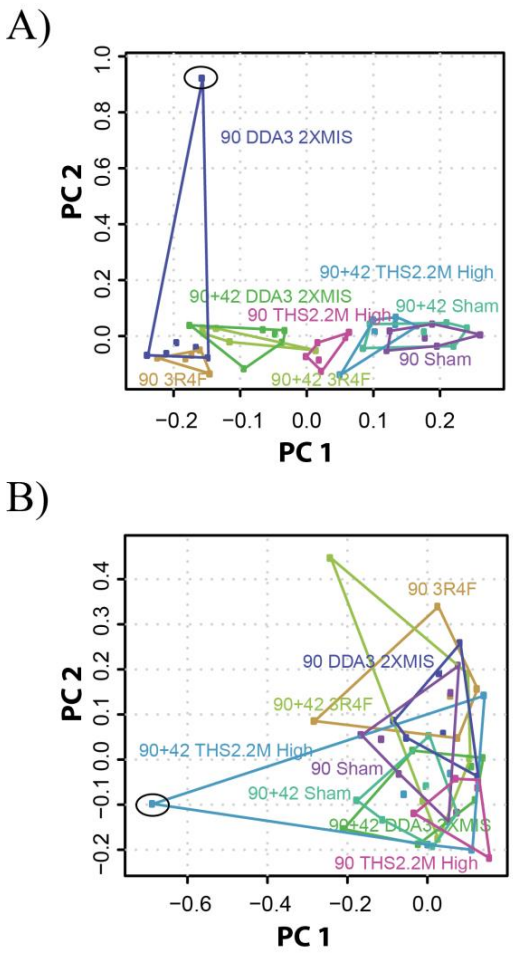


Figure 2: Principal component analysis.

A) Respiratory nasal epithelium, iTRAQ Set 2 (90+42 days): DDA-2xMIS, 90 days (replicate 1) appeared as outlier on PC 2. B) Lung tissue: After quality control, the following samples were excluded from the analysis: iTRAQ Set 2 THS2.2M High, 90+42 days (replicate 6) appeared as outliers on PC 1.

No clear outlier was identified for the liver tissue, and all samples were kept.

Note that outliers were removed to increase the sensitivity of the differential protein identification, i.e., to ensure that relevant exposure effects were detected. However, the global results were checked for consistency; outlier removal did not affect any of the main conclusions, e.g., the recovery effect for the THS2.2M exposed groups (see below).

Table 5A summarizes the number of replicates effectively available for each RNE group. Table 5B summarizes the number of replicates effectively available for each lung tissue

group. Table 5C summarizes the number of replicates effectively available for each liver tissue group.

Table 5: Number of valid replicates for proteomics analysis.

A)

			iTRAQ Set 1		iTRAQ Set 2	
			90 d		90 d	90+42 d
Group Code	Long Name	Target Nicotine (µg/L)	Male	Female	Female	
012	Sham	0	6	6	6	6
013	3R4F	23	6	5	5	5
014	DDA3 1xMIS	23	6	6		
015	DDA3 2xMIS	23	6	6	5	6
016	THS2.2M Low	15	6	6		
017	THS2.2M Medium	23	6	6		
018	THS2.2M High	50	6	6	6	6

B)

		iTRAQ Set 1		iTRAQ Set 2	
		90 d		90 d	90+42 d
Long Name	Target Nicotine (µg/L)	Male	Female	Female	
Sham	0	6	6	6	6
3R4F	23	6	5	5	5
DDA3 1xMIS	23	6	6		
DDA3 2xMIS	23	6	6	6	6
THS2.2M Low	15	6	6		
THS2.2M Medium	23	6	6		
THS2.2M High	50	6	6	6	5

(Table continues)

C)

		iTRAQ Set 1		iTRAQ Set 2	
		90 d		90 d	90+42 d
Long Name	Target Nicotine (µg/L)	Male	Female	Female	
Sham	0	6	6	6	6
3R4F	23	6	5	5	5
DDA3 1xMIS	23	6	6		
DDA3 2xMIS	23	6	6	6	6
THS2.2M Low	15	6	6		
THS2.2M Medium	23	6	6		
THS2.2M High	50	6	6	6	6

A) Number of valid replicates of nasal epithelium proteomics profiles. B) Number of valid replicates of lung proteomics profiles. C) Number of valid replicates for liver proteomics profile.

In total, for nasal epithelium, 4,370 proteins were identified and quantified for iTRAQ Set 1 (90 days) and 3,706 proteins were identified and quantified for iTRAQ Set 2 (90+42 days). For the identification of differentially expressed proteins compared with the sham exposure group, only proteins quantified in at least two thirds of one compared group were considered. The number of proteins considered after filtering for each comparison is given in Table 6 A.

In total, for lung tissue, 3,544 proteins were identified and quantified for iTRAQ Set 1 (90 days) and 3,226 proteins were identified and quantified for iTRAQ Set 2 (90+42 days). For the identification of differentially expressed proteins compared with the sham exposure group, only proteins quantified in at least two thirds of one compared group were considered. Table 6 B displays the number of proteins considered after filtering for each comparison.

In total, for liver, 2,489 proteins were identified and quantified for iTRAQ Set 1 (90 days) and 2,435 proteins were identified and quantified for iTRAQ Set 2 (90+42 days). For the identification of differentially expressed proteins compared with the sham exposure group,

only proteins quantified in at least two thirds of one compared group were considered. Table 6 displays the number of proteins considered after filtering for each comparison.

More details for the iTRAQ LC-MS/MS procedure are available in the Study Plan "15025_176500 THS SP".

Table 6: Number of proteins for differential expression analysis.

A)

			iTRAQ Set 1		iTRAQ Set 2	
			90 d		90 d	90+42 d
Group Code	Long Name	Target nicotine (µg/L)	Male	Female	Female	
012	Sham	0	REF	REF	REF	REF
013	3R4F	23	2552	2466	2370	2370
014	DDA3 1xMIS	23	2534	2553		
015	DDA3 2xMIS	23	2599	2560	2370	2370
016	THS2.2M Low	15	2530	2517		
017	THS2.2M Medium	23	2594	2567		
018	THS2.2M High	50	2557	2526	2370	2370

B)

			iTRAQ Set 1		iTRAQ Set 2	
			90 d		90 d	90+42 d
Group Code	Long Name	Target Nicotine (µg/L)	Male	Female	Female	
012	Sham	0	REF	REF	REF	REF
013	3R4F	23	2020	2081	2141	2141
014	DDA3 1xMIS	23	2164	2112		
015	DDA3 2xMIS	23	2057	2105	2142	2141
016	THS2.2M Low	15	2095	2101		
017	THS2.2M Medium	23	2116	2080		
018	THS2.2M High	50	2123	2101	2142	2141

(Table continues)

C)

			iTRAQ Set 1		iTRAQ Set 2	
			90 d		90 d	90+42 d
Group Code	**Long Name**	**Target Nicotine (µg/L)**	**Male**	**Female**	**Female**	
012	Sham	0	REF	REF	REF	REF
013	3R4F	23	1536	1512	1478	1478
014	DDA3 1xMIS	23	1540	1537		
015	DDA3 2xMIS	23	1542	1523	1478	1478
016	THS2.2M Low	15	1513	1502		
017	THS2.2M Medium	23	1553	1542		
018	THS2.2M High	50	1543	1548	1478	1478

A) Number of proteins in nasal epithelium. B) Number of proteins in lung. C) Number of proteins in liver. Sham group is the reference (REF).

7.14 Lipidomics

7.14.1 Samples and Platforms

The following samples were sent to Zora Biosciences Oy, Finland:

Table 7: Number of samples processed by Zora.

A)

		90 d	90+42 d
Long Name	**Target Nicotine (µg/L)**	**M/F**	**M/F**
Sham PLUS	0	6/6	0/6
3R4F PLUS	23	6/5	0/5
DDA3 2xMIS PLUS	23	6/6	0/6
THS2.2M Medium PLUS	23	6/6	0/0
THS2.2M High PLUS	50	6/6	0/6
Total		30/29	0/23

B)

		90 d
Long Name	**Target Nicotine (µg/L)**	**M/F**
Sham PLUS	0	6/6
3R4F PLUS	23	5/5
DDA3 2xMIS PLUS	23	6/6
THS2.2M Medium PLUS	23	6/6
THS2.2M High PLUS	50	6/6
Total		29/29

A) Lung samples, B) Liver samples. No recovery samples (90+42 days) were sent.

The lipidomics platforms used for the lung samples were Shotgun, Ceramide, and Eicosanoid. The platforms used for liver were Shotgun and Ceramide. Table 8 lists the platform details.

Table 8: Lipidomics platforms and lipid classes measured in the lung and liver.

Platform	**Monitored lipid classes**
Shotgun Lipidomics (SG)	Cholesteryl esters (CE) Phosphatidylcholines (PC) Lysophosphatidylcholines (LPC) and other lysophospholipids (LPL) Ether-linked phosphatidylcholines (PC O) and other ether-linked phospholipids (PL O) Phosphatidylserines (PS) Phosphatidylethanolamines (PE) Phosphatidylglycerols (PG) Phosphatidylinositols (PI) Phosphatidic acid (PA) Sphingomyelins (SM) Diacylglycerols (DAG)
Ceramide and cerebroside Lipidomics (CER)	Ceramides (Cer) Cerebrosides (Lactosylceramides (LacCer), Galactosyl- and Glucosylceramides (Gal/GlcCer), globotriaosylceramides (Gb3Cer))
Eicosanoid Lipidomics (EC)	Arachidonic acid (AA) Eicosapentaenoic acid (EPA) Docosahexaenoic acid (DHA) Prostaglandins (PG) Thromboxanes (TX) Hydroxyeicosapentaenoic acids (HEPEs) Hydroxyeicosatetraenoic acids (HETEs) Dihydroxyeicosatrienoic acids (DiHETrEs/DHETs) Hydroxyoctadecadienoic acids (HODEs) Hydroxyoctadecatrienoic acids (HOTrEs) Leukotrienes (LT) Lipoxines (LX)

No Eicosanoid lipidomics were performed in liver samples.

7.14.2 Sample Preparation and Lipid Extraction

The lipid analyses of tissue samples were performed according to the Standard Operating Procedures (SOP), the Lab Method Sheets (LMS), and data Processing Method Sheets (PMS) of Zora Biosciences Oy (Jung 2011).

The tissue samples were pulverized with CP02 cryoPREP Dry Pulverization System (Covaris, Woburn, MA, USA), and resuspended in ice-cold methanol containing 0.1% butyl-hydroxy-toluene (BHT) in a concentration of 100 mg/mL. Lipids (ceramides, glycerolipids, and glycerophospholipids) were extracted using a modified Folch lipid extraction (Jung 2011) performed on a Hamilton Microlab STAR robot. Samples were spiked with known quantities of non-endogenous synthetic internal standards. After lipid extraction, samples were reconstituted in chloroform:methanol (1:2, v/v), and synthetic external standards were spiked to the extracts. The extracts were stored at −20°C prior to MS analysis.

Eicosanoids were extracted using solid-phase extraction (SPE) as described by (Deems 2007). Known quantities of isotope-labeled standards were included as synthetic internal and external standards. The SPE wells were washed with 35% methanol and eluted in 100% acetonitrile. The samples were then evaporated until dry and reconstituted in methanol, followed by the addition of an external standard mixture.

7.14.3 Mass Spectrometric Analyses

In Shotgun lipidomics, lipid extracts were analyzed using a hybrid triple quadrupole/linear ion trap mass spectrometer (QTRAP 5500) equipped with a robotic nanoflow ion source (NanoMate HD) according to Ståhlman et al. (Ståhlman 2009). Molecular lipids were analyzed in both positive and negative modes using Multiple Precursor Ion Scanning (MPIS)-based methods (Ekroos 2002, Ekroos 2003). Triacylglycerols (TAG) were analyzed using Precursor Ion Scanning (PIS) and Neutral Loss scanning (NL)-based methods (McAnoy 2005). The molecular lipid species were identified and quantified in semi-absolute or absolute quantities according to the corresponding LMS.

Targeted molecular lipids were analyzed on a hybrid triple quadrupole/linear ion trap mass spectrometer (QTRAP 5500) equipped with an ultra-high pressure liquid chromatography (UHPLC) system (Eksigent 100-XL) using a multiple reaction monitoring (MRM)–based method in negative ion mode according to the corresponding LMS.

Sphingolipids were analyzed as in (Merrill 2005) using an Acquity BEH C18, 2.1×50 mm column with a particle size of 1.7 µm (Waters, Milford, MA, USA). A 25 min gradient was

used with 10 mM ammonium acetate in water with 0.1% formic acid (mobile phase A) and 10 mM ammonium acetate in acetonitrile:2-propanol (4:3, v/v) containing 0.1% formic acid (mobile phase B). Eicosanoids were analyzed as in (Deems 2007). The mass spectrometry data obtained from MS instruments were exported as .wiff or .txt files that represent the basic raw files of lipidomic analysis. These files contain information on masses of identified molecules and their counts (intensities and areas). Masses and counts of detected peaks were converted into a list of corresponding lipid names and concentrations.

Calibration lines were generated to determine the dynamic quantification range for each lipid monitored, e.g., the quantification limits. As the internal standards used behave in the same way as endogenous lipids, they were used for quantifying endogenous lipids.

The MS data files were processed using LipidView™ 1.2 or MultiQuant™ 3.0 for producing a list of lipid names and peak areas. Lipids were normalized to their respective internal standard (the peak area of the endogenous lipid was divided by the peak area of the corresponding internal standard) and sample volume. The concentrations of molecular lipids are presented as pmol/µl or pmol/µg tissue wet weight for plasma or tissue samples, respectively.

7.14.4 Acceptance Criteria for the Results

The ratio of synthetic Internal Standards (IS) to corresponding post-extract spiked External Standards (ES), and MS analysis of extracted matrix and solvents served as quality controls (QC) of the analysis. In addition, extracted reference plasma/tissue samples were analyzed for monitoring the instruments' performance.

Calibration lines using synthetic standards were obtained prior to sample analysis. The calibration lines consisted of a minimum of four accepted standard points covering the linear quantification range. The calibration lines were used to determine the quantification limits of the method.

The analysis was accepted based on the linearity of the calibration lines. The linear regression must exceed 0.95 based on at least four out of six non-zero standards.

The analysis is accepted based on the identification of sample-specific IS.

8 Statistical Methods and Computational Methods

8.1 Sample Randomization Protocol

As we wanted to compare the effect of THS2.2M vs. references, the effect of a recovery period, and the effect of sex, all samples (=107 per tissue) needed to be randomized and processed together.

For cryoslicing, the 90-day group and the 90+42-day group were randomized in two batches.

For transcriptomics randomization, we took into account potential cryoslicing batch effects, RNA extraction batch effects, and different Affymetrix fluidics stations. A randomization plan was provided by the bioinformatics team. For iTRAQ, samples were randomized according to the plan provided by the bioinformatics team.

8.2 Computational Methods

8.2.1 Gene/Protein-Set Analysis

Gene-set analysis (GSA) of transcriptomics and proteomics data was performed using the *Piano* package in the R statistical environment (Varemo 2013). Pathway maps were obtained from the KEGG database (Kanehisa 2014a) and exported as R objects into the package *graphite* (Sales 2012). Gene-set enrichment was assessed using over-representation analysis (ORA) and gene-set analysis. For the ORA, a one-tailed Fisher's exact test was employed. For the GSA, the fold-change was used as the gene-level statistic, the mean was used as the set statistic, and sample permutation (Q2) was used to assess statistical significance (Ackermann 2009). For each test, the *p*-value was adjusted using the Benjamini–Hochberg procedure.

8.2.2 Network Perturbation Amplitude

The collection of causal biological networks used in the study(s) was the rat network suite CBN v1.3. These networks range between a few dozen and two hundred nodes in size.

Network scoring exploits the network backbone nodes that are connected to downstream mRNA-abundance-nodes based on their known relationship reported in the literature. These signed relationships can be the backbone node increasing or decreasing the abundance of certain mRNAs and are used to infer the activation of a backbone node using

transcriptomics data. Since not all backbone nodes have downstream mRNA nodes, the network models need to be prepared for scoring to improve the specificity and relevancy of the overall NPA score. Only backbone nodes that are on a directed path that starts and ends with a node that has downstream mRNA nodes are considered. After removing the nodes that do not satisfy the above, the largest connected component is kept. Finally the edges "causesNoChange" are disregarded for the scoring.

The Network Perturbation Amplitude (NPA) methodology (Hoeng 2014, Martin 2012) aims at contextualizing the high dimensional transcriptomics data by combining gene expression (log_2) fold-changes, β, into fewer differential node values (one value for each node of the network), *f*. The differential nodes values are determined by a fitting procedure that infers the values that best satisfy the directionality of the causal relationships (positive or negative signs) contained in the network model, while being constrained by the experimental data (the gene log_2-fold-changes, which are described as downstream effects of the network itself):

$$f = L_3^{-1} L_2^T \beta$$

where L is the signed weighted Laplacian of the network and the extra edges and nodes describing the downstream effects (to gene expression nodes); L_3 is the sub-matrix of L for the nodes in the network; and L_2 is the sub-matrix corresponding to the edges connecting the network nodes to the downstream gene expression nodes. The differential node values are in turn summarized as a single positive number, referred to as the amplitude of perturbation ("NPA scores").

$$NPA = \frac{1}{|E|} \sum_{e\ in\ E} (f(e_0) - \sigma(e) f(e_1))^2$$

where E is the set of edges in the network; |E| is its size; and e_0 and e_1 denote the start and the end, respectively, of an edge, e. The sum computing the NPA score can be expressed as $f^T Q f$, where Q is the signed Laplacian of the network when all of the edge signs have been reversed.

All the details of the methodology is described in a previous publication (Martin 2014).

For the NPA scores, a confidence interval accounting for the experimental variation and the associated p-value are computed. In addition, companion statistics are derived to inform on the specificity of the NPA score with respect to the biology described in the subnetwork model and are shown as *O and K* if their p-values are below the significance level (0.05).

A network is considered to be significantly impacted if all of the three values (the p-value for experimental variation, *O, and K* statistics) are below 0.05.

8.2.3 Biological Impact Factor

The methodology Biological Impact Factor (BIF) (Martin 2014, Martin 2012) provides a unified and coherent framework for investigating mechanistic effects at each level of granularity of the biological processes represented in the network models. This methodology enables the derivation of the relative BIF, which is a measure of the overall biological impact across all network models. The BIF allows an assessment of the exposures in an objective, systematic, and quantifiable manner, computing a systems-wide and pan-mechanistic biological impact measure for a given substance, mixture, or test item.

The network models are organized into five major families, representing global biological processes: cell stress, cell proliferation, inflammation, tissue repair, and cell fate. Each of them comprised of various subnetwork models, representing the specific processes within a given network family.

An aggregation of the NPA should satisfy the following criteria:

1. *Credibility*: The BIF should be an intuitive and logical aggregation scheme.
2. *Fairness*: All network families are equally important.
3. *Understandable*: Each decision or step has a defined rationale.

To fulfil the first criteria, network scores are aggregated via a weighted sum (as every scoring in NPA is additive). In addition, only networks that have the three statistics p-values below 0.05 (*O, *, K*) will be considered (denoted by N_i^*). The BIF is defined as:

$$BIF = \sum_{\mathcal{N}_i^*} w_i NPA(\mathcal{N}_i) = \sum_{\mathcal{N}_i^*} w_i \sum_{e \in E(\mathcal{N}_i)} (f(e_0) + \sigma(e) f(e_1))^2$$

Where, f denotes the function on the network nodes describing the differential node values; $E(N_i^*)$ denotes the network edges; and e_0 and e_1 denote the start and the end, respectively, of an edge, e .

For the second criteria, a "fair" BIF would represent the equality of the biological processes (networks) in a given system (e.g., 2D normal human bronchial epithelial cells, 3D organotypic tissue cultures, or lung tissue samples from in-vivo studies). If all subnetworks models were perfectly fitted by the gene expression data, the contribution of each subnetwork to the BIF is assumed to be equal. Therefore, the methodology considers that all specific processes represented in the subnetwork models, are equally involved and

important for a given network family (e.g., cell stress). A perfect fit of the network will maximize the NPA value while being smooth over the network. Using the notation above, a "perfect" network response (differential node values) is both maximizing the f^TQf with $||f||_2 = 1$ and minimizing the f^TL_3f (the NPA criteria (Hoeng 2014)). Additionally, there is a constraint that L_3f is vanishing for the network nodes that do not have direct downstream gene expression nodes (Hoeng 2014, Martin 2012), as those are expected to be in the image of L^T_2. Such nodes are denoted as *NH*. Therefore, the following optimization problem will be solved:

$$argmax_{f\ s.t.(L_3f)|_{NH}=0}\ \frac{f^TQf}{f^TL_3f}$$

To rebalance the network families, the average over the subnetworks will be considered.

For each edge $e = (e_0, \sigma(e), e_1)$, the number of occurrence of an edges, *e,* in the set of networks used in the BIF calculation is denoted by o(e). Therefore, the maximum occurrence-corrected amplitude of a network N_i can be defined as:

$$NPA_{max}(\mathcal{N}_i) \doteq \sum_{e\in E(\mathcal{N}_i)} \frac{1}{o(e)}(f_{max}(e_0) + \sigma(e)f_{max}(e_1))^2$$

Finally, to normalize the NPAs, a correction factor of $|E(N_i)|/NPA_{max}(N_i)$ is applied. Considering all of these factors, the BIF is defined as the weighted sum (F denotes the subnetwork families), as follows:

$$\sum_{\mathcal{F}} \frac{1}{|\mathcal{F}|} \sum_{\mathcal{N}_i^*\in\mathcal{F}} \frac{1}{NPA_{max}(\mathcal{N}_i)} \sum_{e\in E(\mathcal{N}_i)} \frac{1}{o(e)}(f(e_0) + \sigma(e)f(e_1))^2$$

Therefore, the contribution of each subnetwork F is:

$$\frac{\frac{1}{|\mathcal{F}|}\sum_{\mathcal{N}_i^*\in\mathcal{F}} \frac{1}{NPA_{max}(\mathcal{N}_i)} \sum_{e\in E(\mathcal{N}_i)} \frac{1}{o(e)}(f(e_0) + \sigma(e)f(e_1))^2}{BIF_{SDP}}$$

8.3 Statistical analysis of Lipidomics data

Statistical analysis of the lipidomics data was conducted analogous to the transcriptomics and proteomics analyses. Samples with a total summed lipid concentration below the first quartile − 1.5 × the interquartile range were excluded. For the detection of differentially expressed lipids, only those lipid species that were present/quantified in at least 50% of the

samples of each compared group were included. A linear model was fitted for each exposure condition and its respective sham group, and *p*-values from a moderated t-statistic were calculated with the empirical Bayes approach (Gentleman 2004a). The Benjamini–Hochberg FDR method was then used to correct for multiple testing effects. Lipids with an adjusted *p*-value < 0.05 were considered differentially abundant.

9 Results

9.1 Body Weight

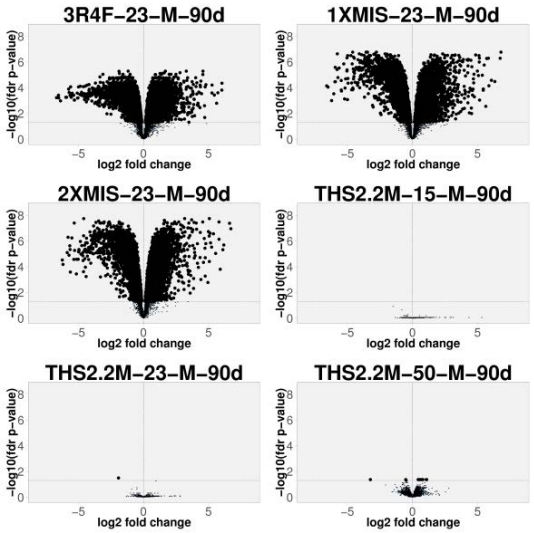
The body weight trends in the OECDplus groups before exposure, during the first week of adaptation, and progression during the 90-day exposure and post-exposure periods were very similar to those of the OECD groups, with all animals gaining weight over time throughout the 90-day exposure period. Only females were included in the recovery groups, and the trends depicted a more rapid body weight gain in the 42-day post-inhalation recovery period, as seen in the OECD groups.

9.2 Respiratory Nasal Epithelium Transcriptome after 90 Days of Exposure and after a 42-day Recovery Period in Male and Female Rats

9.2.1 Differentially Expressed Genes in Respiratory Nasal Epithelium after 90 Days of Exposure to Reference Cigarettes and THS2.2M, or after a 42-day Recovery Period

The amplitude (expressed as log fold change, x-axis) and statistical significance (expressed as −log of the FDR p-value) of gene expression changes in nasal epithelium for 3R4F-, DDA3 1xMIS-, DDA3 2xMIS-, and THS2.2M-exposed rats after 90 days of exposure or after a 42-day recovery period (females only) were compared with the sham group and graphed as volcano plots (Figure 3).

A)



B)

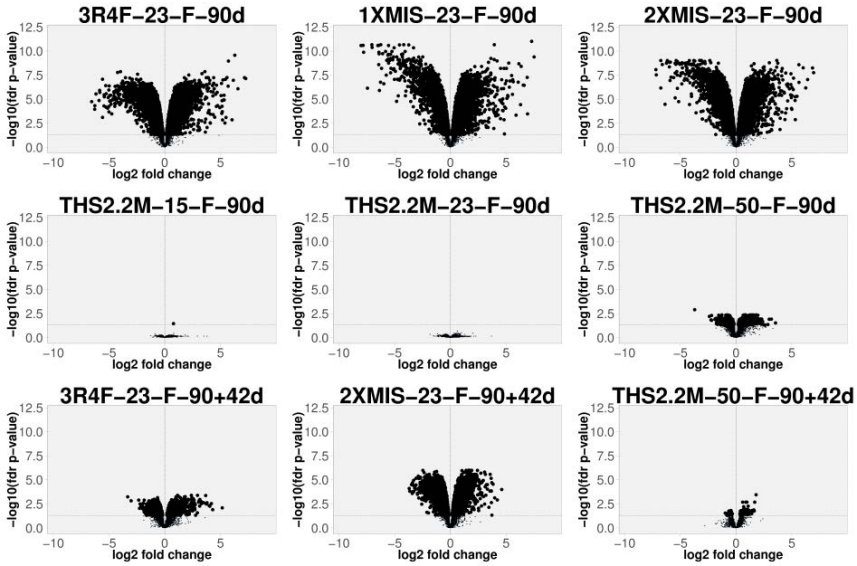


Figure 3: Volcano plots representing the systems response profiles in respiratory nasal epithelium.

For each gene, the change in gene expression, calculated as the log2 fold change, was plotted on the x-axis; statistical significance, proportional to the negative log10-FDR *p*-value, was plotted on the y-axis. Dark black

dots highlight genes that are statistically significantly up- and down-regulated (right and left quadrants, respectively) compared with sham at the same time point. A) Male rats, B) female rats. The exposure vs. sham group comparisons are labeled according to "test item – nicotine concentration – Male/Female – time point". For example, 3R4F-23-F-90d represents the group of female rats exposed to 3R4F at a nicotine concentration of 23 µg/L for the 90d time point; THS2.2-15-F-90+42d represents the group of female rats exposed to THS2.2 at a nicotine concentration of 15 µg/L for the 90+42d time point.

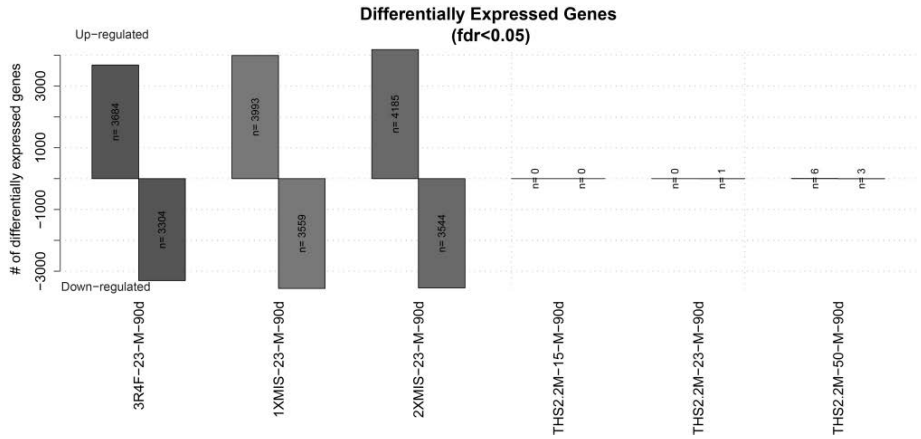
In the respiratory epithelium of 3R4F-, DDA3 1xMIS-, and DDA3 2xMIS-exposed male and female rats after 90 days of exposure, more than 7,000 genes were differentially expressed (adj. *p*-value < 0.05) (Figure 3).

After exposure to the high dose of THS2.2M (50 µg/L nicotine) for 90 days, only nine genes were differentially expressed in the RNE of male rats, only one gene when the THS2.2M concentration with the same nicotine amount as in the 3R4F group was used (23 µg/L nicotine), and no differentially expressed gene was identified for the lowest THS2.2M concentration (15 µg/L nicotine) after 90 days of exposure.

For female rats, after exposure to the high dose of THS2.2M (50 µg/L nicotine) for 90 days, more than 2,100 genes were differentially expressed in the RNE. Only one or no genes were differentially expressed in THS2.2M at lower doses, 15 and 23 µg/L nicotine, respectively. After 42 days of recovery in THS2.2M (50 µg/L nicotine)-exposed rats, differential expression was not detected anymore for most of these genes; only 120 genes were still differentially expressed.

Figure 4 displays an overview of the number of differentially expressed genes after reference cigarette and THS2.2M exposure.

A)



(Figure continues)

B)

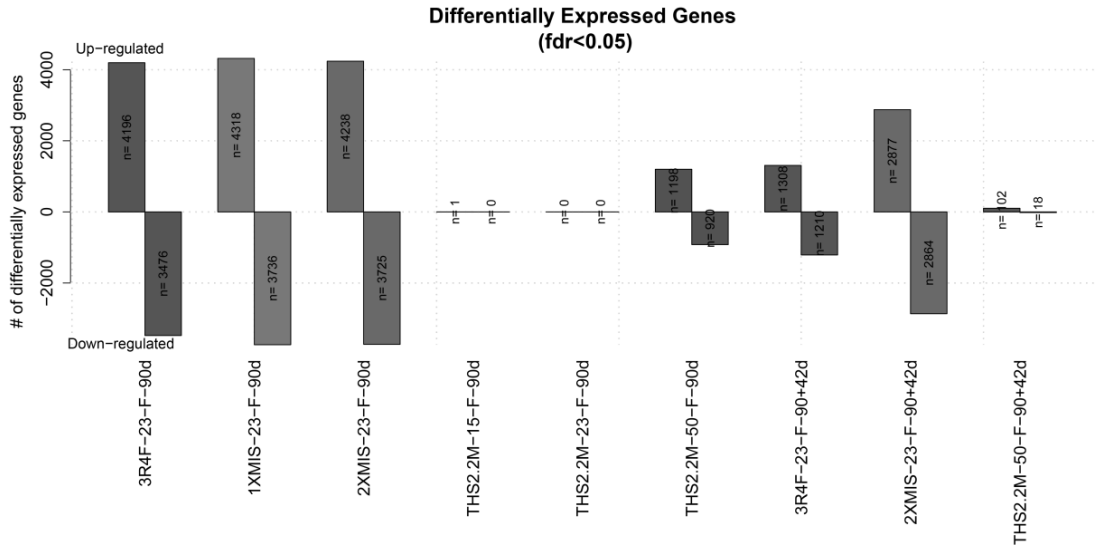
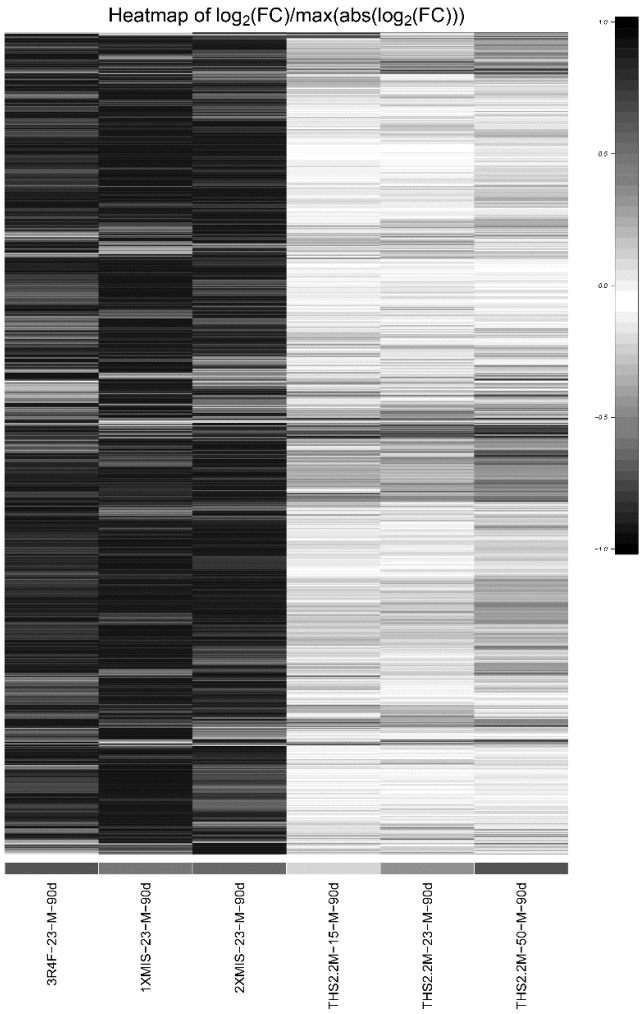


Figure 4: Number of significant differentially expressed genes in RNE tissue.

Bar plots represent the number of differentially expressed genes. A) Female rats, B) male rats.

We generated a heat map (Figure 5) to display an overview of the differential gene expression trends over the various exposure groups, and to graph the overlap of differentially expressed genes.

A)



(Figure continues)

B)

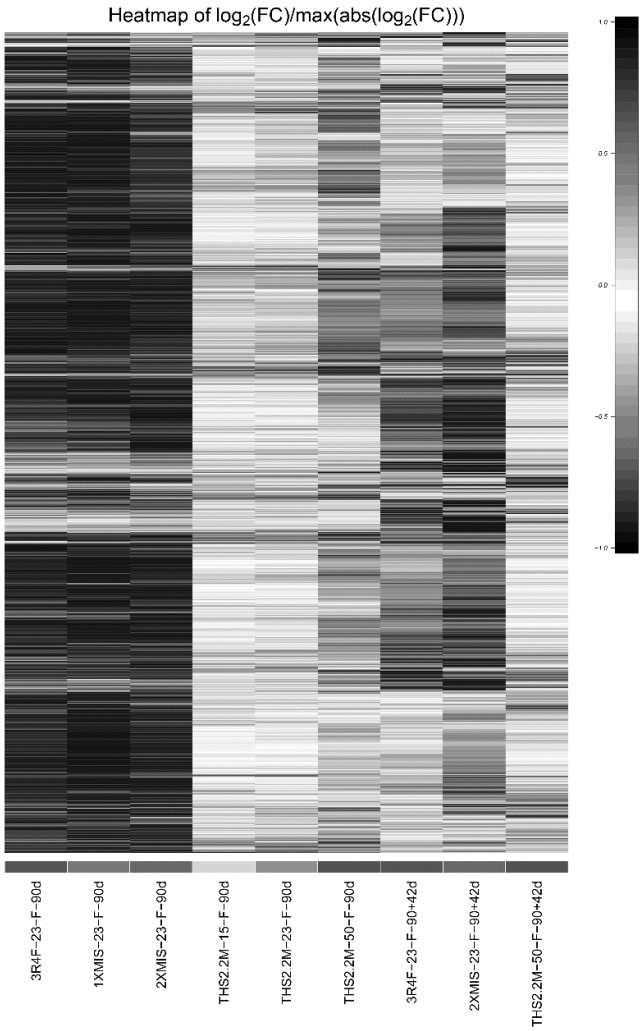


Figure 5: Heat map of gene expression in respiratory nasal epithelium.

Heat map representing the log2(fold-change)/max(abs(log2(fold-change))) for all genes which induced a significant expression change, at least in one comparison. The grayscale is based on the absolute values (range from -1 to 1). A) Male rats after 90 days of exposure, B) female rats after 90+42 days of exposure.

We can see in the heat map that in comparison with the reference exposures (3R4F, DDA3 1xMIS, and DDA3 2xMIS), the corresponding fold changes in THS2.2M groups were generally lower.

After exposure to the highest concentration of THS2.2M, all differentially expressed genes in the RNE from male rats were also differentially expressed after exposure to at least one of the reference cigarettes.

After exposure to the highest concentration of THS2.2M, about 94% of the differentially expressed genes in the RNE from female rats were also differentially expressed by at least one of the reference cigarettes groups (i.e., 2,158 DEGs vs. 1,995 overlapping DEGs).

The genes that were significantly differentially expressed only after THS2.2M exposure are listed in Table 9.

Table 9: Unique genes that were differentially expressed only in RNE of female rats after THS2.2M exposure.

	Differentially Expressed Genes in Female Rats Uniquely Significant for THS2.2M Group								
Gene ID	**3R4F-23-F 90d**	**1XMIS-23-F 90d**	**2XMIS-23-F 90d**	**THS2.2M-15-F 90d**	**THS2.2M-23-F 90d**	**THS2.2M-50-F 90d**	**3R4F-23-F 90+42d**	**2XMIS-23-F 90+42d**	**THS2.2M-50-F 90+42d**
Acsl3	0.04	0.11	0.14	0.25	0.15	0.38 *	0.37 *	0.13	0.12
Acsl4	0.25	0.33	0.29	0.4	0.37	0.55 *	0.25	0.32 *	0.47
Adamts15	0.23	0.02	-0.1	-0.45	-0.51	-0.72 *	0.28	0.04	-0.38
Ahcyl1	0.23	0.13	0.24	0.15	0.01	0.42 *	0.45 *	0.32 *	0.34
Alox12e	0.1	-0.12	0.18	0.78	0.68	1.56 *	0.26	0.12	-0.01
Apln	-0.03	-0.11	0.06	-0.19	-0.37	-0.46 *	0.04	0.08	-0.09
Armcx4	0	-0.12	-0.23	0.19	-0.01	0.47 *	0.39	0.33	0.68
Asun	0.08	0.05	0.19	0.09	0.19	0.35 *	0.04	0.02	0.15
Atp5e	0.02	-0.11	0.04	0.04	0.1	0.21 *	-0.04	-0.18	-0.15
Atpif1	0.07	0.03	0.06	0.02	0.2	0.32 *	0.05	-0.08	-0.07
Avp	-0.21	0.06	-0.02	0.16	0.22	0.37 *	-0.31	-0.31	0.03
Bmper	-0.37	-0.39	0.17	-0.81	-1.17	-0.94 *	1.38 *	0.9 *	-0.4
Calb1	0.13	-0.13	0.26	-0.03	-0.2	-0.26 *	0.99	0	-0.01
Cd164	0.09	0.18	0.1	0.2	0.19	0.2 *	0.07	0.17	-0.01
Creb3l4	0.27	0.35	0.18	0.08	0.18	0.61 *	-0.24	0.17	-0.36
Cyp2s1	0.01	-0.3	-0.17	-0.02	0.15	0.53 *	0.03	0.19	0.26
Ddit4l	0.55	0.4	0.45	0.08	0.38	1.04 *	0.4	-0.08	-0.12
Defb1	0.6	1.16	0.51	-0.13	0.26	-0.59 *	0.06	-0.19	-0.21
Dmrt1	-0.09	-0.07	-0.19	0.27	0.15	0.54 *	0.24	0.15	0.24
Dnajc18	0.01	0.05	0.15	0.17	0.11	0.38 *	0.1	0.14	0.17
Dock9	0.16	0.12	0.08	-0.05	-0.03	-0.39 *	-0.1	-0.06	0.04
Dzip3	0.1	0.22	-0.06	0.46	0.38	0.39 *	0.08	-0.06	0.13
E2f7	-0.05	-0.34	-0.15	0.26	0.46	0.9 *	0.38	0.2	0.98
Fam115a	0.01	0.13	0.2	0.12	0.08	0.3 *	0.23	0.25 *	0.28
Fbxo30	0.22	0.06	0.14	0.23	0.17	0.32 *	0.22	0.16	0.3
Fubp1	0.11	0.02	0.01	0.18	0.12	0.38 *	0.3	0.2	0.47
Gan	0.41	0.4	0.15	-0.36	-0.27	-0.41 *	-0.33	-0.46 *	-0.17
Gramd1b	-0.19	-0.17	-0.12	0.26	0.19	0.43 *	-0.21	-0.07	0.03
Hdac2	0.07	0.09	0.09	0.17	0.04	0.27 *	0.55 *	0.4 *	0.49 *
Hist1h2af	0.09	0.03	-0.03	0.21	0.24	0.35 *	0.14	0.06	0.25
Hpd	-0.12	-0.08	-0.2	-0.05	0	-0.29 *	-0.13	-0.3 *	-0.12
Ica1	-0.26	-0.19	-0.25	-0.17	-0.16	-0.41 *	-0.44 *	-0.26	-0.2
Kank3	-0.02	-0.06	0.01	-0.24	-0.24	-0.34 *	0.12	0.24	-0.08
Klhl18	-0.12	-0.02	-0.17	-0.06	0.07	-0.31 *	-0.23	-0.07	-0.08
Lars	0.1	0.14	-0.02	0.04	0.01	0.23 *	-0.24	-0.16	-0.09
LOC102549471	0.21	0.2	0.03	0.1	0.13	0.29 *	-0.11	-0.37 *	-0.03
LOC102554586	0.15	0.05	-0.16	-0.3	-0.01	-0.41 *	-0.57 *	-0.48 *	-0.13
LOC301124	0.1	0.06	0.11	0	0.14	0.22 *	0.08	0.08	-0.22
LOC690155	-0.05	0.06	0.06	0.37	0.29	0.61 *	1.1 *	0.58	0.8
Marcks	0.05	0.1	0.21	0.3	-0.01	0.52 *	0.86 *	0.53 *	0.72 *
Masp1	0.06	0.09	0.1	-0.07	-0.02	-0.35 *	-0.25	-0.11	-0.15
Mex3b	-0.03	-0.38	-0.13	0.57	0.23	0.94 *	0.86 *	0.2	1.44 *
Mmgt2	0.13	0.18	0.08	0.31	0.34	0.43 *	0.23	0	0.1
Mtmr1	-0.11	-0.14	-0.14	-0.12	-0.14	-0.23 *	-0.1	-0.16	-0.03
Ngf	0.05	0	-0.02	-0.2	-0.09	-0.3 *	0.03	-0.01	-0.04
Nudt21	0.13	0.07	0.09	0.12	0.08	0.37 *	0.36 *	0.26 *	0.33
Otud7b	-0.11	-0.15	-0.1	-0.06	-0.04	-0.22 *	-0.2	-0.09	-0.17
Pde4b	-0.12	-0.01	0.08	-0.07	-0.06	-0.34 *	0.31	0.15	0.08
Pdlim4	0.02	-0.15	-0.02	-0.04	-0.01	0.56 *	0.02	-0.11	0.03
Pfas	0.04	0	0.02	0.02	0.1	0.29 *	-0.03	-0.17	0.21
Pip4k2a	-0.15	-0.01	0.05	-0.11	-0.15	-0.36 *	0.01	-0.35 *	-0.14
Plac9	-0.16	-0.19	-0.07	-0.2	-0.25	-0.32 *	-0.12	-0.01	-0.13
Plk4	-0.01	-0.12	0.16	0.83	0.78	1.66 *	0.79	0.34	1.42 *
Prkab2	-0.05	-0.07	0	-0.1	-0.23	-0.28 *	0.1	0.07	0.08
R3hcc1l	-0.01	-0.08	-0.07	0.03	-0.03	-0.23 *	0	-0.05	0.01
Rasgef1b	-0.11	-0.01	-0.06	0	0.08	-0.22 *	-0.13	-0.09	-0.03
Rbx1	-0.14	-0.12	-0.12	0.09	0.04	0.19 *	0.07	0.05	0.03
Rcsd1	-0.35	-0.32	-0.3	-0.27	-0.28	-0.57 *	0.05	0.19	-0.07
RGD1565166	0.02	0.3	0.3	-0.27	-0.35	-0.62 *	-0.04	0.19	-0.23
RGD1565222	0.27	0.12	0.03	0.09	0.16	0.29 *	0.02	-0.02	-0.14
Rnd1	-0.19	-0.29	-0.11	-0.3	-0.39	-0.52 *	-0.01	-0.23	-0.3
Rnf20	0.12	0.1	0.09	-0.01	0.07	0.29 *	0.16	0.08	0.25
Sdr16c5	0.38	0.61	0.53	-0.24	-0.18	0.92 *	-0.2	-0.7 *	-0.27
Sfxn3	-0.16	-0.2	-0.12	-0.06	0	-0.32 *	-0.2	-0.24	-0.02
Slc2a6	-0.02	0.07	0.07	-0.06	-0.13	-0.23 *	0.13	0.03	-0.06
Slc45a4	0.2	0.06	-0.17	-0.16	-0.16	-0.32 *	-0.18	-0.29 *	-0.19
Snrpd1	0.1	0.21	0.09	0.17	0.24	0.34 *	0.16	-0.25	0.28
Snx3	0.1	0.1	0.13	0.03	0.05	0.27 *	0.04	0.04	-0.08
Tcf7l2	0.14	0.09	0.16	0.13	0.18	0.3 *	0.08	0.12	-0.07
Terf1	0.22	0.1	0.12	0.23	0.25	0.54 *	0.23	0.18	0.21
Tlcd1	0.15	0.07	0.12	0.27	0.25	0.28 *	-0.12	-0.22	-0.22
Tnnc1	0.08	-0.03	0.03	-0.08	-0.12	0.39 *	-0.07	-0.14	-0.07
Tpst2	0.02	0.12	0.02	-0.15	-0.11	-0.39 *	-0.18	-0.19	-0.15
Trhr	-0.04	-0.02	0.01	0	-0.04	-0.18 *	-0.06	0.01	-0.02
Tspan15	0.01	0.13	0.13	0.27	0.16	0.5 *	-0.01	0.31	0
Wfdc5	0.06	0.19	0.01	-0.23	-0.01	-0.41 *	-0.2	-0.41 *	-0.2
Xrcc2	0.1	0.2	0.11	0.05	0.01	0.37 *	0.06	-0.05	0.16
Zbtb20	-0.2	-0.23	0	0.03	0.02	-0.35 *	0.19	0.49 *	-0.03
Zfp422	0.05	0.02	0.04	0.12	0.04	0.26 *	0.1	0.21	0.07

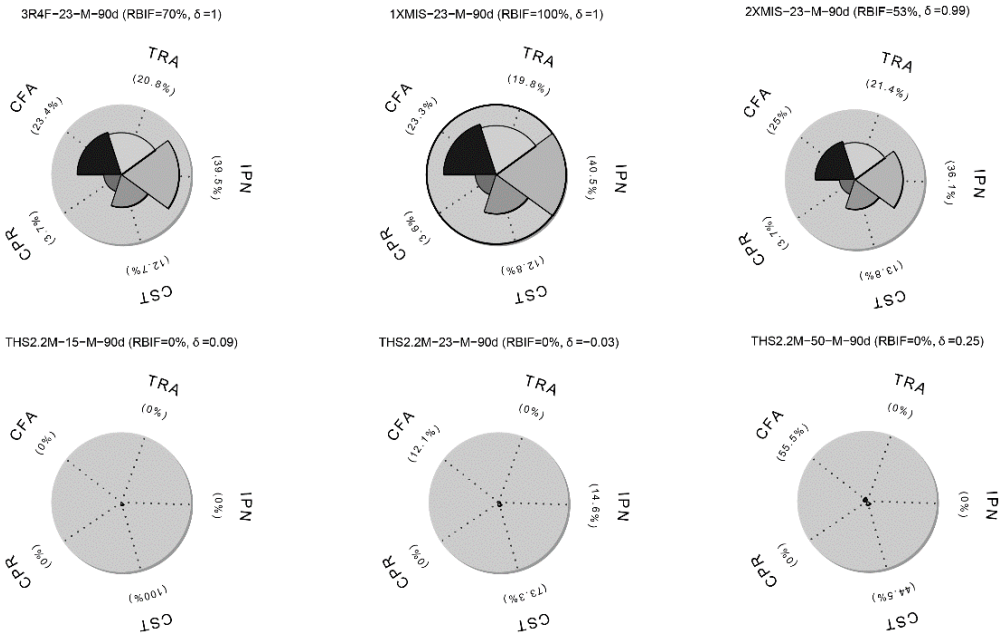
These DEGs were found only in the nasal tissue of female rats after THS2.2M exposure. * FDR < 0.05. Statistically significant differential expression is indicated with an asterisk (*) (BH-adjusted *p*-value < 0.05).

9.2.2 Biological Network Perturbation Amplitude Analysis in Nasal Epithelium Tissue after 90 Days of Exposure to Reference Cigarettes and THS2.2M, or after a 42-day Recovery Period

We calculated the perturbation of computational networks to get an overview of the biological networks impacted by the different exposures. We investigated the processes of cell fate (CFA), tissue repair and angiogenesis (TRA), inflammatory process network (IPN), cell stress (CST), and cellular proliferation (CPR).

The star plots in Figure 6 display the biological processes that contributed to network perturbation.

A)



(Figure continues)

B)

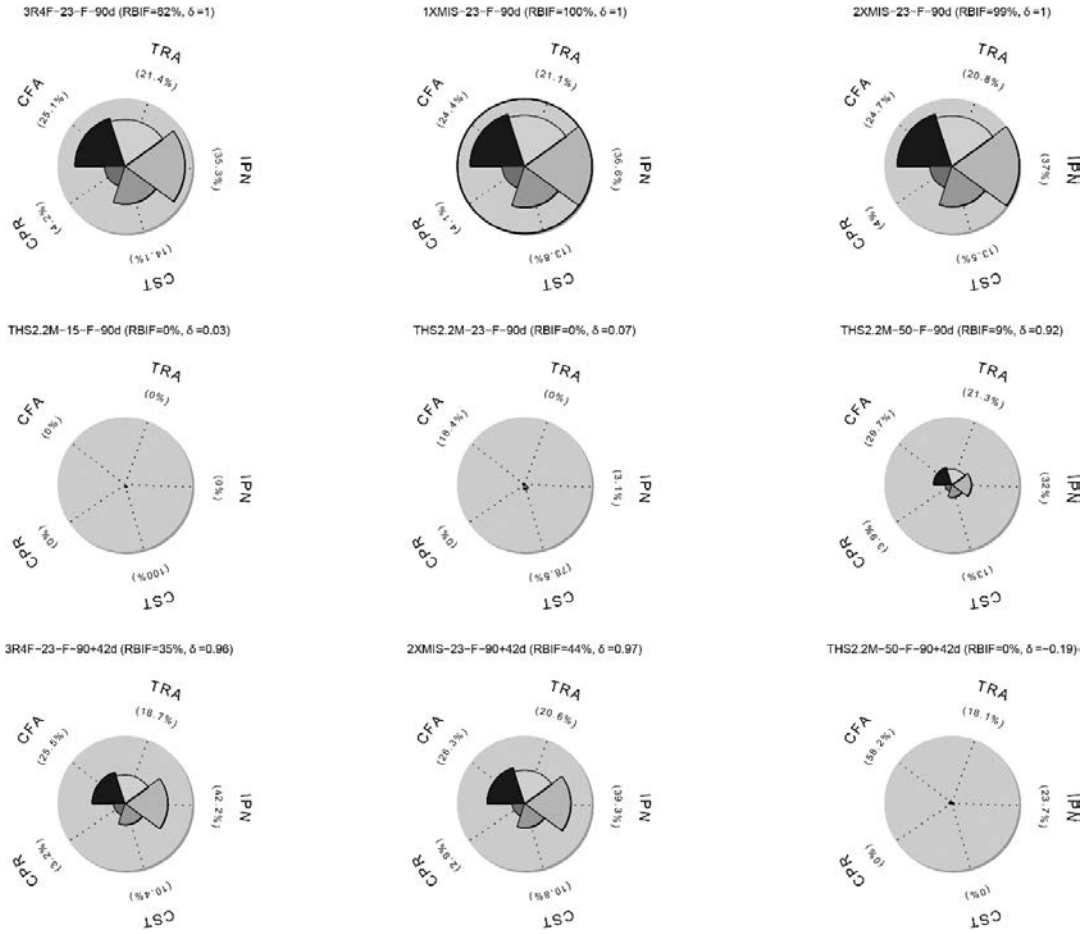


Figure 6: Biological impact calculated from respiratory nasal epithelium tissue.

Star plots illustrating five mechanistic components for each exposure group. The surface area of each slice is proportional to the contribution within a particular treatment of each network perturbation (labeled as %), and is adjusted by the overall relative BIF for the treatment compared with the reference, such that the sum of the slice areas for each treatment equals the RBIF for the treatment. The pie chart represents the distribution of the sum of contributions for each network across all treatment groups. A) Male rats, B) female rats. CFA, cell fate; TRA, tissue repair and angiogenesis; IPN, inflammatory process network; CST, cell stress; CPR, cell proliferation.

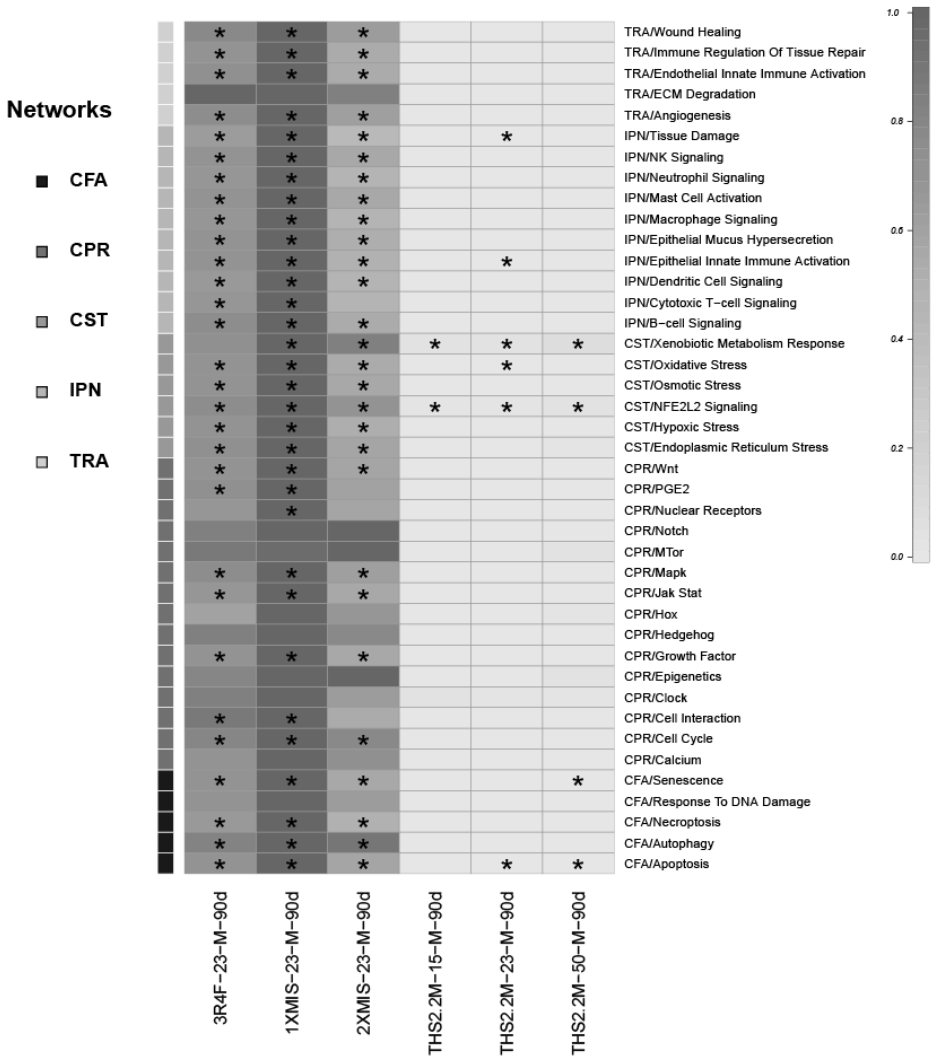
In the respiratory epithelium of male rats, all tested network categories appeared to be impacted after exposure of 90 days to the reference cigarettes 3R4F, DDA3 1xMIS, and DDA3 2xMIS (all with 23 µg/L nicotine). The inflammatory process network contributed the most perturbation. Very minor network perturbation was found after exposure to THS2.2M with all three concentrations (Figure 6 A).

In the respiratory epithelium of female rats after 90 days of exposure to the reference cigarettes, the inflammatory process network was the most impacted process, but all other tested networks were also perturbed. The low THS2.2M concentration (15 µg/L nicotine) and the medium/equal to the reference cigarettes concentration (23 µg/L) did not show any perturbed networks. The high THS2.2M concentration (50 µg/L) showed detectable network perturbation, with a highly similar pattern, also emphasizing the inflammatory process network. The perturbation amplitude was much lower than we found after exposure to the reference cigarettes.

Of note, 42 days of recovery were enough to re-establish pre-exposure conditions only in THS2.2M rats at the highest nicotine concentration. In fact, the two groups exposed to reference cigarettes 3R4F and DDA3 2xMIS (all with 23 µg/L nicotine) after 42 days of recovery showed a reduction in the perturbation amplitude but without reaching the initial conditions.

The biological processes depicted in the star plots can be separated into different biological sub-processes to obtain a higher level of mechanistic insight. A detailed view of these sub-networks within each of the mechanistic components that displayed a significant perturbation in at least one of the exposure groups is presented in Figure 7.

A)



(Figure continues)

B)

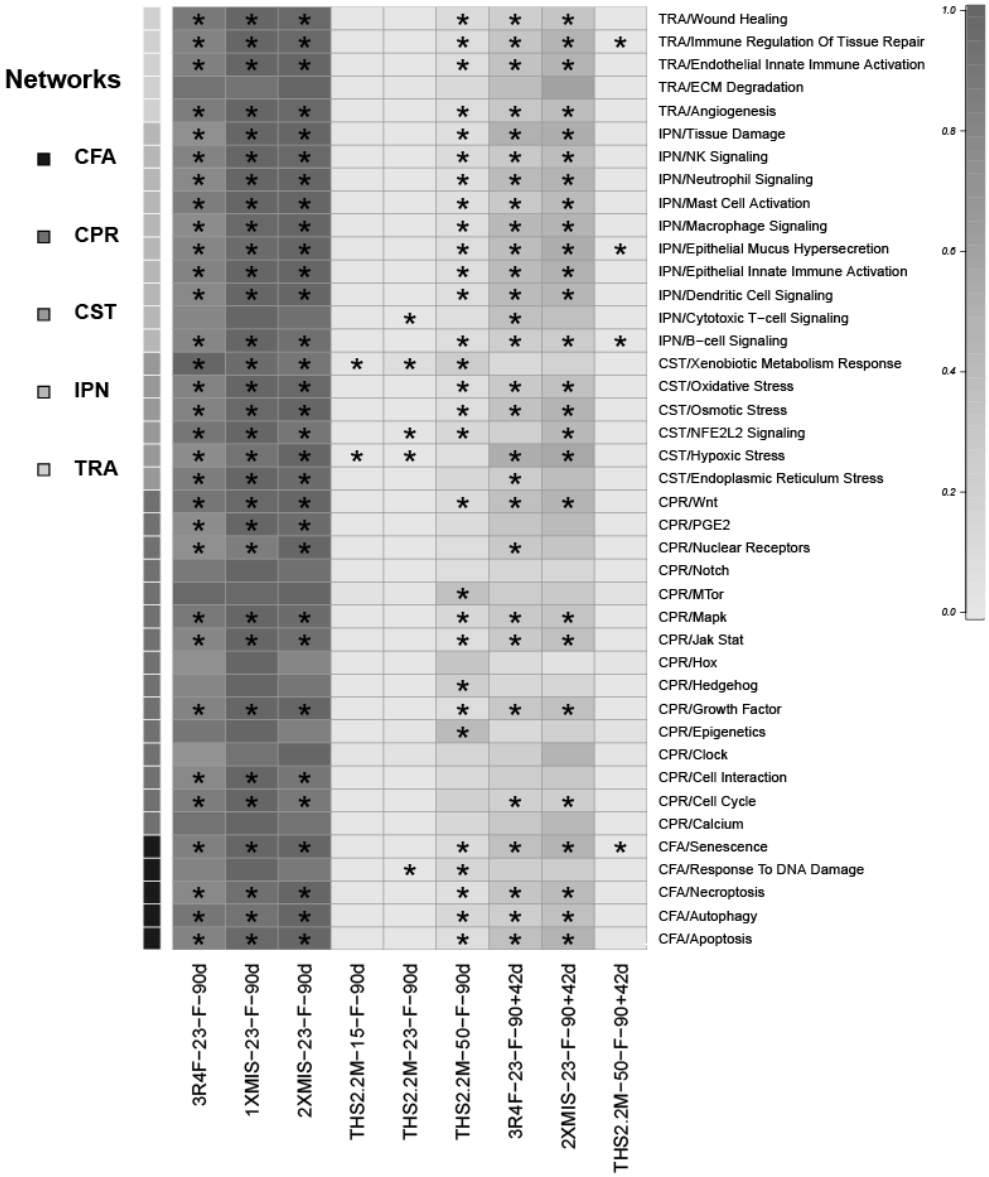


Figure 7: Heat map of network perturbation in nasal respiratory epithelium.

Heat map summarizing the sub-networks are shown. A network is considered perturbed if, in addition to the statistical significance of the NPA score with respect to the experimental variation, the two companion statistics (O and K), derived to inform on the specificity of the NPA score with respect to the biology described in the network, are significant. A) Male rats, B) female rats. * denotes O and K statistic p-values below 0.05 and statistical significance with respect to the experimental variation.

All sub-networks impacted by THS2.2M were also impacted by reference cigarette exposure in the respiratory nasal epithelium of male rats. For all tested THS2.2M concentrations, the xenobiotic metabolism responses and NFE2L2 signaling networks were pertubed.

In the respiratory epithelium of female rats, the response pathways to DNA damage, epigenetic changes, mTOR, cytotoxic T−cell signaling, and hedgehog signaling were only significantly perturbed after THS2.2M exposure, and not after reference cigarette exposure.

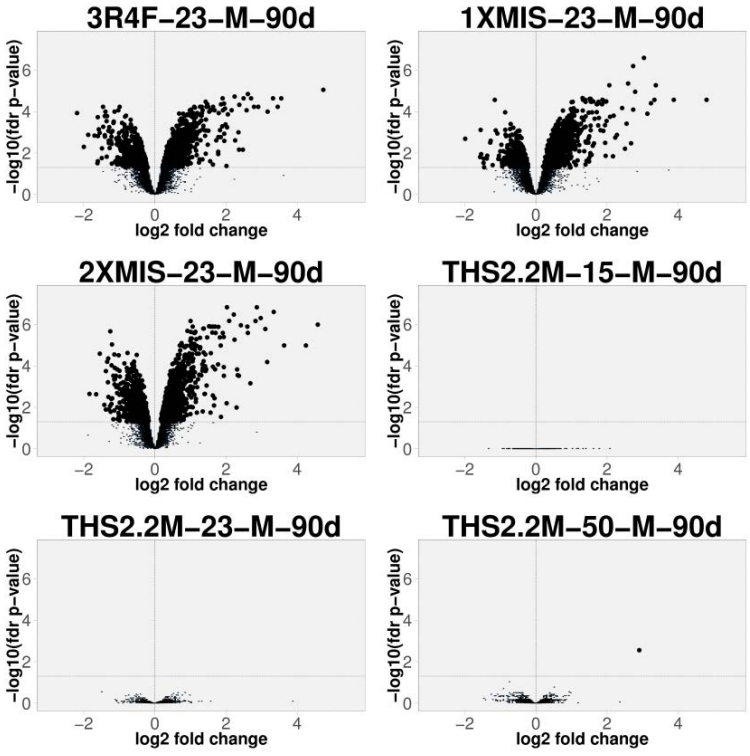
In general, only a few sub-networks were impacted after exposure to the low or medium dose of THS2.2M, in comparison with the perturbations caused by the reference cigarettes. The observed sub-networks which were perturbed after exposure to the high dose of THS2.2M were similar to those that were perturbed after exposure to the reference cigarettes, but the amplitude was much lower.

9.3 Lung Transcriptome after 90 Days of Exposure and after a 42-day Recovery Period in Male and Female rats

9.3.1 Differentially Expressed Genes in Lung Tissue after 90 Days of Exposure to 3R4F or THS2.2M, or after a 42-day Recovery Period

The amplitude (expressed as log fold change, x-axis) and statistical significance (expressed as –log of the FDR *p*-value) of gene expression changes in lung tissue for 3R4F-, DDA3 1xMIS-, DDA3 2xMIS-, and THS2.2M-exposed rats after 90 days of exposure or after a 42-day recovery period (females only) were compared with the sham group and graphed as volcano plots (Figure 8).

A)



(Figure continues)

B)

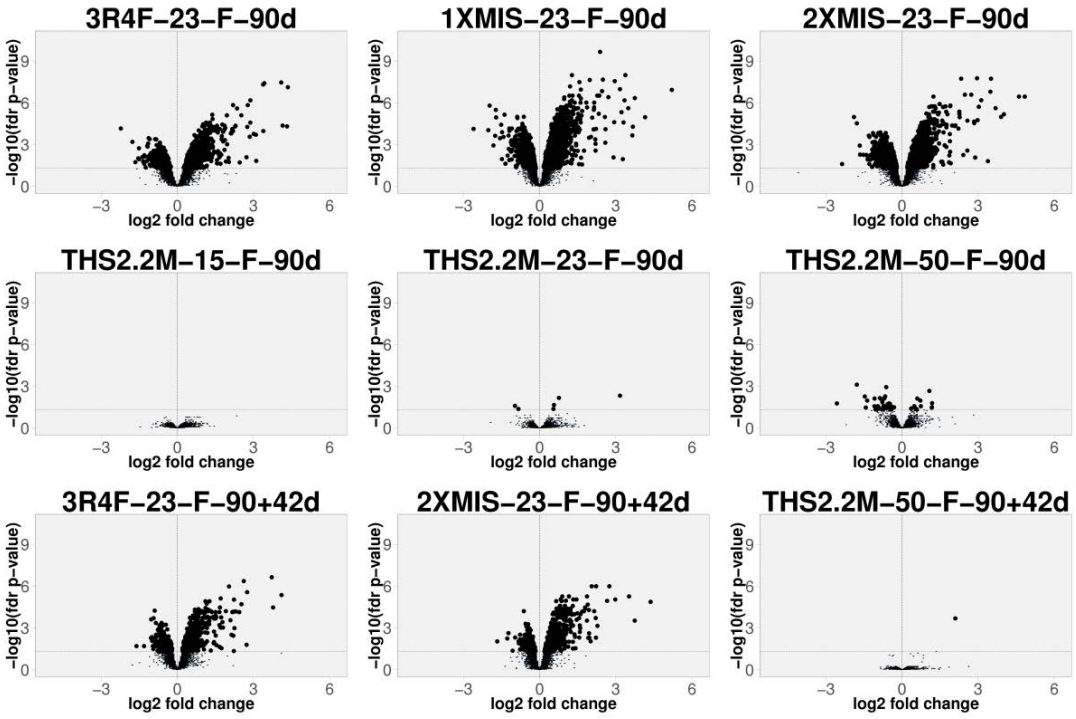


Figure 8: Volcano plots representing the systems response profiles in lung tissue.

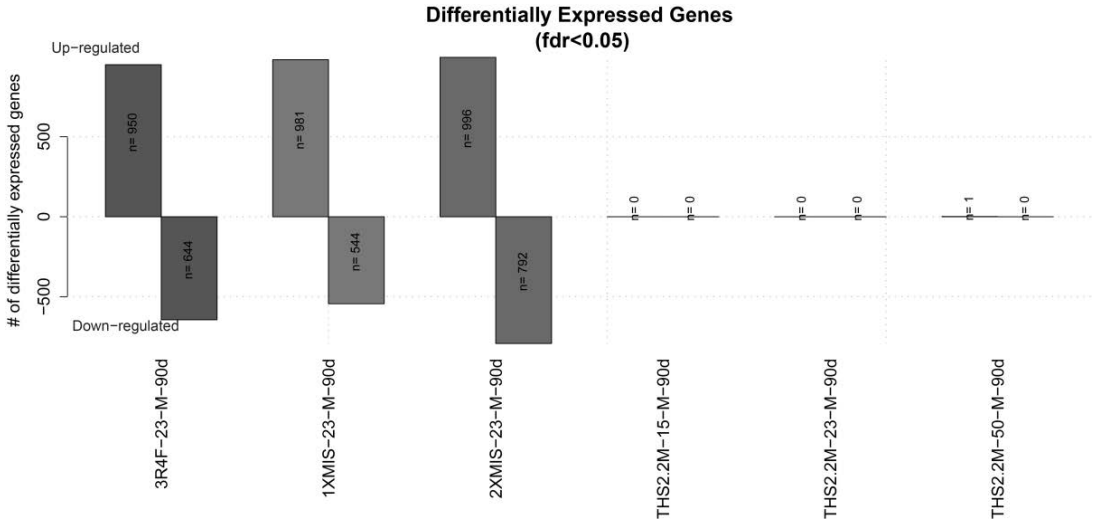
For each gene, the change in gene expression, calculated as the log2 fold change, is plotted on the x-axis; statistical significance, proportional to the negative log10-FDR *p*-value, is plotted on the y-axis. Dark black dots highlight genes that are statistically significantly up- and down-regulated (right and left quadrants, respectively) compared with the sham at the same time point. A) Male rats, B) female rats.

Between 1,525 and 1,788 genes were differentially expressed in the lung tissue after exposing male rats for 90 days to the reference cigarettes 3R4F, DDA3 1xMIS, and DDA3 2xMIS (Figure 9). In contrast, only one gene was differentially expressed with the high THS2.2M concentration, and no differentially expressed genes were found after THS2.2M exposure with the low and the medium dose.

Between 1,245 and 2,865 genes were differentially expressed in the lung tissue after exposing female rats for 90 days to the reference cigarettes 3R4F, DDA3 1xMIS, and DDA3 2xMIS (Figure 9). In contrast, only six genes were differentially expressed when the rats were exposed to the medium dose of THS2.2M (the same concentration as reference

cigarettes, 23 µg/L nicotine). 45 genes were differentially expressed after a 90-day exposure to the high concentration of THS2.2M. Of note, 42 days of recovery were enough to reduce to only one the number of differentially expressed genes in THS2.2M. Contrarily, in the reference groups, although reduced, a consistent number of genes were still significantly up- or down-regulated.

A)



B)

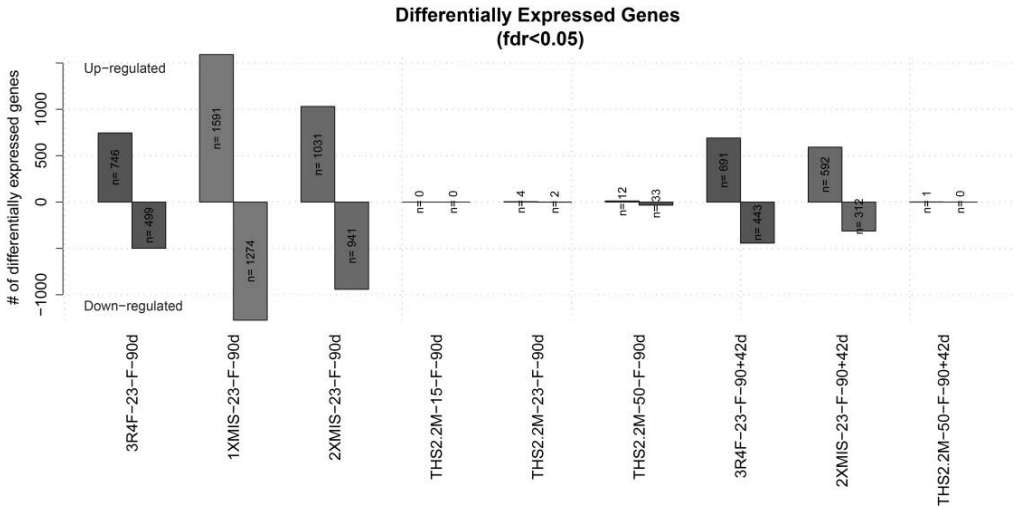
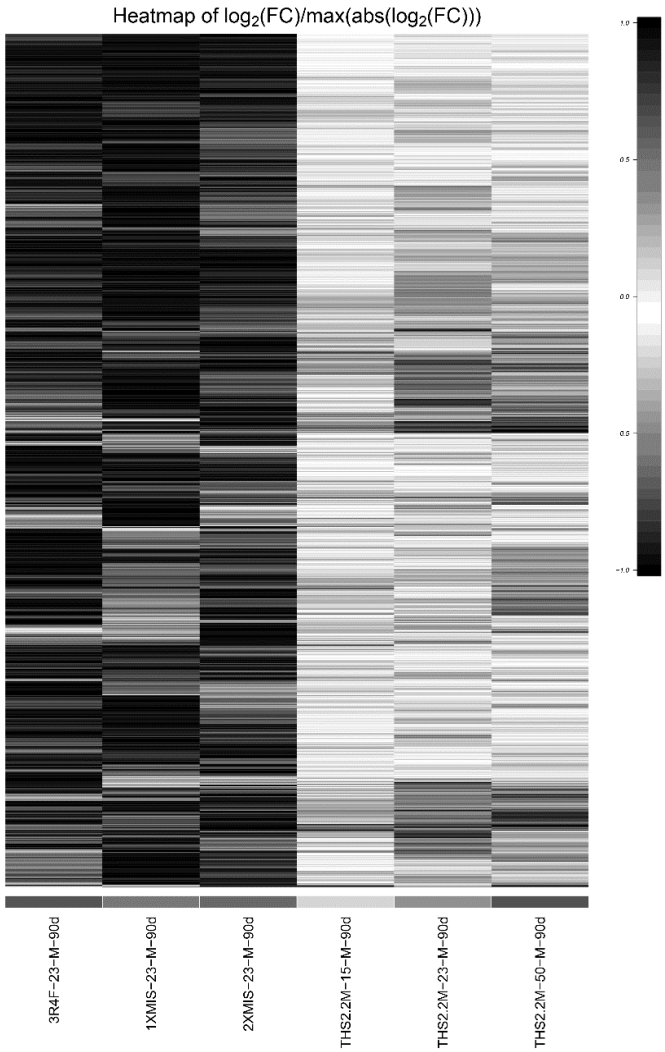


Figure 9: Number of significant differentially expressed genes in lung tissue.

Bar plots depicting differentially expressed genes with FDR < 0.05. A) Male rats, B) female rats.

We generated a heat map (Figure 10) to obtain an overview of the differential gene expression trends over the various exposure groups, and to graph the overlap of differentially expressed genes.

A)



(Figure continues)

B)

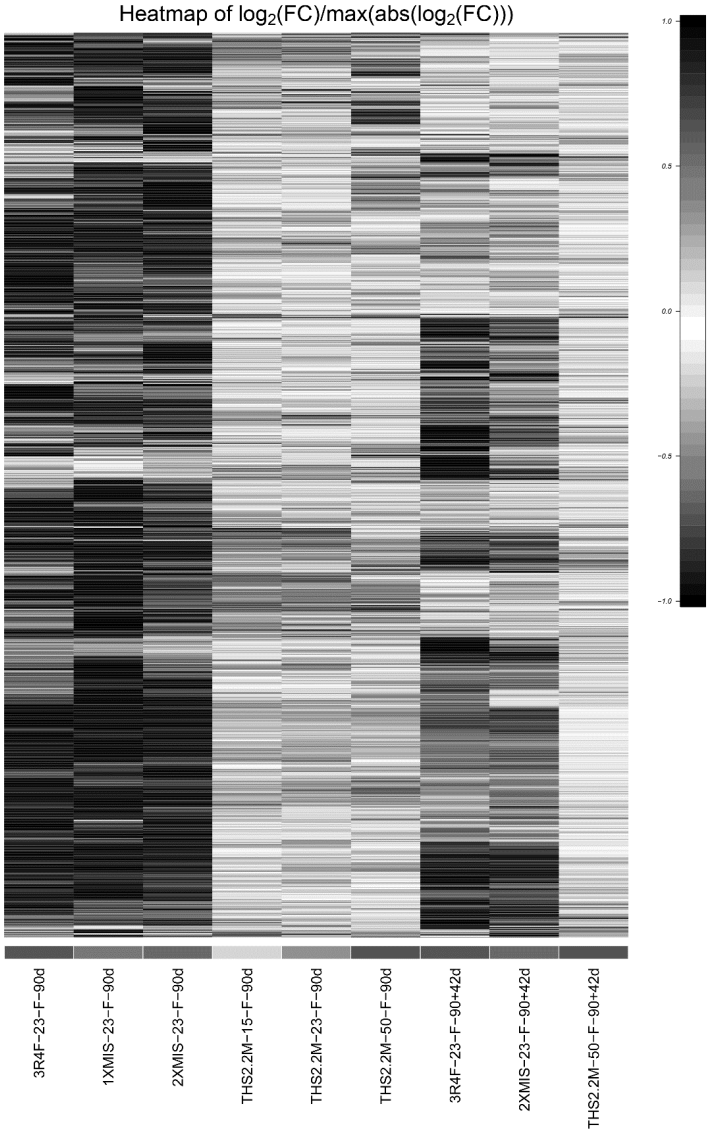


Figure 10: Heat map of gene expression in lung tissue.

Heat map representing the log2(fold-change)/max(abs(log2(fold-change))) for all genes which induced a significant change in expression, at least comparatively. The grayscale is based on the absolute values (range from -1 to 1). A) Male rats 90 days of exposure, B) female rats 90+42 days of exposure.

The heat map showed that the overall fold changes of the differentially expressed genes were relatively lower in the THS2.2M exposed groups, compared with the fold changes in the reference cigarette exposed groups.

The differentially expressed genes in the lung tissue from male rats exposed to the highest concentration of THS2.2M was also differentially expressed after exposure to at least one of the reference cigarettes.

In the lung tissue from female rats exposed to the highest concentration of THS2.2M, of the 45 differentially expressed genes, 42 were also differentially expressed by at least one of the reference cigarettes groups (i.e., DEGs vs. overlapping DEGs) (Table 10).

Table 10: Unique expressed genes after THS2.2M treatment found in the lung tissue.

	Differently Expressed Genes in Female Rats Uniquely Significant for THS2.2M Group								
GENE ID	3R4F-23-F 90d	1XMIS-23-F 90d	2XMIS-23-F 90d	THS2.2M-15-F 90d	THS2.2M-23 F-90d	THS2.2M-50 F-90d	3R4F-23-F 90+42d	2XMIS-23-F 90+42d	THS2.2M-50 F-90+42d
RGD1566401	-0.16	-0.04	-0.17	0.48	0.62	0.58 *	-0.53 *	-0.47 *	-0.38
Slfn2	0.05	-0.23	-0.18	0.09	-0.14	-0.45 *	0.12	0.18	-0.04
Usp18	-0.43	-0.43	-0.22	0.45	-0.20	-1.09 *	0.24	0.43	0.02

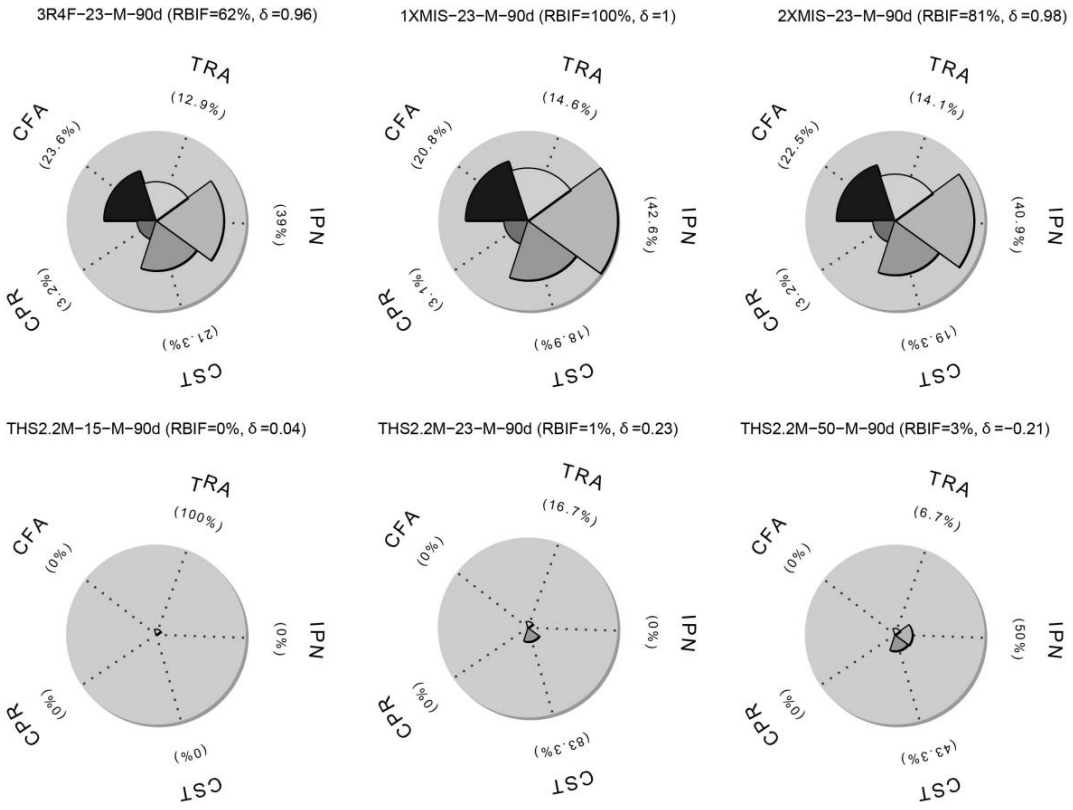
Table for female genes; * FDR < 0.05. Statistically significant differential expression is indicated with an asterisk (*) (BH-adjusted *p*-value < 0.05).

9.3.2 Biological Network Perturbation Amplitude Analysis in Lung Tissue after 90 Days of Exposure to Reference Cigarettes and THS2.2M, or after a 42-day Recovery Period

We calculated the perturbation of computational networks to get an overview of the biological networks that were impacted by the different exposures. The processes that were investigated were cell fate (CFA), tissue repair and angiogenesis (TRA), inflammatory process network (IPN), cell stress (CST), and cellular proliferation (CPR).

The star plots in Figure 11 depict the biological processes that contributed to network perturbation.

A)



(Figure continues)

B)

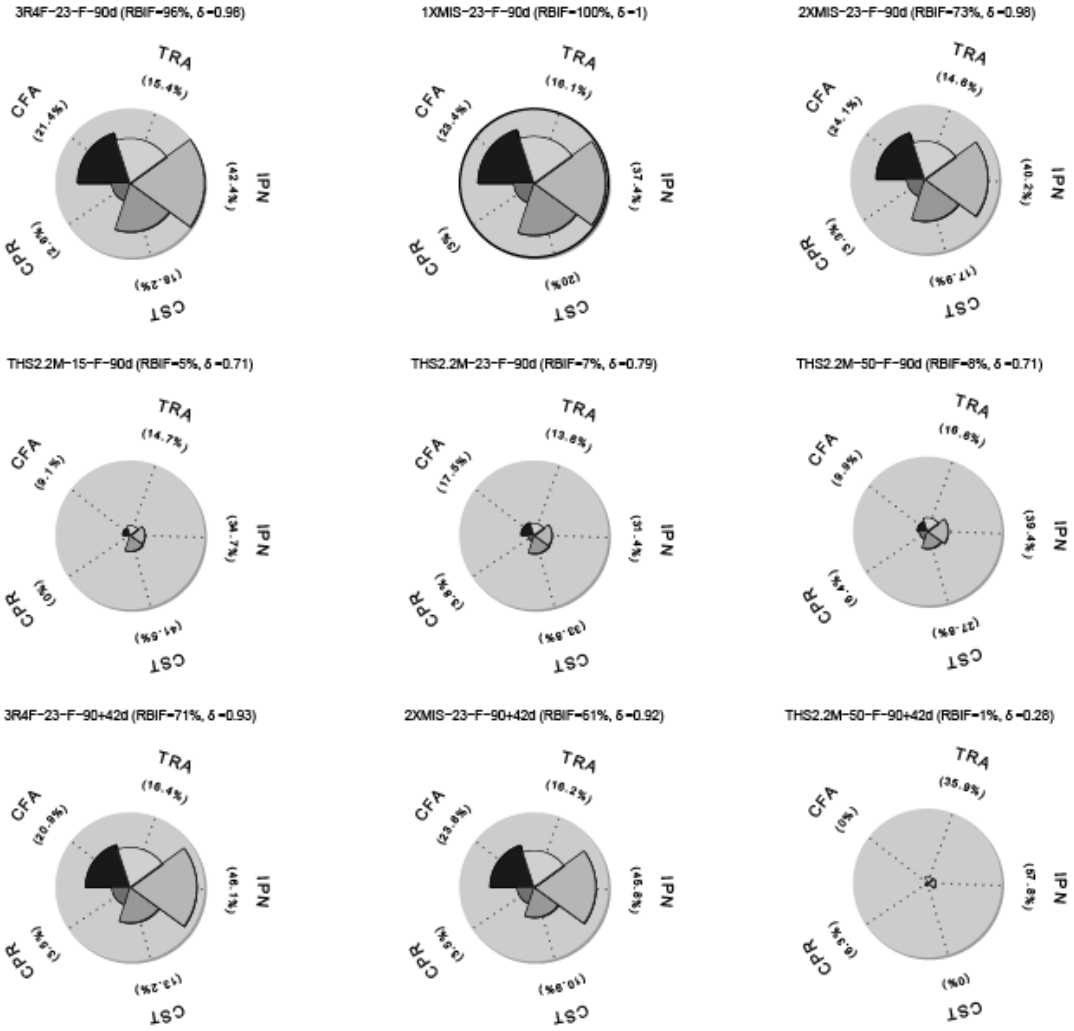


Figure 11: Biological impact calculated from lung tissue.

Star plots illustrating five mechanistic components for each exposure group. The surface area of each slice is proportional to the contribution within a particular treatment of each network perturbation (labeled as %), and is adjusted by the overall relative BIF for the treatment compared with the reference, such that the sum of the slice areas for each treatment equals the RBIF for the treatment. The pie chart represents the distribution of the sum of contributions for each network across all treatment groups. A) Male rats, B) female rats.

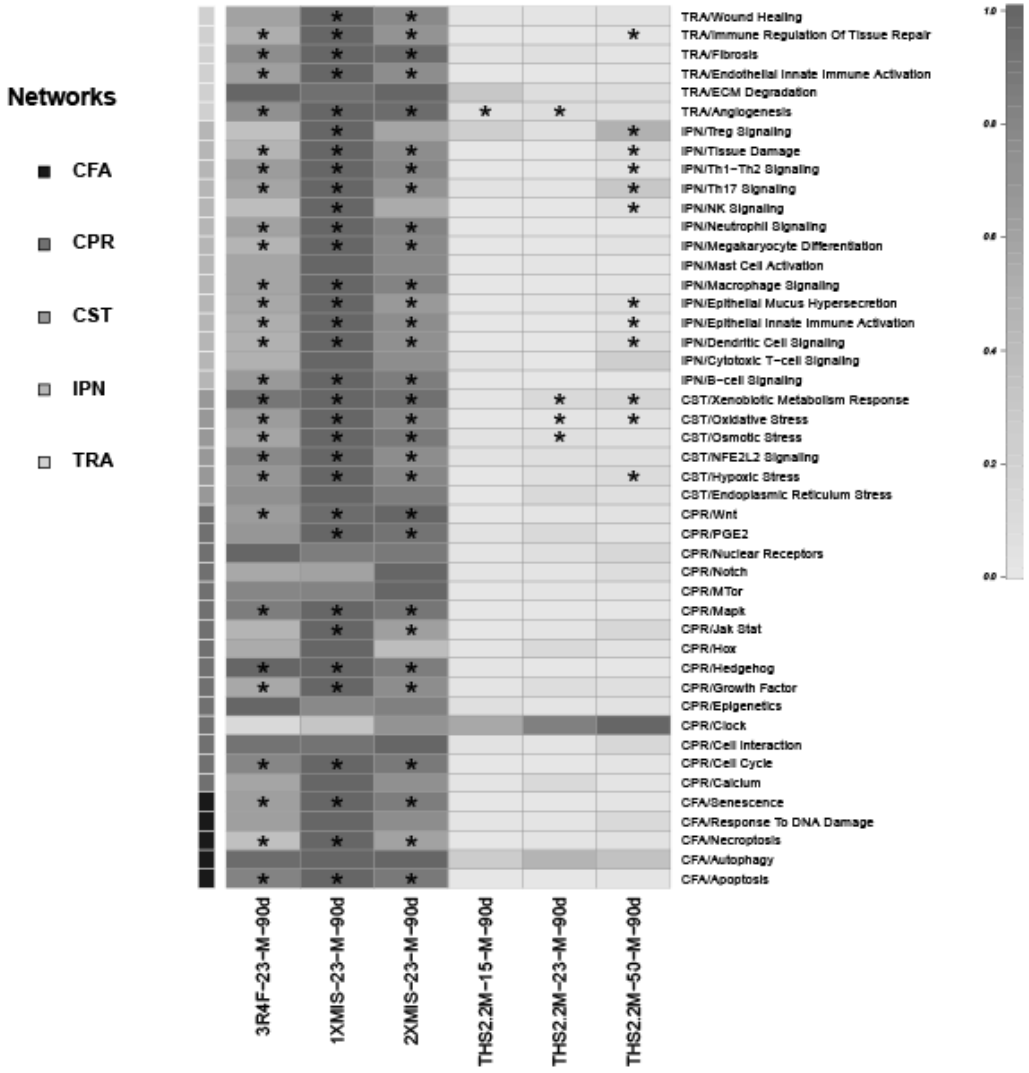
In the lung tissue of male rats, all tested networks appeared to be impacted after exposure of 90 days to the reference cigarettes 3R4F, DDA3 1xMIS, and DDA3 2xMIS (all with 23 µg/L nicotine). The inflammatory process network contributed to the perturbation more than other networks. After 90 days of exposure to the low THS2.2M concentration (15 µg/L nicotine), no network perturbation was evident in the lung tissue. After 90 days of exposure to the medium concentration of THS2.2M (23 µg/L nicotine), we found perturbation of the cell stress network. After 90 days of exposure to the high concentration of THS2.2M (50 µg/L nicotine), a perturbation of the cell stress network was accompanied by a perturbation of the inflammatory process network. The amplitudes of perturbation were much lower when compared with those found after exposure to the reference cigarettes.

In the lung tissue of female rats, the inflammatory process network was the most impacted after 90 days of exposure to the reference cigarettes, but all other tested networks appeared perturbed as well. Exposure to THS2.2M showed perturbation of the cell stress and the inflammatory process networks, and to a minor extent, perturbation of cell fate, tissue repair and angiogenesis, and cellular proliferation. The amplitudes of the perturbation after THS2.2M exposure were lower than those seen after reference cigarette exposure.

Of note, 42 days of recovery were enough to re-establish pre-exposure conditions only in THS2.2M rats exposed to the highest nicotine concentration. The two groups exposed to reference cigarettes 3R4F and DDA3 2xMIS (all with 23 µg/L nicotine) showed a small reduction in the perturbation amplitude.

The biological processes modulated above can be separated into different biological sub-process groups to obtain a higher level of mechanistic insight. Figure 12 presents a detailed view of the sub-networks within each mechanistic component that displayed a significant perturbation in at least one of the exposure groups.

A)



(Figure continues)

B)

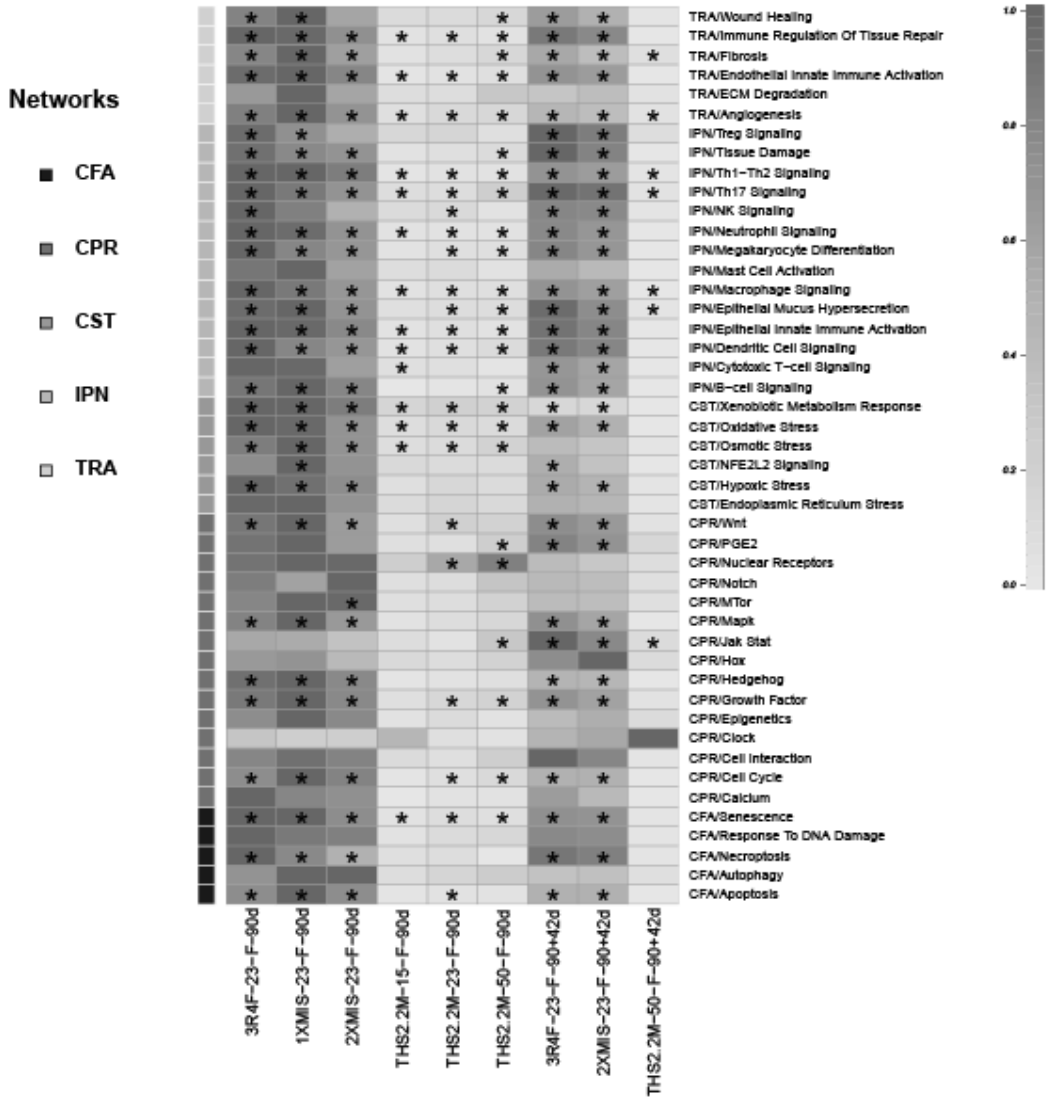


Figure 12: Heat map of network perturbation in lung tissue.

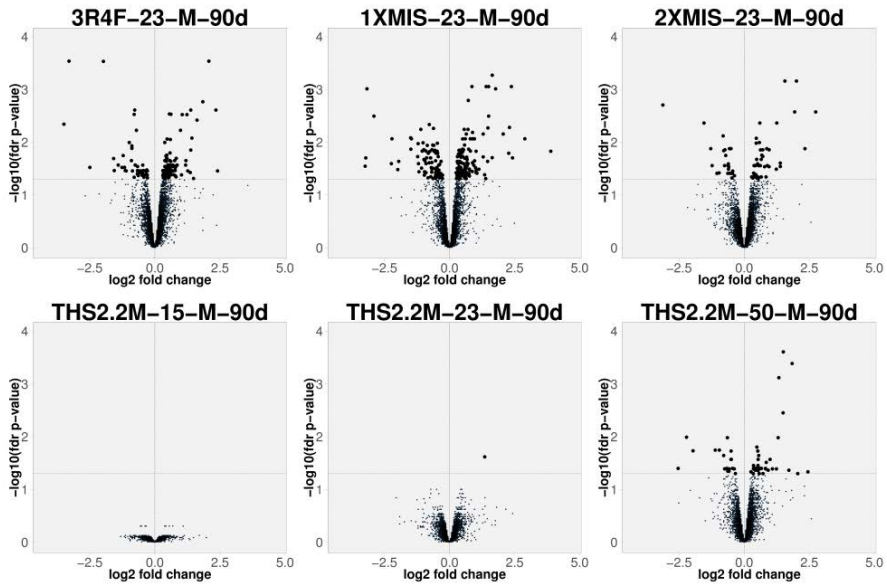
Heat map summarizing the sub-networks are shown. A network is considered perturbed if, in addition to the statistical significance of the NPA score with respect to the experimental variation, the two companion statistics (O and K), derived to inform on the specificity of the NPA score with respect to the biology described in the network, are significant. * denotes O and K statistic *p*-values below 0.05 and statistical significance with respect to the experimental variation. A) Male rats, B) female rats

9.4 Liver Transcriptome after 90 Days of Exposure and after a 42-day Recovery Period in Male and Female rats

9.4.1 Differentially Expressed Genes in Liver Tissue after 90 Days of Exposure to 3R4F or THS2.2, or after a 42-day Recovery Period

The amplitude (expressed as log fold change, x-axis) and statistical significance (expressed as –log of the FDR *p*-value) of gene expression changes in liver tissue for 3R4F-, DDA3 1xMIS-, DDA3 2xMIS-, and THS2.2M-exposed rats after 90 days of exposure or after a 42-day recovery period (females only) were compared with the sham group and graphed as volcano plots (Figure 13).

A)



(Figure continues)

B)

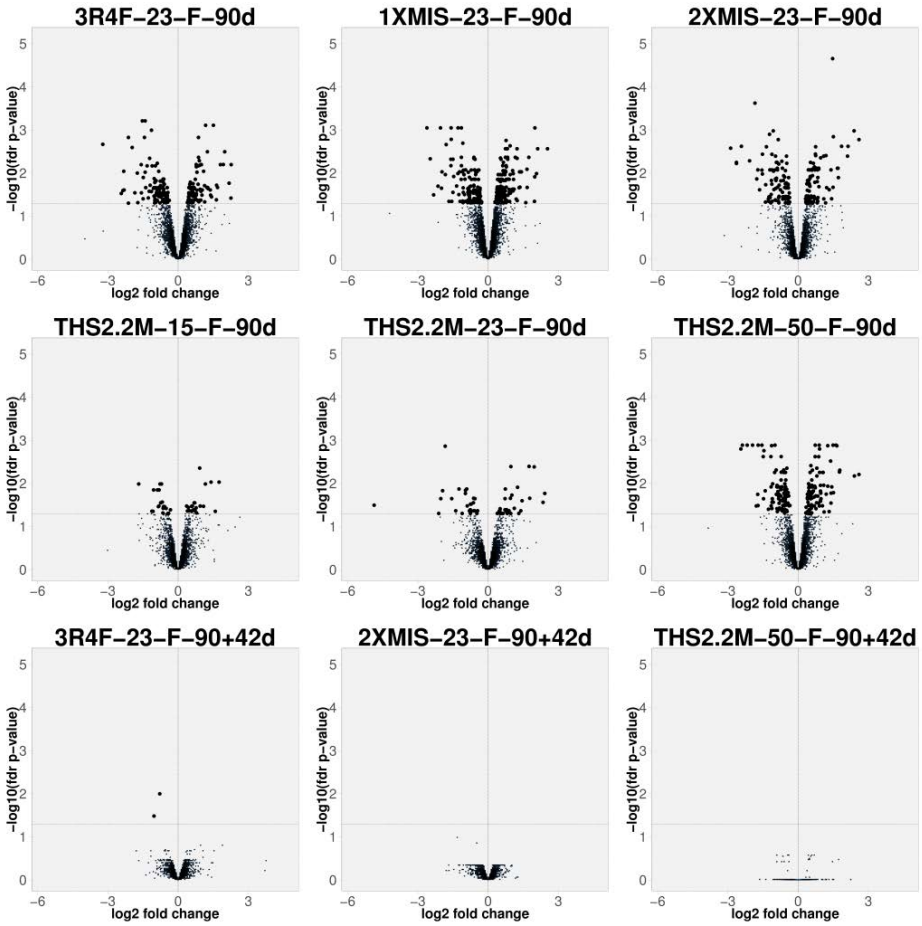


Figure 13: Volcano plots representing the systems response profiles in liver tissue.

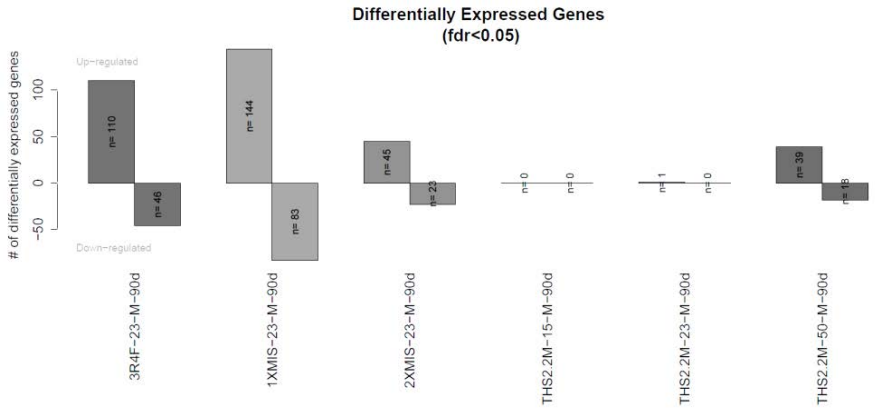
For each gene, the change in gene expression, calculated as the log2 fold change, is plotted on the x-axis; statistical significance, proportional to the negative log10-FDR *p*-value, is plotted on the y-axis. Dark black dots highlight genes that are statistically significantly up- and down-regulated (right and left quadrants, respectively) compared with the sham at the same time point. A) Male rats, B) female rats.

In the liver of 3R4F-, DDA3 1xMIS-, and DDA3 2xMIS-exposed male rats after 90 days of exposure, between 68 (DDA3 2xMIS) and 227 (DDA3 1xMIS) genes were differentially expressed. After exposure to THS2.2M at same time point (90 days) in male rats, only the high dose of nicotine (50 µg/L) seemed to affect gene expression, with 57 genes differentially expressed (Figure 14). Moreover, the lower (15 µg/L) concentration did not

affect gene expression at all, while the medium (23 µg/L) concentration determined the up-regulation of only one gene in the liver.

The liver of 3R4F-, DDA3 1xMIS-, and DDA3 2xMIS-exposed female rats after 90 days of exposure showed the regulation of between 185 and 287 genes (Figure 14). THS2.2M at the lower (15 µg/L) and medium (23 µg/L) nicotine concentrations' exposure determined a reduction in the number of differentially expressed genes (43 and 60, respectively). However, the higher concentration of nicotine (50 µg/L) determined the significant up- and down-regulation of a total of 195 genes. After 42 days of recovery, almost all genes resumed their regular expression rate in the three experimental groups (3R4F, DDA3 2xMIS, and THS2.2M High). Only two genes were still differentially expressed in the 3R4F group.

A)



(Figure continues)

B)

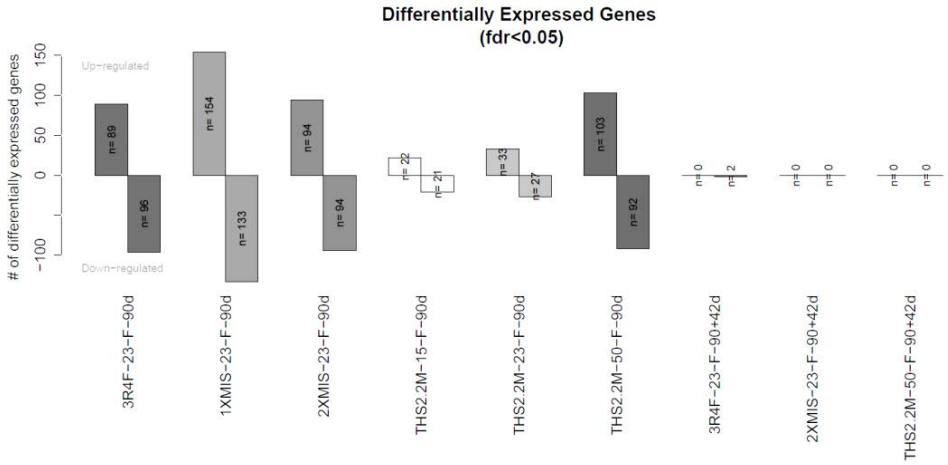
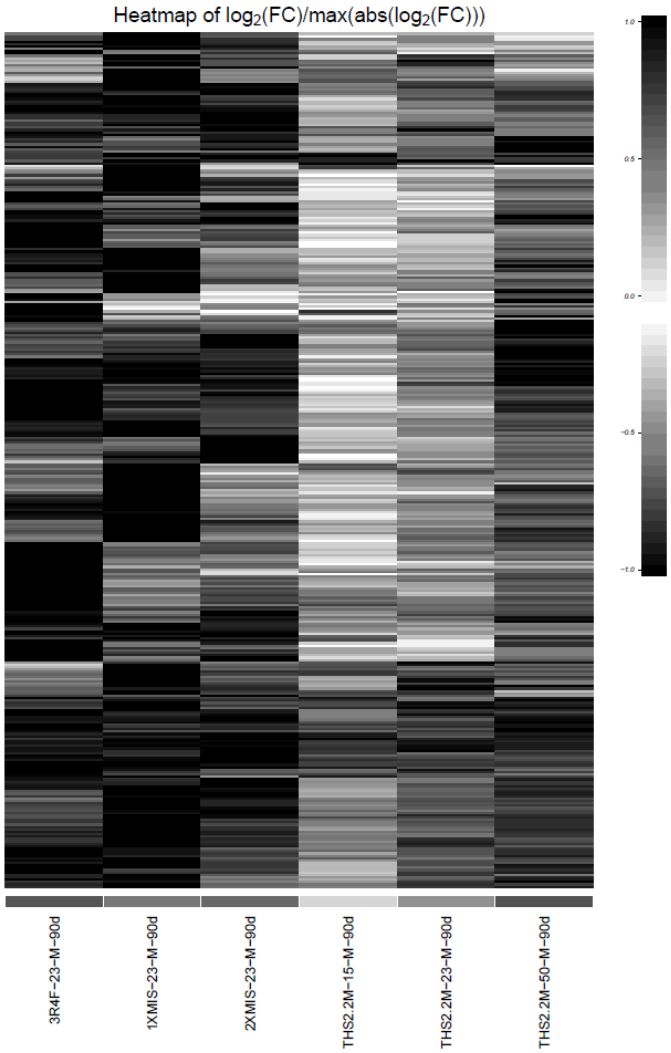


Figure 14: Number of significant differentially expressed genes in liver tissue.
Bar plots depicting differentially expressed genes with FDR < 0.05. A) Male rats, B) female rats.

We generated a heat map to obtain an overview of the distribution of differential gene expression over the various exposure groups, and to graph the overlap of differentially expressed genes.

A)



(Figure continues)

B)

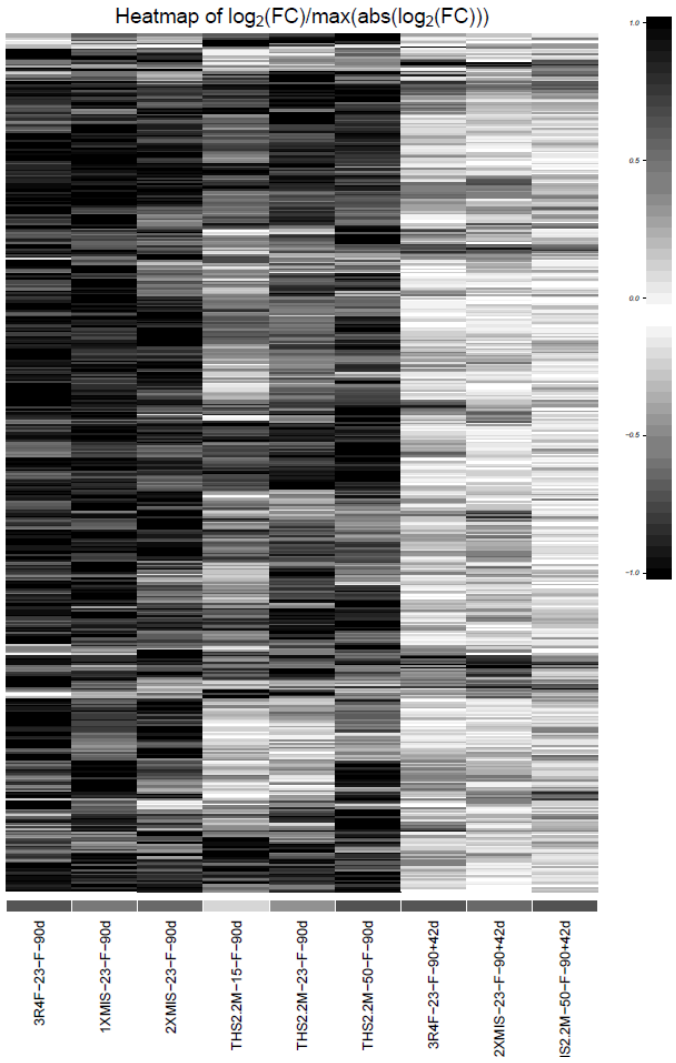


Figure 15: Heat map of gene expression in liver tissue.

Heat map representing the log2(fold-change)/max(abs(log2(fold-change))) for all genes which induced a significant change in expression, at least comparatively. The grayscale is based on the absolute values (range from -1 to 1). A) Male rats 90 days of exposure, B) female rats 90+42 days of exposure.

The heat map showed that, overall, the fold changes of gene expression were reduced upon THS2.2M treatment, at the matching (23 µg/L) and the lower (15 µg/L) concentration,

compared with the reference exposures. This trend was present in both male and female rats with a clear dose-dependency. In fact, the differentially expressed genes in the liver tissue from male and female rats exposed to the highest concentration of nicotine in THS2.2M increased in term of number and expression level. Of note, 42 days of recovery in female rats were enough to reduce both the number (Figure 14) and the fold change (Figure 15) of differentially expressed genes in the liver. Table 11 lists the genes that were significantly expressed only after THS2.2M treatment in male (A) and female (B).

Table 11: Unique expressed genes found in the liver tissue after THS2.2M treatment.

A)

	Differentially Expressed Genes in Male Rats Uniquely Significant for THS2.2M Group					
GENE ID	3R4F-23 90d	1XMIS-23 90d	2XMIS-23 90d	THS2.2M-15 90d	THS2.2M-23 90d	THS2.2M-50 90d
Synj2	0.3	0.45	0.32	0.27	0.22	0.56 *
Abcg8	-0.2	-0.11	-0.07	-0.16	-0.15	-0.5 *
Atp5o	0.22	0.19	0.19	0.13	0.13	0.26 *
Tubg1	0.26	0.23	0.35	0.03	0.19	0.36 *
Ms4a7	-0.43	-0.28	-0.33	-0.22	-0.38	-0.57 *
Mbnl3	-0.53	-0.35	-0.6	-0.22	-0.35	-0.67 *
Atp13a5	-0.41	-0.27	-0.4	-0.18	-0.2	-0.44 *
Spc24	0.2	0.63	0.12	0.11	0.17	0.58 *
Apoo	0.45	0.53	0.25	0.19	0.44	0.6 *
Islr	-0.14	-0.34	0.01	0.1	-0.03	-0.34 *
Kank2	0.16	0.37	0.22	0.32	0.51	0.46 *
LOC100363236	-0.48	-0.12	-0.3	-0.06	0.05	-0.51 *
LOC103692119	0.54	0.61	0.66	0.24	0.55	0.85 *

(Table continues)

B)

	Differentially Expressed Genes in Female Rats Uniquely Significant for THS2.2M Group								
GENE ID	3R4F-23 90d	1XMIS-23 90d	2XMIS-23 90d	THS2.2M-15 90d	THS2.2M-23 90d	THS2.2M-50 90d	3R4F-23 90+42d	2XMIS-23 90+42d	THS2.2M-50 90+42d
Junb	-0.21	-0.35	-0.44	0.13	-0.32	-0.86 *	0.33	0.38	0.65
Me1	0.06	0.18	0.21	1.09 *	1.09	0.86	-0.34	-0.07	-0.1
Acsm3	-0.91	-0.67	-0.62	-1.05 *	-0.97	-0.75	0.11	-0.13	-0.42
Ccl2	-0.52	-0.24	-0.44	-0.26	-0.33	-0.61 *	-0.19	-0.14	-0.02
Ptger3	0.57	0.41	0.75	0.79 *	0.37	0.85	0.21	0.17	0.07
Cyp51	0.44	0.36	0.44	0.33	0.52	0.54 *	0.17	0.04	0.09
Tmod1	-0.03	0.28	0.07	0.41	0.4	0.42 *	-0.08	-0.09	-0.1
Fabp2	0.92	0.98	0.68	0.51	0.78	0.96 *	-0.47	-0.67	-0.02
Apoa2	-0.32	-0.48	-0.4	-0.28	-0.2	-0.38 *	-0.14	-0.06	-0.05
Stmn3	0.34	0.39	0.15	0.56 *	0.93	0.75	0.19	0.29	0.11
Slc6a6	0.99	1.11	1.16	-0.07	0.3	1.41 *	0.97	0.14	-0.02
Ptgfrn	0.41	0.43	0.47	0.28	0.44	0.4 *	0.12	0.19	0.12
Tgm1	0.75	0.78	0.77	0.56	0.89 *	0.22	0.02	0.07	-0.12
Cd14	-0.56	-0.43	-0.38	-0.82 *	-0.89	-0.71 *	0.05	-0.23	-0.32
Prom1	-1.01	-1.01	-1.24	-0.76	-1.11 *	-0.84	-0.59	-1.07	-0.31
Ddah1	0.63	0.51	0.49	0.34	0.46	0.73 *	0.18	0.12	0.18
Pde4dip	0.01	0.31	0.4	0.58 *	0.18	0.54 *	0.02	0.08	0.16
Ascl1	-1.18	-1.22	-2.13	-1.07 *	-1.25	-0.79	-0.52	-0.88	-0.53
Zmat3	0.24	0.32	0.27	0.32	0.39	0.47 *	-0.29	-0.1	-0.04
Aacs	0.89	0.84	0.8	0.79	1.06	1.09 *	0.54	0.2	0.53
Hsd17b2	-0.51	0.18	-0.05	1.59 *	1.17	0.1	-0.1	0.44	0.5
Mvd	0.55	0.51	0.39	0.47 *	0.59	0.63 *	-0.07	-0.05	0.04
Fads2	0.29	0.29	0.11	0.61 *	0.59	0.43	0.52	0.2	0.38
Fads1	0.47	0.41	0.33	0.49	0.48	0.59 *	0.2	0.12	0.21
Cxadr	0.27	0.27	0.24	0.18	0.24	0.5 *	0.14	-0.03	0.09
Kif1c	0.6	0.47	0.41	0.26	0.42	0.56 *	-0.14	-0.21	-0.22
Sc5d	0.23	0.14	0.37	0.36 *	0.18	0.29	0.17	0.05	0.08
Slfn3	-0.61	-1.09	-1.02	0.54	-0.27	-1.4 *	0.57	0.37	0.28
Coro1a	-0.2	-0.39	-0.4	-0.24	-0.13	-0.58 *	0.31	0	0.12
Hdgfrp2	0.42	0.41	0.04	0.38	0.45	0.46 *	-0.24	-0.28	-0.11
Prss8	-0.54	-0.62	-0.68	-0.62	-0.75	-0.89 *	-0.08	-0.44	-0.28
Dnajc21	0.25	0.27	0.22	0.34	0.28	0.48 *	-0.21	-0.09	-0.19
Hspa4	0.34	0.39	0.37	0.36	0.29	0.58 *	-0.23	-0.06	0.01
Sorbs3	-0.23	-0.26	-0.25	-0.15	-0.2	-0.42 *	0.03	-0.03	-0.01
Pgp	0.32	0.35	0.3	0.38	0.51	0.58 *	-0.1	0.02	-0.04
Nuak2	-0.01	-0.22	-0.32	-0.67 *	-0.55	-0.41	0.07	-0.28	-0.2
Serpinb1a	-0.22	-0.4	-0.41	-0.52	-0.21	-0.57 *	0.18	-0.19	0.12
Snrpd1	0.15	0.67	0.39	0.64	1.14	1.39 *	0.31	0.38	0.72
Rgs7bp	-0.4	-0.41	-0.47	-0.46	-0.46	-0.52 *	-0.16	-0.12	-0.18
Ttpal	0.44	0.42	0.31	0.27	0.5	0.63 *	-0.31	-0.35	-0.24
Mknk2	0.46	0.4	0.22	0.51	0.64 *	0.28	0.02	0.15	0.16
Rora	-0.12	-0.15	0.03	-0.51 *	-0.46	-0.13	-0.2	-0.2	-0.24
Dhx58	-0.4	-0.5	-0.5	-0.16	-0.11	-0.59 *	0.2	0.04	0.12
Pgs1	0.52	0.66	0.44	0.55	0.66	0.76 *	-0.1	-0.07	0.08
Mrpl12	0.21	0.27	0.21	0.22	0.32	0.34 *	-0.02	0.04	0.01
Cyyr1	0.62	0.98	0.82	1	0.39	1.27 *	0.11	-0.85	-0.19
Foxk1	-0.39	-0.31	-0.38	-0.41 *	-0.4	-0.43 *	-0.2	-0.04	-0.06
Psph	0.12	0.26	0.1	0.24	0.42	0.49 *	-0.1	-0.14	0.04
Tbc1d9	0.4	0.38	0.27	0.3	0.41	0.61 *	0.19	0.1	0.13
Tmem129	0.33	0.31	0.18	0.19	0.3	0.39 *	-0.02	-0.01	-0.01
Unc5d	-0.54	-0.55	-0.64	-0.23	-0.97 *	-0.4	-0.01	-0.42	-0.38
Gpt2	-0.36	-0.3	-0.15	-0.07	-0.33	-0.69 *	-0.35	-0.2	-0.06
Usp10	0.3	0.39	0.26	0.38	0.38	0.54 *	-0.17	-0.08	0.04
Tomm40	0.2	0.35	0.13	0.24	0.53 *	0.23	0.03	-0.05	0.09
Egln1	0.36	0.36	0.3	0.09	0.33	0.42 *	-0.15	0	-0.13
Ppp1r3c	-0.41	-0.37	-0.36	-0.81 *	-0.8 *	-0.28	0.27	0.03	-0.12
Prdm1	-0.32	-0.4	-0.24	-0.64 *	-0.48	-0.22	-0.26	-0.37	-0.36
Pofut1	0.33	0.24	0.29	0	0.38	0.52 *	0.3	0.07	0.01
Acss2	0.46	0.42	0.46	0.46	0.52	0.51 *	0.31	0.31	0.24
Lrp6	-0.01	-0.16	-0.28	-0.34	-0.45 *	-0.24	-0.21	-0.24	-0.15
Coro2a	0.33	0.45	0.35	0.43	0.51	0.61 *	-0.22	0.01	-0.29
Ctps1	0.27	0.52	0.43	0.44	0.56	0.69 *	-0.46	-0.13	-0.21
Spsb1	0.4	0.39	0.35	0.47	0.5 *	0.46 *	0.27	0.26	0.32
Chordc1	0.17	0.4	0.27	0.4	0.48	0.69 *	-0.28	-0.19	0.03
Tbcc	0.17	0.29	0.2	0.06	0.28	0.33 *	-0.08	-0.12	-0.05
Mpzl1	-0.46	-0.43	-0.45	-0.63 *	-0.39	-0.41	-0.13	0.1	0.04
Sult2a2	-3.18	-4.23	-3.17	-3.03	-4.87 *	-3.86	1.43	1.2	2.25
Rnls	0.42	0.42	0.42	0.26	0.21	0.39 *	0.02	-0.02	0.03
Alg14	0.13	0.14	0.15	0.02	0.16	0.35 *	-0.15	-0.16	-0.09
Fam13a	0.13	-0.25	0.17	-0.75 *	-0.34	0.24	-0.28	-0.52	-0.35
Mthfr	0.38	0.38	0.3	0.42	0.35	0.54 *	-0.4	-0.25	0.01
Csrnp1	-0.63	-0.62	-0.68	-0.11	-0.29	-0.64 *	-0.02	0.42	0.33
Fastkd5	0.06	0.17	0.12	0.35	0.47	0.5 *	-0.07	-0.04	0.21
Fn3k	0.62	0.72	0.7	0.69 *	0.77	0.56	-0.08	-0.05	-0.03
Plekhd1	0.32	0.54	0.47	0.47	1.07	0.96 *	0.61	0.02	0.54
RGD1565356	-0.64	-0.77	-0.58	-0.39	-0.45	-0.83 *	0.4	-0.11	0.19
Dnajc12	-0.44	-0.37	-0.53	-0.65 *	-0.74	-0.42	-0.28	-0.5	-0.26
LOC681383	-0.6	-0.83	-0.78	-0.97	-0.51	-0.9 *	0.39	0.27	0.23
Tmem41a	0.18	0.31	0.22	0.34	0.47	0.4 *	-0.25	-0.12	-0.13

Table for A) male and B) female genes; * FDR < 0.05. Statistically significant differential expression is indicated with an asterisk (*) (BH-adjusted *p*-value < 0.05).

9.4.2 Biological Network Perturbation Amplitude Analysis in Liver Tissue after 90 Days of Exposure to Reference Cigarettes and THS2.2M, or after a 42-day Recovery Period

As no liver-specific networks were available yet, no analysis could be performed.

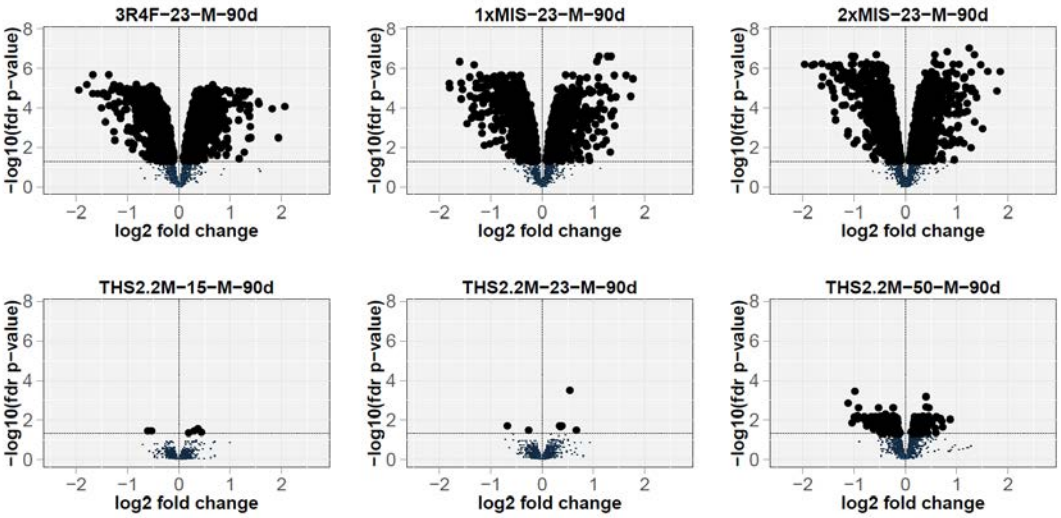
9.5 Respiratory Nasal Epithelium Proteome after 90 Days of Exposure and after a 42-day Recovery Period in Male and Female Rats

To assess how the different exposure conditions quantitatively affected the proteome of nasal epithelium, we employed a robust LC-MS/MS-based quantitative proteomics approach. This isobaric tag-based quantification method allowed for the multiplexed analysis of up to eight samples in a single mass-spectrometry run, making use of up to eight different peptide-reporter labeling reagents. Here, we defined two different multiplexed iTRAQ labeling sets, to facilitate the analysis of the relevant sample group comparisons. The first iTRAQ set contained all sample groups after 90 days (iTRAQ Set 1), and the second iTRAQ set contained the sample groups for the 90-day vs. 90+42-day comparison (iTRAQ Set 2). For the number of biological replicates for proteomics profiling, please see sub-section 7.13.

9.5.1 Differentially Expressed Proteins in Respiratory Nasal Epithelium

To evaluate the global impact on the proteome of each exposure condition compared with the sham exposure, the amplitude (expressed as log2 fold change, x-axis) and statistical significance (expressed as –log10 of the adjusted *p*-value, y-axis) of differential protein expression were graphed as volcano plots. In these plots, proteins demonstrating statistically significant differential expression compared with the sham exposure are above the significance line (BH-adjusted p-value < 0.05), and are marked with bold black dots. Figure 16 and Figure 17 depict the volcano plots for iTRAQ Set 1 and Set 2, respectively. The numbers of identified differentially expressed proteins across the exposure conditions are summarized in Figure 18.

A)



B)

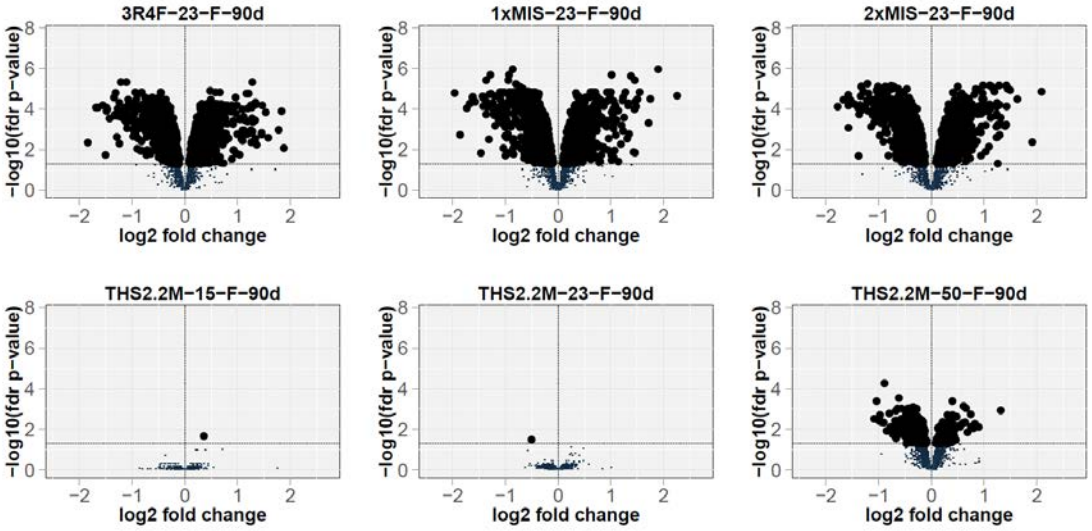


Figure 16: Volcano plots representing the proteome response profiles in RNE (comparisons for 90 days, Set 1).

For each protein, the protein expression change compared with the respective sham group, calculated as the log2 fold change, is plotted on the x-axis; statistical significance, proportional to the negative log10-adjusted *p*-value, is plotted on the y-axis. Bold, black dots highlight genes that are statistically significantly up- or down-regulated compared with the sham group at each respective time point (Benjamini–Hochberg adjusted *p*-value < 0.05). A) Response in male rats, B) response in female rats.

After 90 days of exposure, a clear proteome response was detected in 3R4F-, DDA3 1xMIS-, and DDA3 2xMIS-exposed male and female rats (top panel of Figure 16, A and B). In THS2.2M-exposed rats, the response was much reduced (bottom panel of Figure 16, A and B). At the matched nicotine concentration of 23 µg/L, THS2.2M induced a much lower number of differentially expressed proteins than the DDA3 1xMIS or DDA3 2xMIS exposure. At a THS2.2M exposure of 50 µg/L nicotine, the response, although increased compared with the other THS2.2M groups, was still lower than the response for DDA3 1xMIS or DDA3 2xMIS at approximately half of the nicotine concentration (23 µg/L).

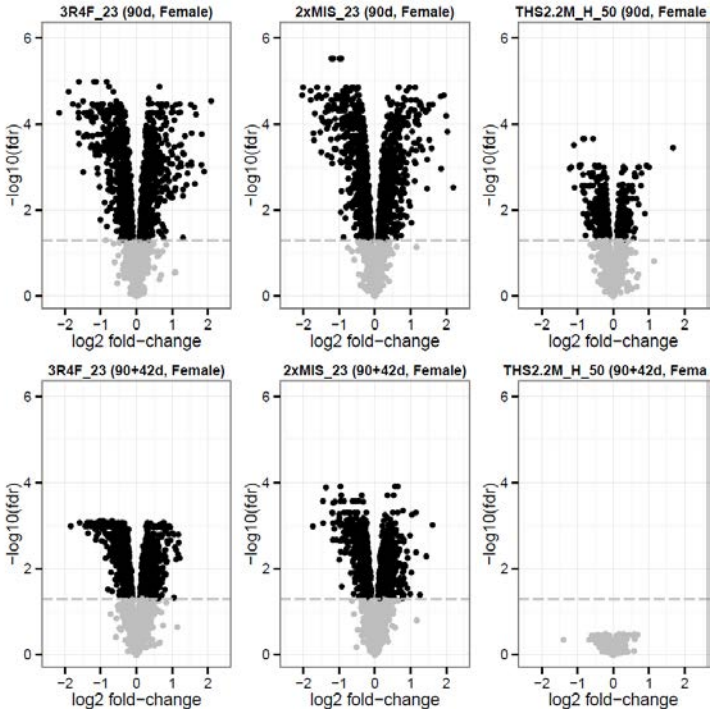


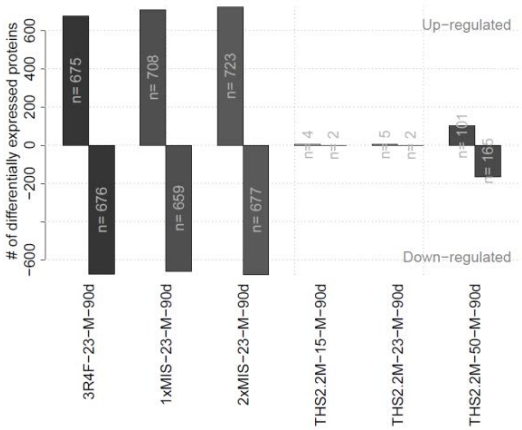
Figure 17: Volcano plots representing the proteome response profiles in RNE (comparison between 90 days and 90+42 days, Set 2).

For each protein, the protein expression change compared with the respective sham group, calculated as the log2 fold change, is plotted on the x-axis; statistical significance, proportional to the negative log10-adjusted *p*-value, is plotted on the y-axis. Bold, black dots highlight genes that are statistically significantly up- or down-regulated compared with the sham group at each respective time point (Benjamini–Hochberg adjusted *p*-value < 0.05).

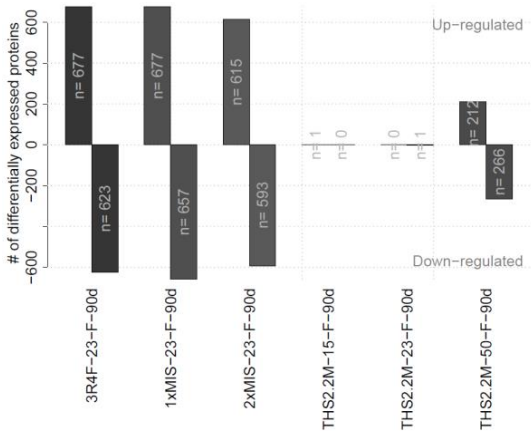
After the 42-day recovery period, the protein expression changes were reduced in all groups (Figure 17). Whereas the effects of DDA3 2xMIS and 3R4F exposure (both at 23 µg/L nicotine) were still clearly detectable, the effects of THS2.2M exposure (at 50 µg/L nicotine) largely disappeared after the 42-day recovery period (Figure 17).

Figure 18 depicts the numbers of differential expressed proteins.

A)



B)



C)

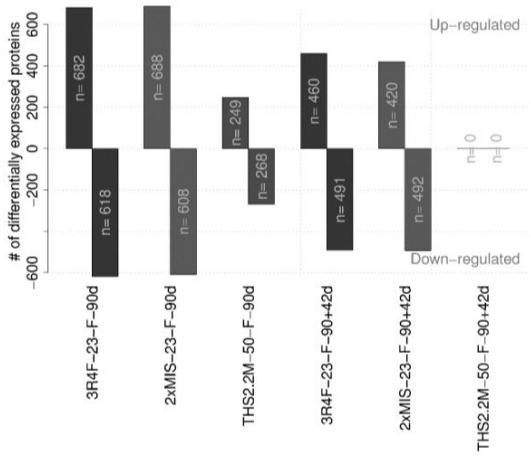


Figure 18: Numbers of differentially expressed proteins in RNE.
A) Comparisons for 90 days, male rats, Set 1; B) comparisons for 90 days, female rats, Set 1; C) comparisons for 90+42 days, female rats, Set 2. For each comparison with the respective sham group, the number of differentially up- and down-regulated proteins is shown. The false discovery rate was controlled at the 5% level using the Benjamini–Hochberg approach.

To compare the exposure response across conditions more directly, we graphed the fold change and statistical significance for each differentially expressed protein in any of the conditions in a vertical bar chart (Figure 19). This graph demonstrates the overall similarity of the exposure response in the 3R4F, DDA3 1xMIS, and DDA3 2xMIS groups for both sexes. In contrast, THS2.2M exposure at a nicotine concentration of 15 µg/L and 23 µg/L showed a very limited response – a clear effect on the proteome was observed only for THS2.2M at 50 µg/L nicotine, which, however, remained below the response to DDA3 1xMIS and DDA3 2xMIS exposure (23 µg/L nicotine).

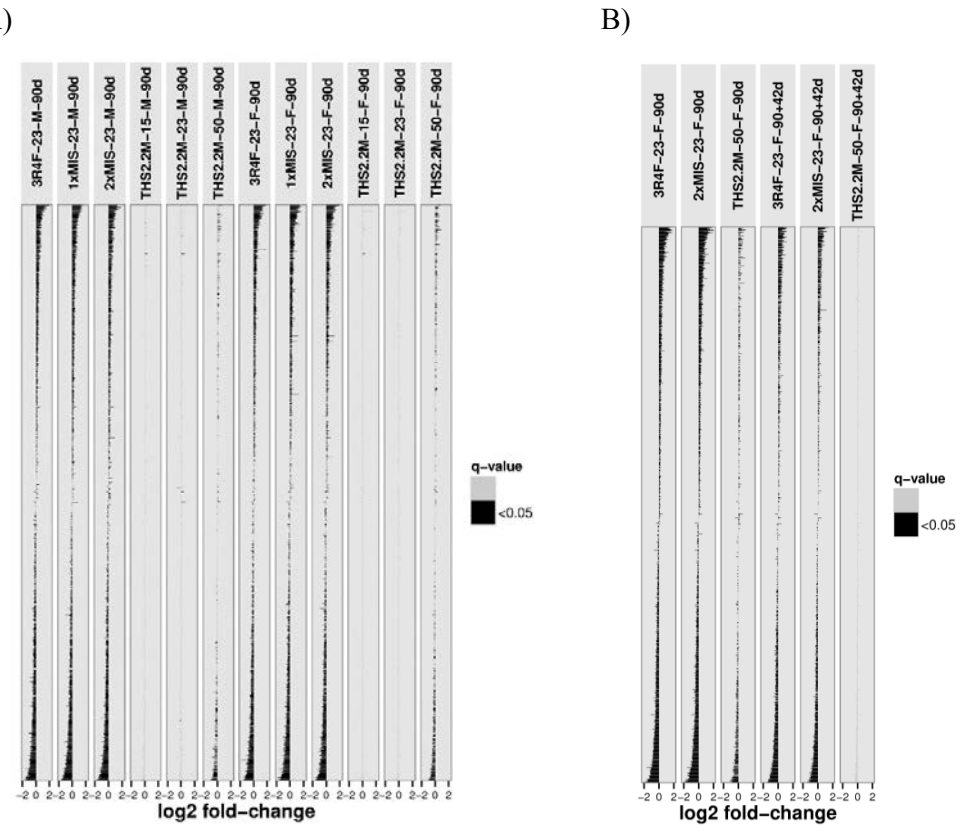


Figure 19: Fold change and significance in protein profiles across the exposure conditions.

Differential expression bar plots for proteins significantly affected by any of the different exposure conditions. Differential protein expression of treatments vs. sham is graphed as bar plots. The length of the bars represents the log2 fold change compared with sham exposure (right = up-regulated, left = down-regulated). Significant changes are indicated with black bars (BH-adj. *p*-value < 0.05). Only significantly regulated proteins (adj. *p*-value < 0.05) in any of the comparisons are shown. A) iTRAQ Set 1, B) iTRAQ Set 2.

Overall, the THS2.2M exposed groups showed a strong reduction in the number of differentially expressed proteins in RNE compared with the DDA3 1xMIS, DDA3 2xMIS, and 3R4F exposure groups. For male rats, THS2.2M exposure resulted in only approximately 0.5% of the number of differentially expressed proteins of the DDA3 1xMIS, DDA3 2xMIS, and 3R4F exposure groups at the same nicotine concentration (23 µg/L). When male rats were exposed to the high THS2.2M concentration (50 µg/L nicotine), the number of differentially expressed proteins was still lower than 20% of the proteins found for the reference smoke exposures. Importantly, the 266 differentially expressed proteins from exposure to THS2.2M (50 µg/L nicotine) were mostly also differentially regulated by 3R4F (243 of 266 proteins), DDA3 1xMIS (248 of 266 proteins), and DDA3 2xMIS (244 of 266 proteins).

For female rats, THS2.2M exposure resulted in only approximately 0.1% of the number of differentially expressed proteins of the DDA3 1xMIS, DDA3 2xMIS, and 3R4F exposure groups at the same concentration (23 µg/L nicotine). When female rats were exposed to the high THS2.2M concentration (50 µg/L nicotine), the number of differentially expressed proteins was still lower than 40% of the proteins found for the reference smoke exposures. Importantly, the 478 differentially expressed proteins from exposure to THS2.2M (50 µg/L nicotine) were mostly also differentially regulated by 3R4F (433 of 478 proteins), DDA3 1xMIS (437 of 478 proteins), and DDA3 2xMIS (435 of 478 proteins).

All proteins that were uniquely expressed after THS2.2M exposure in one of the groups but were not found differentially regulated after exposure to the reference cigarettes are displayed in Table 12. For comparison, the fold changes of the respective proteins are also presented.

Table 12: Unique MRTP proteins.

A)

	ID	3R4F-23-M-90d	1xMIS-23-M-90d	2xMIS-23-M-90d	THS2.2M-15-M-90d	THS2.2M-23-M-90d	THS2.2M-50-M-90d	3R4F-23-F-90d	1xMIS-23-F-90d	2xMIS-23-F-90d	THS2.2M-15-F-90d	THS2.2M-23-F-90d	THS2.2M-50-F-90d
Glb1	D3ZUM4	0.06	0.06	0.07	0.12	0.15	0.21 *	-0.02	-0.05	0.02	0.11	0.08	0.2 *
Nt5c	D3ZWR1	0.02	-0.02	0.14	-0.03	-0.12	-0.03	-0.15	-0.11	-0.06	-0.19	-0.18	-0.18 *
Lsm4	D4A2C6	0.02	0.03	-0.04	-0.01	-0.04	0	0.12	0.1	-0.1	0.05	0.07	0.16 *
Cbx1	D4A3T3	0	0.05	0.03	-0.06	0.04	0	0.15	0.07	0.15	0.06	0.08	0.19 *
Bin1	D4A4P1	0.06	0	0.06	-0.04	-0.13	0	-0.1	-0.17	0.03	-0.12	0.02	-0.21 *
Srsf4	G3V798	-0.03	-0.03	-0.05	-0.01	-0.02	-0.05	0	-0.03	-0.04	0.1	0.07	0.12 *
Grpel1	P97576	-0.04	0.04	0.02	-0.04	0.04	0.05	0.03	0.05	-0.05	0.08	0.07	0.12 *
Krt8	Q10758	-0.08	-0.04	-0.03	0.03	0.16	0.2 *	-0.11	-0.12	-0.13	0	0.06	0.19 *
Rbm8a	Q27W01	0.1	0.11	0.07	0.02	0.02	0.13	0.08	0.1	0.05	0.06	0.11	0.14 *
Ctsa	Q6AYS3	-0.02	0.03	0.04	0.07	0.07	0.19 *	0.02	0.03	0	0.06	0.07	0.13 *
Marcksl1	Q9EPH2	-0.06	-0.13	-0.09	-0.03	0.04	-0.06	-0.08	-0.11	-0.02	0.22	0.16	0.19 *
Urod	B0BN55	-0.01	0.02	-0.05	0.02	0.11	0.16 *	-0.05	0.01	-0.02	0	0.09	0.05
Prkar1b	F1M9X5	NA	NA	NA	NA	NA	-0.19 *	NA	NA	NA	NA	NA	NA
Rbbp9	O88350	-0.04	-0.14	-0.08	-0.11	-0.1	-0.18 *	-0.11	-0.05	-0.13	-0.11	-0.09	-0.17
Mgat4a	Q5M854	0.12	-0.02	0	0.16	0.13	0.26 *	NA	NA	NA	NA	NA	NA
Cmas	Q5M963	-0.06	-0.03	-0.07	0.08	0.07	0.14 *	-0.02	-0.05	-0.09	0.04	0.09	0.12
		male						female					

B)

Protein	ID	3R4F-23 (90d, Female)	2xMIS-23 (90d, Female)	THS2.2M-H-50 (90d, Female)	3R4F-23 (90+42d, Female)	2xMIS-23 (90+42d, Female)	THS2.2M-H-50 (90+42d, Female)
Prkaca	A1L1M0	0.06	-0.06	-0.3 *	-0.08	-0.11	0.01
Bcas2	B5DFM8	0.01	0.05	0.13 *	-0.07	-0.06	0.01
Phpt1	D3ZP47	-0.09	-0.08	-0.1 *	-0.01	0	-0.01
Glb1	D3ZUM4	-0.01	0.01	0.14 *	-0.01	0.08	-0.01
Lsm7	D4A2D8	0.13	0.09	0.2 *	0.13	0.1	0.04
Uba6	D4A8H3	0	-0.06	-0.21 *	-0.04	-0.1	0
Smarca5	F1LNL2	-0.03	0.01	0.24 *	-0.01	0.09	0.18
Rbm25	F1LT30	0.11	0.09	0.16 *	-0.06	0	-0.04
Srsf6	G3V6S8	-0.04	0.34	0.16 *	-0.05	-0.08	0.07
Prrc1	G3V834	0.13	0.05	0.17 *	0.04	0.01	0.1
Hprt1	P27605	-0.03	-0.03	-0.11 *	-0.04	-0.01	-0.06
Arsb	P50430	-0.04	0.07	0.17 *	-0.06	-0.13	-0.07
Mtpn	P62775	-0.08	-0.07	-0.26 *	-0.05	0.07	0.07
Edf1	P69736	0.22	0.14	0.22 *	0.05	-0.03	-0.05
Grpel1	P97576	0.17	-0.01	0.18 *	-0.11	-0.03	0.08
Krt8	Q10758	-0.08	-0.12	0.23 *	-0.12	-0.04	-0.05
Hexa	Q641X3	-0.04	-0.01	0.14 *	0.01	0.01	0.04
Nasp	Q66HD3	0.15	0.11	0.3 *	0.05	-0.01	0.22
Hexb	Q6AXR4	-0.02	-0.01	0.18 *	0.12	0.09	0
Ctsa	Q6AYS3	0.05	0.03	0.17 *	-0.03	0	-0.02
Pdhx	Q7TQ85	-0.12	-0.07	-0.15 *	-0.13	-0.12	-0.08
		female					

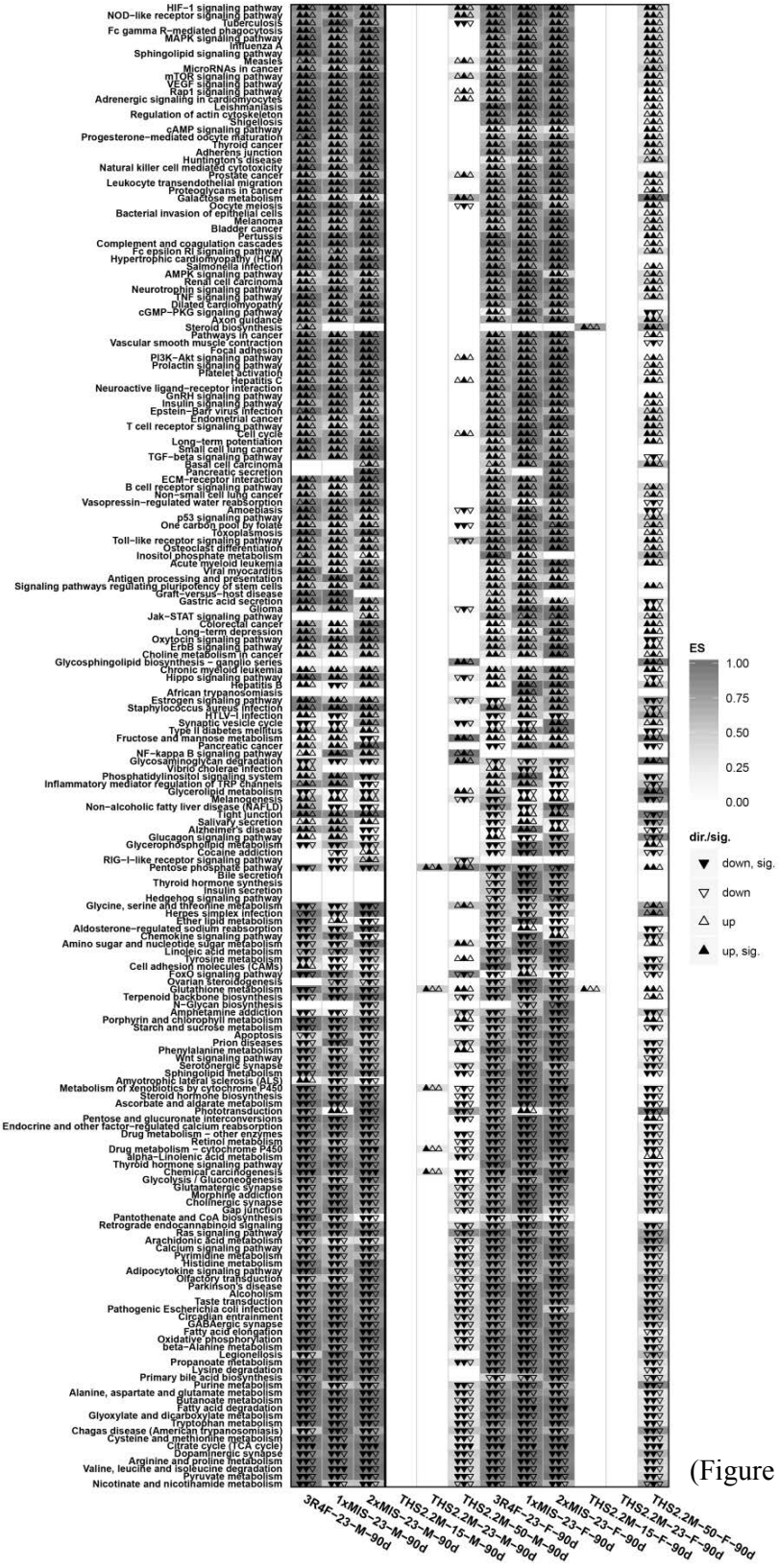
Summary of all proteins that were only significantly differentially expressed in THS2.2M exposed groups, but not in any of the reference exposed groups. A) iTRAQ Set 1, B) iTRAQ Set 2.Statistically significant differential expression is indicated with an asterisk (*) (BH-adjusted *p*-value < 0.05).

9.5.2 Effects of Exposure Conditions on Functional Groups (Set Enrichment Analyses)

We complemented this analysis at the individual protein level by conducting a protein set enrichment analysis (Figure 20). For this assessment, we identified protein sets from the KEGG compendium (Kanehisa 2014b) that were significantly affected by the tested exposure conditions. The KEGG compendium is a comprehensive database of functionally related gene/protein sets. For biological interpretation, it is important to note that not all protein/gene sets in the diverse KEGG collection are necessarily directly relevant for our biological context.

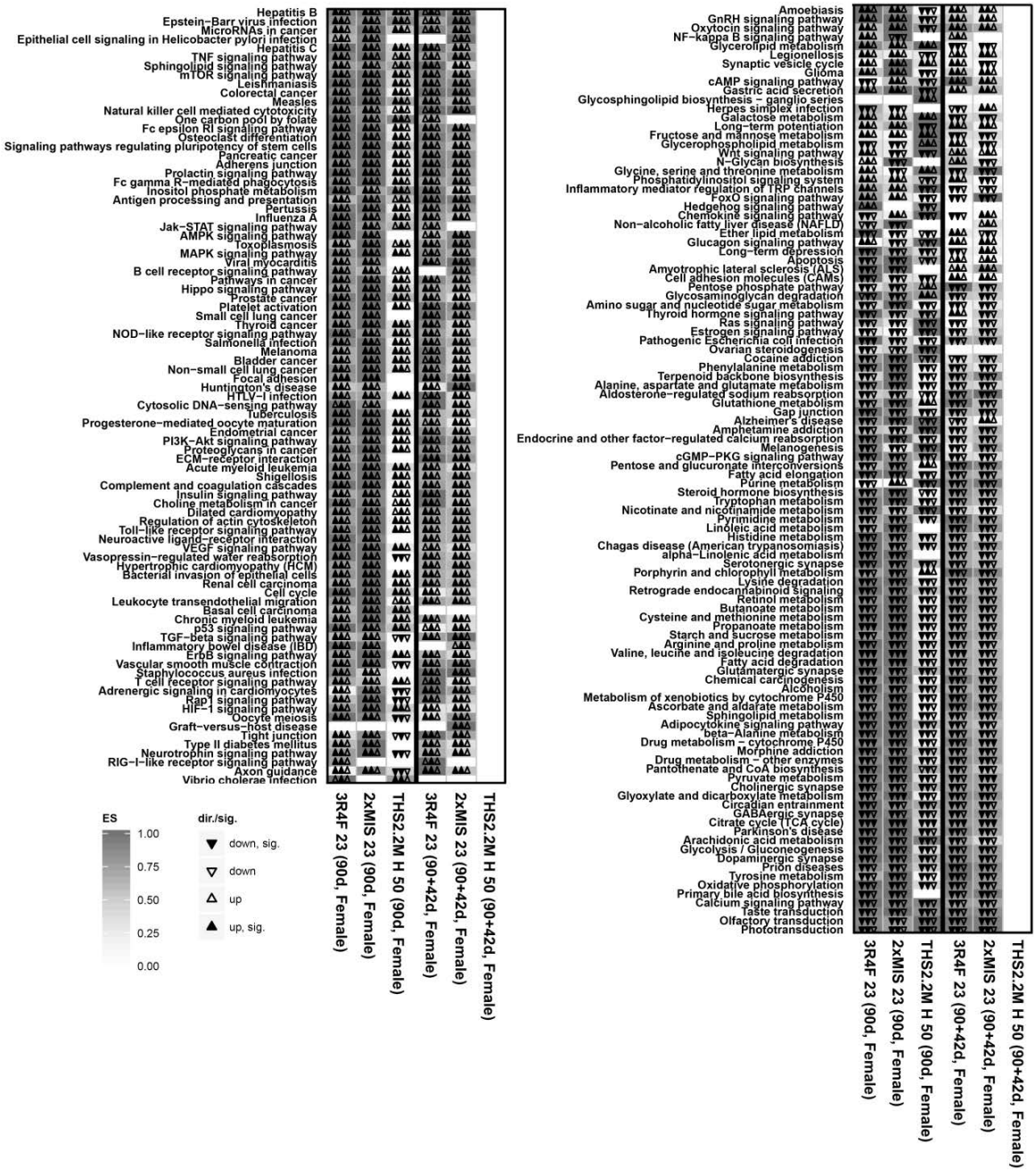
Exposure to reference cigarette smoke (DDA3 1xMIS, DDA3 2xMIS, and 3R4F) at 23 µg/L nicotine induced a strong and consistent response in both male and female rats. In contrast, THS2.2M exposure at the same (23 µg/L) or lower (15 µg/L) nicotine concentration demonstrated only a very limited effect on the level of protein sets. THS2.2M with a nicotine concentration of 50 µg/L (i.e., approximately twice the concentration of the reference cigarettes) showed a clear exposure response. The response in female rats was more pronounced than the response in male rats, however, globally, the exposure response (at this elevated nicotine concentration) always stayed below the response to reference cigarette smoke.

A)



(Figure continues)

B)



(for figure legend please see next page)

Figure 20: Set enrichment results for KEGG pathway collection.

Set enrichment was assessed by over-representation analysis (ORA) and gene-set analysis (GSA). The fold change compared with sham exposure was used as the protein-level statistic, the mean as the set statistic, and sample permutation (Q2) to assess statistical significance. Enrichment results are normalized per pathway and the normalized GSA enrichment score (ES) is mapped to the grayscale (see key). Significance is indicated by a filled triangle (BH-adjusted *p*-value < 0.05), with the direction given by the orientation of the triangle (see key). The first triangle represents the overall adjusted Fisher *p*-value of the GSA and ORA analyses**,** the second triangle the GSA, and the third triangle the ORA results**.** Non-significant associations are left blank. A) iTRAQ Set 1, 90 days; B) iTRAQ Set 2, 90+42 days. (please zoom into PDF version of this document for enlargement).

9.6 Lung Proteome after 90 Days Exposure and after a 42-day Recovery Period in Male and Female Rats

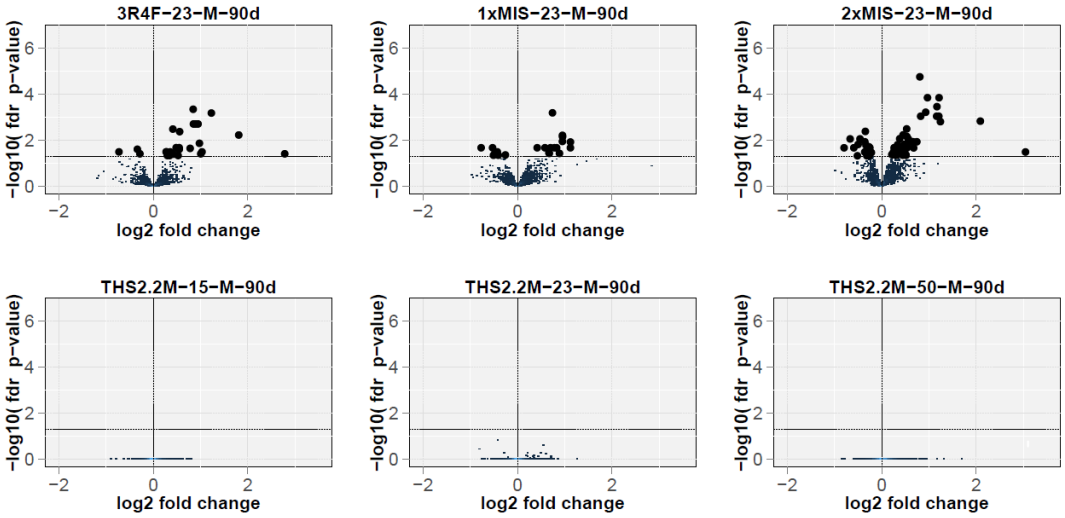
For the lung, we employed a robust LC-MS/MS-based quantitative proteomics approach to assess how the different exposure conditions quantitatively affected the lung proteome. This isobaric tag-based quantification method allows for the multiplexed analysis of up to eight samples, making use of up to eight different peptide-reporter labeling reagents. Here, we defined two different multiplexed iTRAQ labeling sets to facilitate the analysis of the relevant sample group comparisons. The first iTRAQ set contained all sample groups after 90 days (Set 1), and the second iTRAQ set contained the sample groups for the 90-day vs. the 90+42-day comparison (Set 2) (7.13.2). For the number of biological replicates for proteomics profiling, please see sub-section 7.13.4.

9.6.1 Differentially Expressed Proteins in Lung Tissue

To evaluate the global impact on the proteome of each exposure condition compared with the sham exposure, we graphed the amplitude (expressed as log2 fold change, x-axis) and statistical significance (expressed as −log10 of the adjusted *p*-value, y-axis) of differential protein expression as volcano plots. In these plots, proteins demonstrating statistically significant differential expression compared with the sham exposure appear above the significance line (BH-adjusted *p*-value < 0.05), and are marked with bold, black dots.

Figure 21 and Figure 22 depict the volcano plots for iTRAQ Set 1 and Set 2, respectively, and the numbers of identified differentially expressed proteins across the exposure conditions are summarized in Figure 23**.**

A)



B)

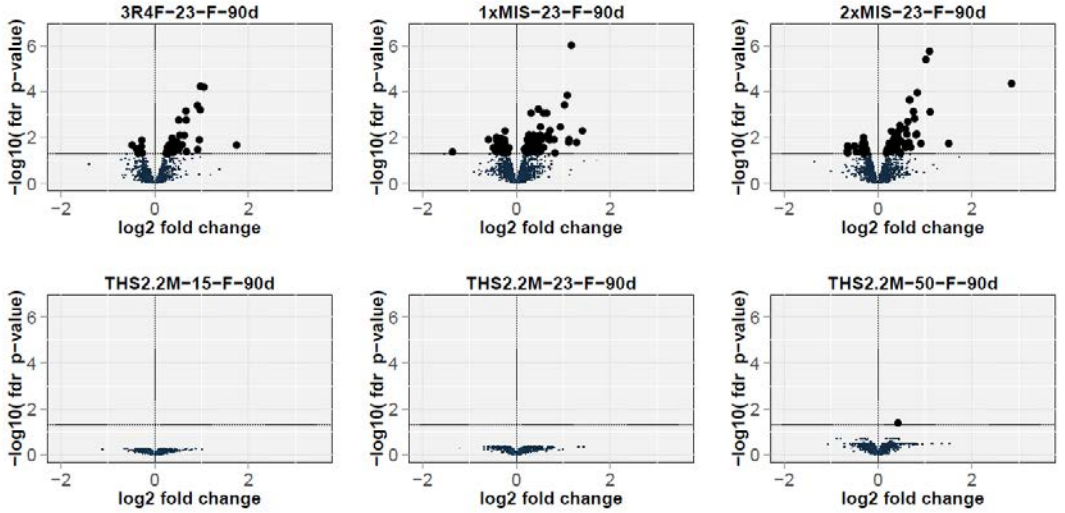


Figure 21: Volcano plots representing the proteome response profiles in lung (comparisons for 90 days, Set 1). A) Male, B) female.

For each protein, the protein expression change compared with the respective sham group, calculated as the log2 fold change, is plotted on the x-axis; statistical significance, proportional to the negative log10-adjusted *p*-value, is plotted on the y-axis. Bold, black dots highlight genes that are statistically significantly up- or down-regulated compared with the sham group at each respective time point (Benjamini–Hochberg adjusted *p*-value < 0.05).

After 90 days of exposure, a clear proteome response was detected in 3R4F-, DDA3 1xMIS-, and DDA3 2xMIS-exposed male and female rats (top panel of Figure 21, A and B). In THS2.2M-exposed rats, the response was much reduced (bottom panel of Figure 21, A and B) – with only one significantly differentially expressed protein (iTRAQ Set 1) for THS2.2M at 50 µg/L nicotine for female rats.

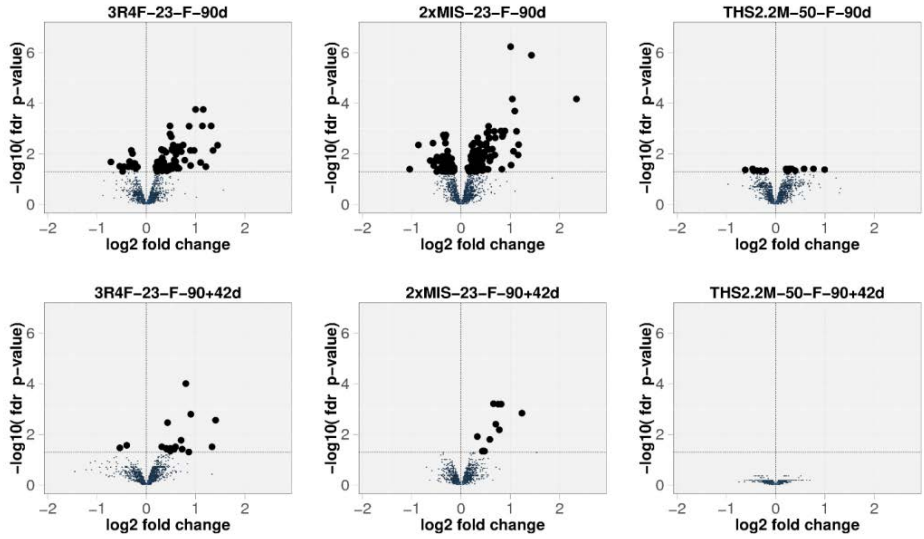


Figure 22: Volcano plots representing the proteome response profiles in lung (comparison between 90 days and 90+42 days, Set 2).

For each protein, the protein expression change compared with the respective sham group, calculated as the log2 fold change, is plotted on the x-axis; statistical significance, proportional to the negative log10-adjusted *p*-value, is plotted on the y-axis. Black dots highlight genes that are statistically significantly up- or down-regulated compared with the sham group at each respective time point (Benjamini–Hochberg adjusted *p*-value < 0.05).

After the 42-day recovery period, the protein expression changes were reduced in all groups (Figure 22). Although the effects of DDA3 2xMIS and 3R4F exposure (both at 23 µg/L nicotine) were still clearly detectable, the effects of THS2.2M exposure (at 50 µg/L nicotine) largely disappeared after the 42-day recovery period (Figure 23).

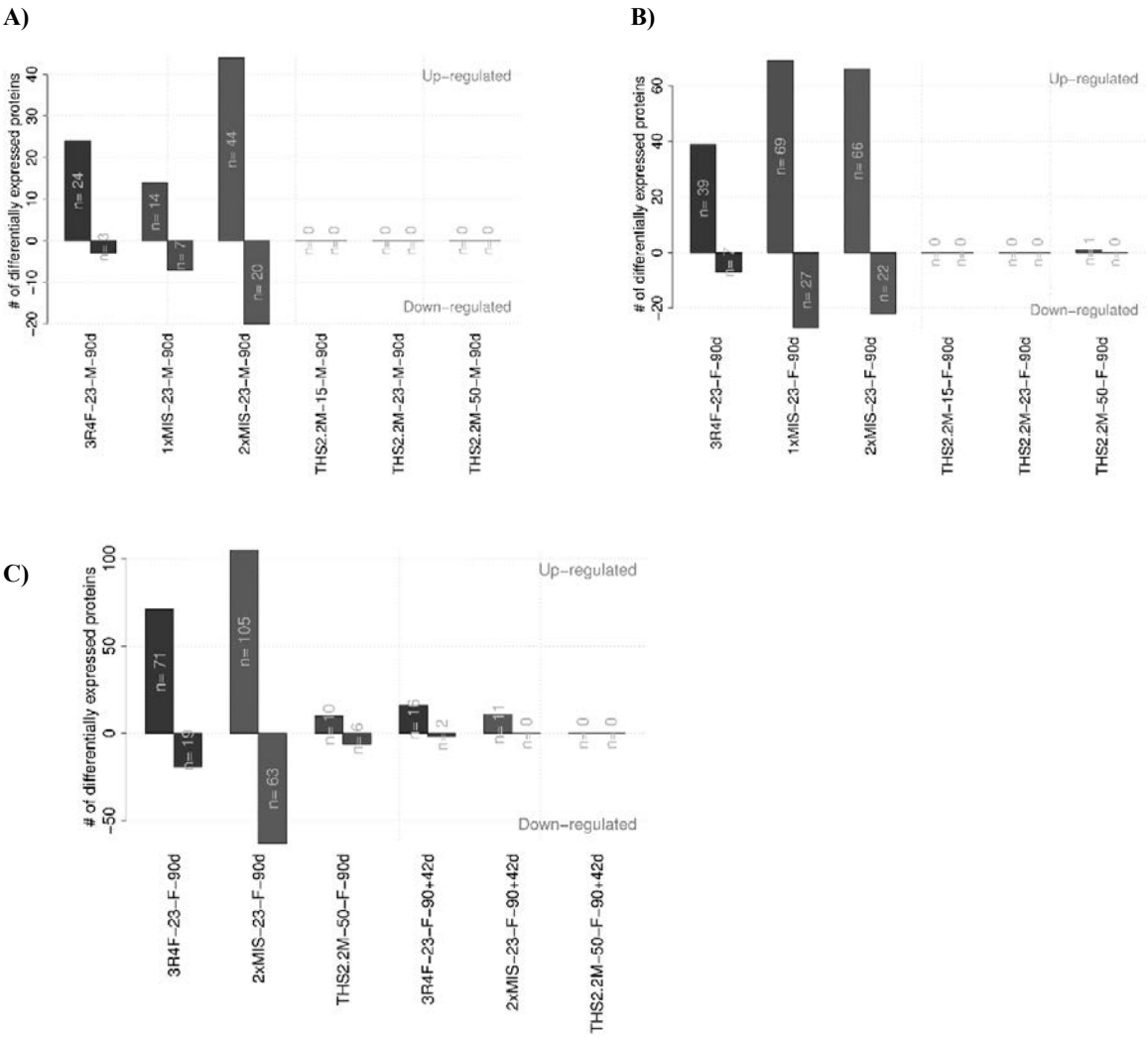
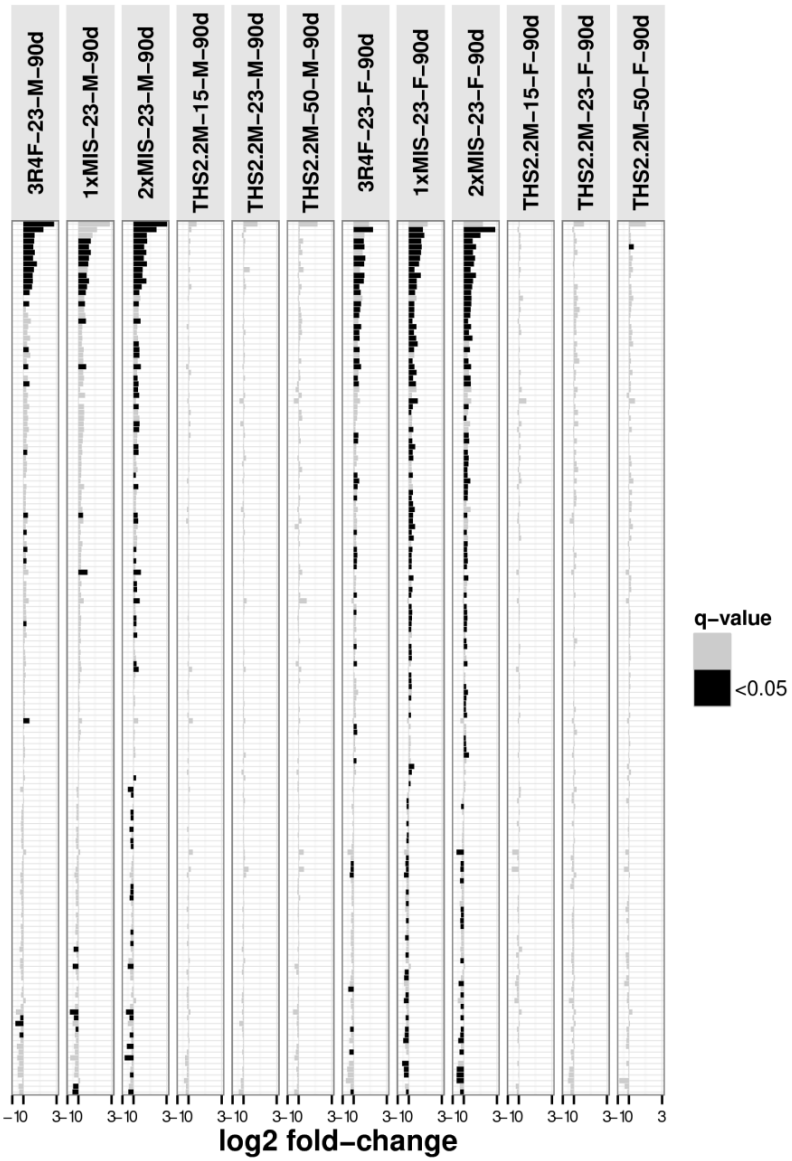


Figure 23: Numbers of differentially expressed proteins in lung.
A) Comparisons for 90 days, Set 1, male rats. B) Comparisons for 90 days, Set 1, female rats. C) Comparisons for 90+42 days, Set 2. For each comparison with the respective sham group, the number of differentially up- and down-regulated proteins is shown. The false discovery rate was controlled at the 5% level using the Benjamini–Hochberg approach.

We graphed the fold change and statistical significance for each differentially expressed protein in any of the conditions in a vertical bar chart, to directly compare the exposure response across conditions (Figure 24). This graph demonstrates the overall similarity of the exposure response in the 3R4F, DDA3 1xMIS, and DDA3 2xMIS groups for both sexes. In contrast, THS2.2M exposure at all three nicotine concentrations (15 µg/L, 23 µg/L, and 50 µg/L) elicited a very limited response.

A)



(Figure continues)

B)

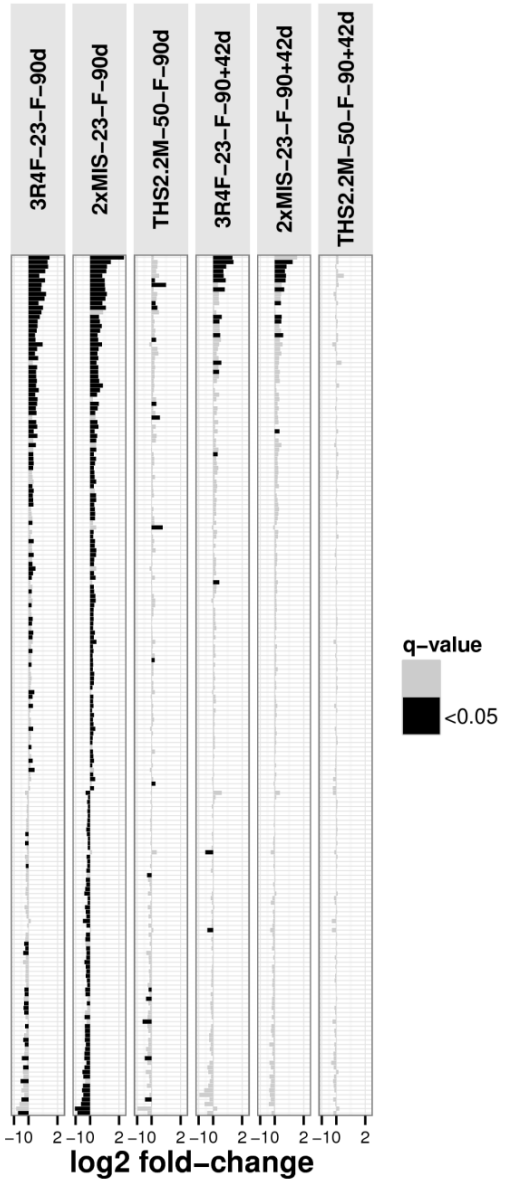


Figure 24: Fold change and significance in protein profiles across the exposure conditions.

Differential expression bar plots for proteins significantly affected by any of the different exposure conditions. Differential protein expression of treatments vs. sham is graphed as bar plots. The length of the bars represents the log2 fold change compared with sham exposure (right = up-regulated, left = down-regulated). Significant changes are indicated with black bars (BH-adj. *p*-value < 0.05). Only significantly regulated proteins (adj. *p*-value < 0.05) in any of the comparisons are shown. A) iTRAQ Set 1, B) iTRAQ Set 2.

In iTRAQ set 2, six proteins were found to be significantly differentially regulated only after THS2.2M exposure in the lung of female rats (Table 13). The direction of regulation is consistent after exposure to the references, but statistical significance was not reached.

Table 13: Unique differentially expressed proteins after THS2.2M treatment.

	ID	3R4F-23-F-90d	2xMIS-23-F-90d	THS2.2M-50-F-90d	3R4F-23-F-90+42d	2xMIS-23-F-90+42d	THS2.2M-50-F-90+42d
Synpo2	D4A702	0.04	0.11	0.26 *	-0.04	-0.07	-0.04
Hnrnph3	D4ABK7	-0.18	-0.23	-0.31 *	0.05	0.03	0.03
Abcd3	F1LR38	0.26	0.37	0.57 *	0.08	0.23	0.05
Mtpn	P62775	-0.05	-0.23	-0.62 *	0	-0.05	-0.25
Rap1a	P62836	-0.33	-0.17	-0.38 *	-0.08	-0.18	0.05
Slc25a4	Q6P9Y4	0.06	0.42	0.77 *	-0.09	-0.1	0.01
	Female						

Log2 fold changes are shown. Statistically significant differential expression is indicated with an asterisk (*) (BH-adjusted *p*-value < 0.05). iTRAQ Set 1 did not display unique THS2.2M proteins in the lung. Only iTRAQ Set 2 is shown.

9.6.2 Effects of Exposure Conditions on Functional Groups (Set Enrichment Analyses)

We complemented this analysis at the individual protein level by conducting a protein set enrichment analysis (Figure 25 and Figure 26). For this assessment, we identified protein sets from the KEGG compendium (Kanehisa 2014b) that were significantly affected by the tested exposure conditions. For biological interpretation, it is important to note that not all protein/gene sets in the diverse KEGG collection are necessarily directly relevant for our biological context.

Exposure to DDA3 1xMIS and DDA3 2xMIS at 23 µg/L nicotine induced an overall strong response, which appeared stronger in female rats. In contrast, THS2.2M exposure at 15 µg/L and 23 µg/L nicotine did not yield any significantly deregulated protein sets. A few affected protein sets were identified for THS2.2M exposure at 50 µg/L nicotine, but the response remained well below the response to reference cigarette smoke.

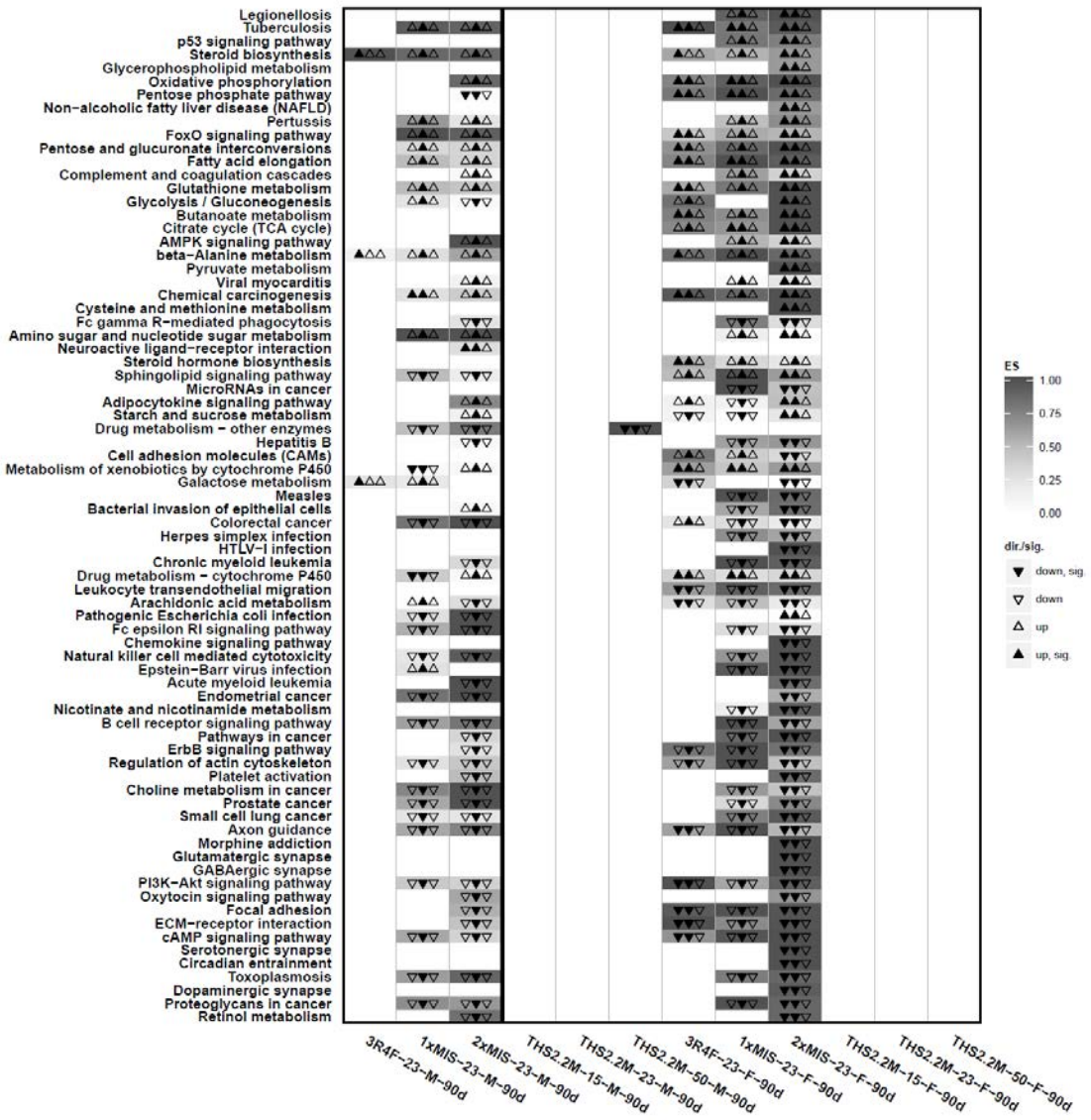


Figure 25: Set enrichment results for 90 days of exposure (Set 1).

Set enrichment was assessed by over-representation analysis (ORA) and gene-set analysis (GSA). The fold change compared with sham exposure was used as the protein-level statistic, the mean as the set statistic, and sample permutation (Q2) to assess statistical significance. Enrichment results are normalized per pathway and the normalized GSA enrichment score (ES) is mapped to the grayscale (see key). Significance is indicated by a filled triangle (BH-adjusted p-value < 0.05), with the direction given by the orientation of the triangle (see key). The first triangle represents the overall adjusted Fisher p-value of the GSA and ORA analyses, the second triangle the GSA, and the third triangle the ORA results. Non-significant associations are left blank (please zoom into PDF version of this document for enlargement).

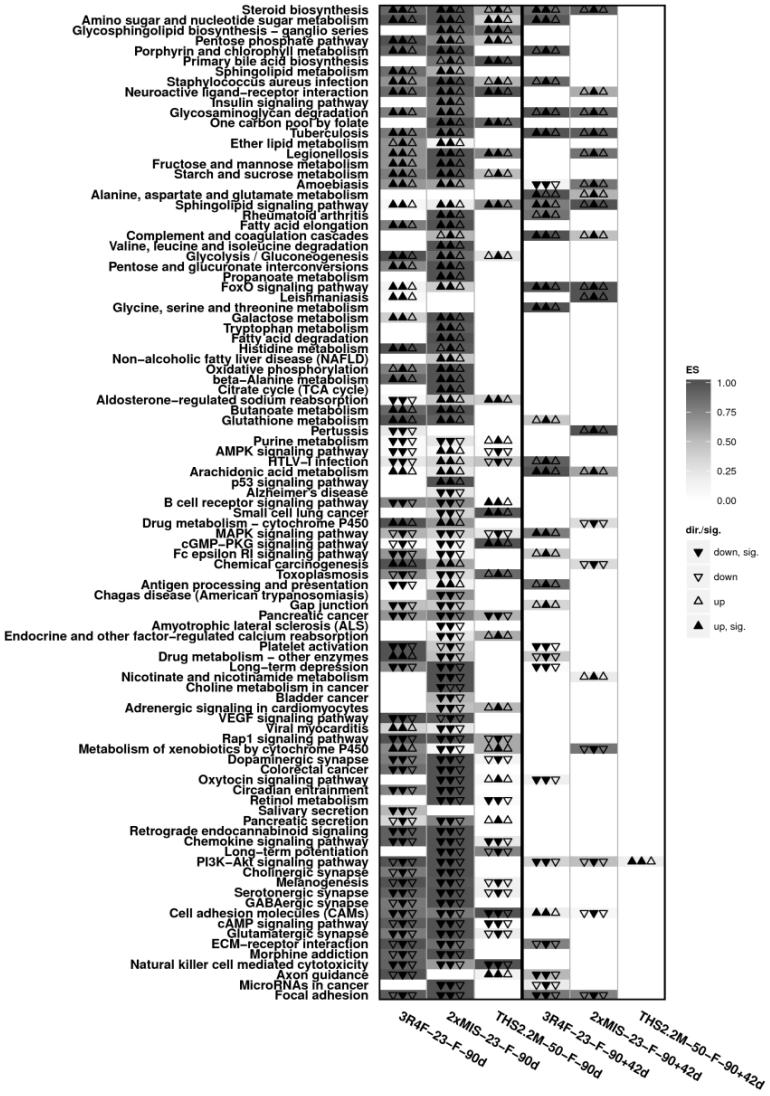


Figure 26: Set enrichment results for 90 days and 90+42-days of exposure (Set 2).

We evaluated protein/gene sets from the KEGG compendium (Kanehisa 2014b). Set enrichment was assessed by over-representation analysis (ORA) and gene-set analysis (GSA). For GSA, the fold change compared with sham exposure was used as the protein-level statistic, the mean as the set statistic, and sample permutation (Q2) to assess statistical significance. Enrichment results are normalized per pathway and the normalized GSA enrichment score (ES) is mapped to the grayscale (see key). Significance is indicated by a filled triangle (BH-adjusted p-value < 0.05), with the direction given by the orientation of the triangle (see key). The first triangle represents the overall adjusted Fisher p-value of the GSA and ORA analyses, the second triangle the GSA, and the third triangle the ORA results. Non-significant associations are left blank (please zoom into PDF version of this document for enlargement).

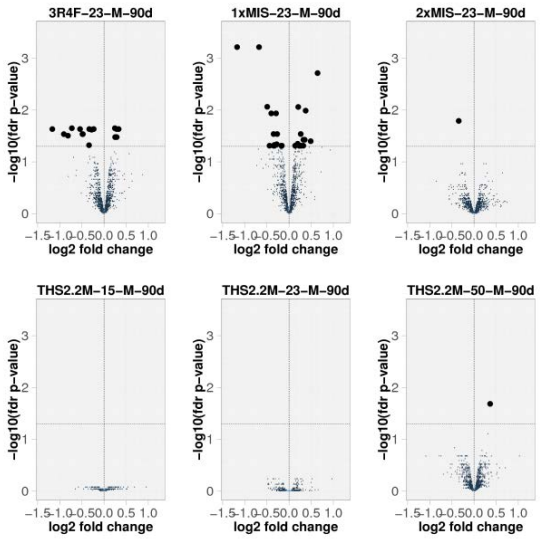
9.7 Liver Proteome after 90 Days Exposure and after a 42-day Recovery Period in Male and Female Rats

As for the nasal epithelium and lung tissue, we employed a robust LC-MS/MS-based quantitative proteomics approach to assess how the different exposure conditions quantitatively affected the liver proteome. This isobaric tag-based quantification method allows for the multiplexed analysis of up to eight samples, making use of up to eight different peptide-reporter labeling reagents. Again, we defined two different multiplexed iTRAQ labeling sets to facilitate the analysis of the relevant sample group comparisons. The first iTRAQ set contained all sample groups after 90 days (Set 1), and the second iTRAQ set contained the sample groups for the 90-day vs. the 90+42-day comparison (Set 2) (7.13.2). For the number of biological replicates for proteomics profiling, see sub-section 7.13.4.

9.7.1 Differentially Expressed Proteins in Liver Tissue

To evaluate the global impact on the proteome of each exposure condition compared with the sham exposure, we graphed the amplitude (expressed as log2 fold change, x-axis) and statistical significance (expressed as −log10 of the adjusted *p*-value, y-axis) of differential protein expression as volcano plots. In these plots, proteins demonstrating statistically significant differential expression compared with the sham exposure appear above the significance line (BH-adjusted p-value < 0.05), and are marked with bold, black dots. Figure 27 and Figure 28 depict the volcano plots for iTRAQ Set 1 and Set 2, respectively, and the numbers of identified differentially expressed proteins across the exposure conditions are summarized in Figure 29.

A)



B)

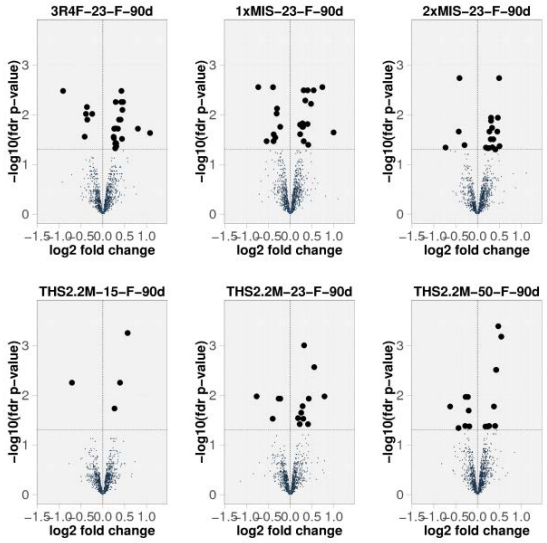


Figure 27: Volcano plots representing the proteome response profiles in liver (comparisons for 90 days, Set 1). A) Male, B) female.

For each protein, the protein expression change compared with the respective sham group, calculated as the log2 fold change, is plotted on the x-axis; statistical significance, proportional to the negative log10-adjusted *p*-value, is plotted on the y-axis. Bold, black dots highlight genes that are statistically significantly up- or down-regulated compared with the sham group at each respective time point (Benjamini–Hochberg adjusted *p*-value < 0.05).

After 90 days of exposure, a proteome response was detected in 3R4F-, DDA3 1xMIS-, and DDA3 2xMIS-exposed male and female rats (top panel of Figure 27A-B and Figure 29 A-B). In THS2.2M-exposed rats, the response was slightly reduced in female but much more reduced in male rats (bottom panel of Figure 27A-B and Figure 29 A-B) with only one significantly differentially expressed protein (iTRAQ Set 1) for THS2.2M at 50 µg/L nicotine for male rats.

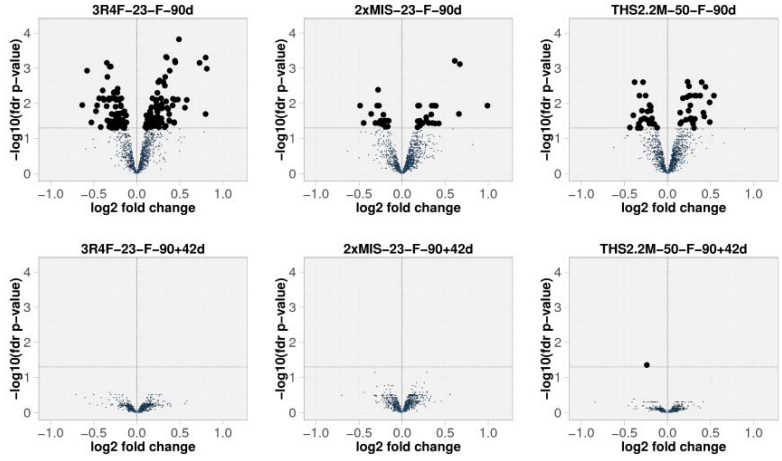


Figure 28: Volcano plots representing the proteome response profiles in liver (comparison between 90 days and 90+42 days, Set 2).

For each protein, the protein expression change compared with the respective sham group, calculated as the log2 fold change, is plotted on the x-axis; statistical significance, proportional to the negative log10-adjusted *p*-value, is plotted on the y-axis. Black dots highlight genes that are statistically significantly up- or down-regulated compared with the sham group at each respective time point (Benjamini–Hochberg adjusted *p*-value < 0.05).

After the 42-day recovery period, the protein expression changes in female livers were reduced in all groups, with only one protein significantly down-regulated in THS2.2M-50 (Figure 28 and Figure 29 C).

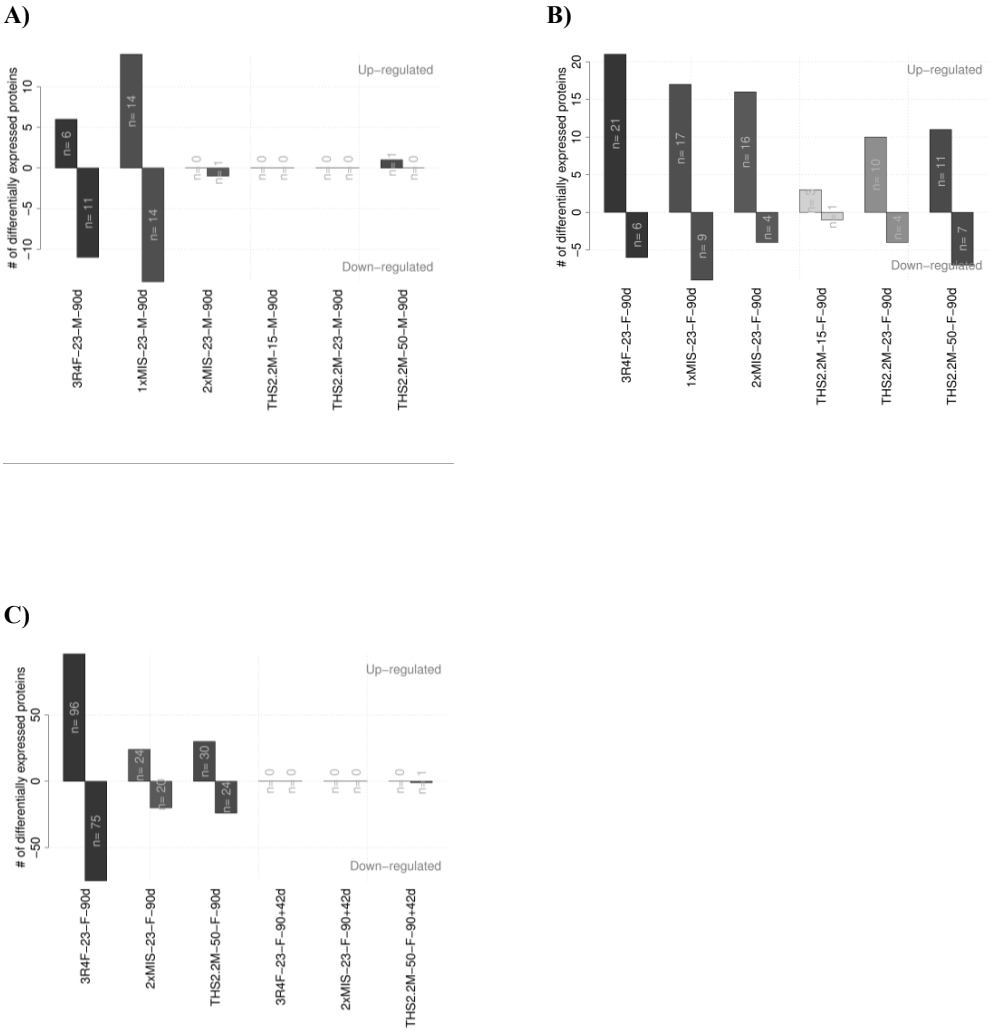


Figure 29: Numbers of differentially expressed proteins in liver.
A) Comparisons for 90 days, Set 1, male rats. B) Comparisons for 90 days, Set 1, female rats. C) Comparisons for 90+42 days, Set 2. For each comparison with the respective sham group, the number of differentially up- and down-regulated proteins is shown. The false discovery rate was controlled at the 5% level using the Benjamini–Hochberg approach.

We graphed the fold change and statistical significance for each differentially expressed protein in any of the conditions in a vertical bar chart, to directly compare the exposure response across conditions (Figure 30). This graph confirmed previous observations. In

fact, in male rats the overall response was higher in the 3R4F and DDA3 1xMIS groups, while THS2.2M exposure showed very limited response at all the concentrations. Of note, the DDA3 2xMIS group showed similarities to the THS2.2M groups. In female rat livers, the system response showed a clear dose-dependent effect in the THS2.2M group. Of note, THS2.2M-23 and THS2.2M-50 showed a consistent number of genes significantly expressed, which, however, remained below the response to the reference groups (3R4F, DDA3 1xMIS, and DDA3 2xMIS).

A) B)

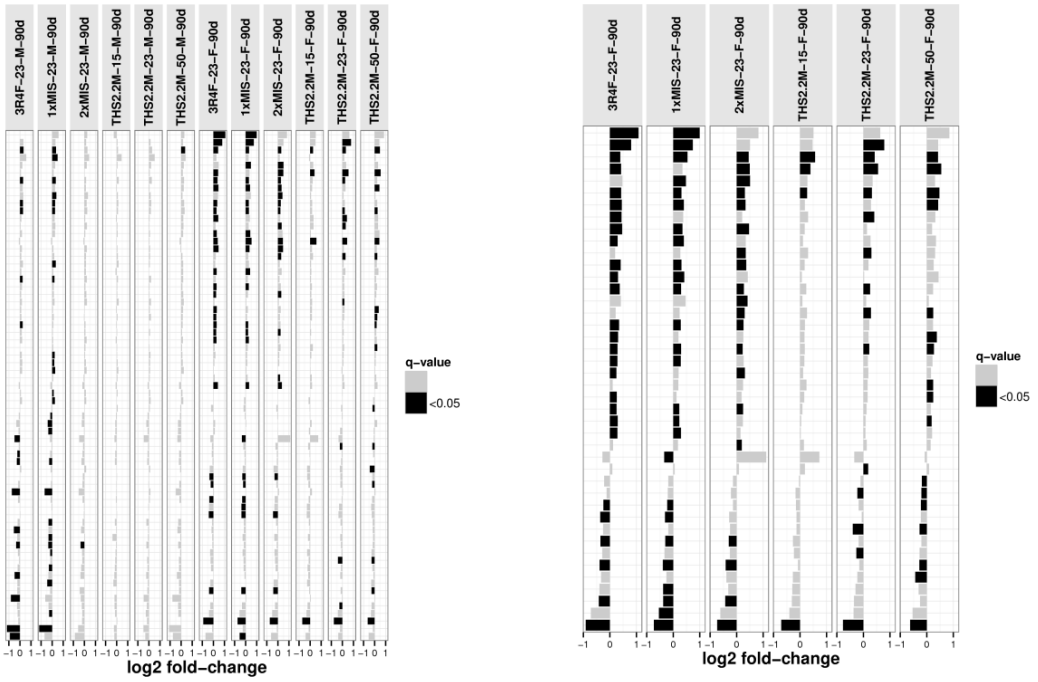


Figure 30: Fold change and significance in protein profiles across the exposure conditions in liver.

Differential expression bar plots for proteins significantly affected by any of the different exposure conditions. Differential protein expression of treatments vs. sham is graphed as bar plots. The length of the bars represents the log2 fold change compared with sham exposure (right = up-regulated, left = down-regulated). Significant changes are indicated with black bars (BH-adj. *p*-value < 0.05). Only significantly regulated proteins (adj. *p*-value < 0.05) in any of the comparisons are shown. A) iTRAQ Set 1, B) iTRAQ Set 2.

Finally, in iTRAQ set 1, seven proteins were found to be only significantly differentially regulated after THS2.2M exposure but not the reference exposures in the liver of female rats (Table 14A). In iTRAQ set 2, ten proteins were found to be only significantly differentially regulated after THS2.2M exposure in the liver of female rats (Table 14B). In general, for these proteins, the direction of regulation was consistent between THS2.2M and the references, but statistical significance was not reached for the latter.

Table 14: Unique differentially expressed proteins after THS2.2M treatment.

A)

	ID	3R4F-23-M-90d	1xMIS-23-M-90d	2xMIS-23-M-90d	THS2.2M-15-M-90d	THS2.2M-23-M-90d	THS2.2M-50-M-90d	3R4F-23-F-90d	1xMIS-23-F-90d	2xMIS-23-F-90d	THS2.2M-15-F-90d	THS2.2M-23-F-90d	THS2.2M-50-F-90d
Prdx3	**G3V7I0**	-0.02	-0.07	0.02	0.1	0.08	-0.07	-0.21	-0.19	-0.14	-0.04	-0.11	-0.19 *
Asgr1	**P02706**	-0.1	-0.05	-0.12	-0.03	-0.07	-0.03	-0.12	-0.2	-0.21	-0.17	-0.23 *	-0.2 *
Sod2	**P07895**	0.12	-0.13	0.16	-0.01	0.11	-0.09	-0.33	-0.26	-0.38	-0.27	-0.23	-0.43 *
Pdlim1	**P52944**	0	0.1	0.09	0.04	0.06	0.08	0.11	0.19	0.24	0.24	0.16	0.24 *
Gphn	**Q03555**	-0.07	-0.17	-0.19	-0.13	-0.15	-0.19	-0.25	-0.19	-0.25	-0.13	-0.4 *	-0.27 *
Fam193a	**D3ZIG8**	-0.26	-0.33	-0.23	-0.19	-0.19	-0.27	-0.28	-0.33	-0.25	-0.23	-0.26 *	-0.27
Got1	**P13221**	0.18	0.22	0.22	0.18	0.19	0.24	0.09	0.05	0.09	0.18	0.18 *	0.08

B)

	ID	3R4F-23-F-90d	2xMIS-23-F-90d	THS2.2M-50-F-90d	3R4F-23-F-90+42d	2xMIS-23-F-90+42d	THS2.2M-50-F-90+42d
Oat	**P04182**	-0.15	-0.14	-0.09	-0.08	-0.14	-0.24 *
RGD15663	**D3ZXS6**	0.2	0.2	0.22 *	-0.08	-0.03	0.02
Ddah1	**O08557**	0.1	0.08	0.28 *	0.04	0.06	0.08
Gsta2	**P04903**	-0.24	-0.31	-0.3 *	-0.16	-0.21	-0.15
G6pdx	**P05370**	0.13	0.19	0.27 *	0.16	0.16	0.11
Cyp2b3	**P13107**	0.19	0.16	0.3 *	0.02	0.04	0.03
Rpl32	**P62912**	0.14	0.19	0.27 *	0.18	0.07	0.03
Nop56	**Q4KLK7**	0.25	0.26	0.27 *	0.19	0.16	-0.04
NA	**D3ZSF3**	0.08	0.08	0.11	-0.11	0.09	-0.02
Lipa	**Q64194**	0.25	0.15	0.28 *	-0.11	0.02	-0.06

Log2 fold changes are shown. Statistically significant differential expression is indicated with an asterisk (*) (BH-adjusted *p*-value < 0.05). A) iTRAQ Set 1, B) iTRAQ Set 2. Note that for the protein with the UniProtKB identifier D3ZSF3, an official name was not available ("NA"), but it has been associated with the name "Gm12728".

9.7.2 Effects of Exposure Conditions on Functional Groups (Set Enrichment Analyses)

We complemented this analysis at the individual protein level by conducting a protein set enrichment analysis (Figure 31 and Figure 32). For this assessment, we identified protein sets from the KEGG compendium (Kanehisa 2014b) that were significantly affected by the tested exposure conditions. For biological interpretation, it is important to note that not all protein/gene sets in the diverse KEGG collection are necessarily directly relevant for our biological context.

Exposure to DDA3 1xMIS and DDA3 2xMIS at 23 µg/L nicotine induced an overall strong response, which appeared stronger in female rats. THS2.2M exposure in male rats at low and medium nicotine concentrations did not induce changes for the analyzed gene sets. However, metabolic pathways for few specific amino acids were affected by THS2.2M at the highest nicotine concentration (50 µg/L).

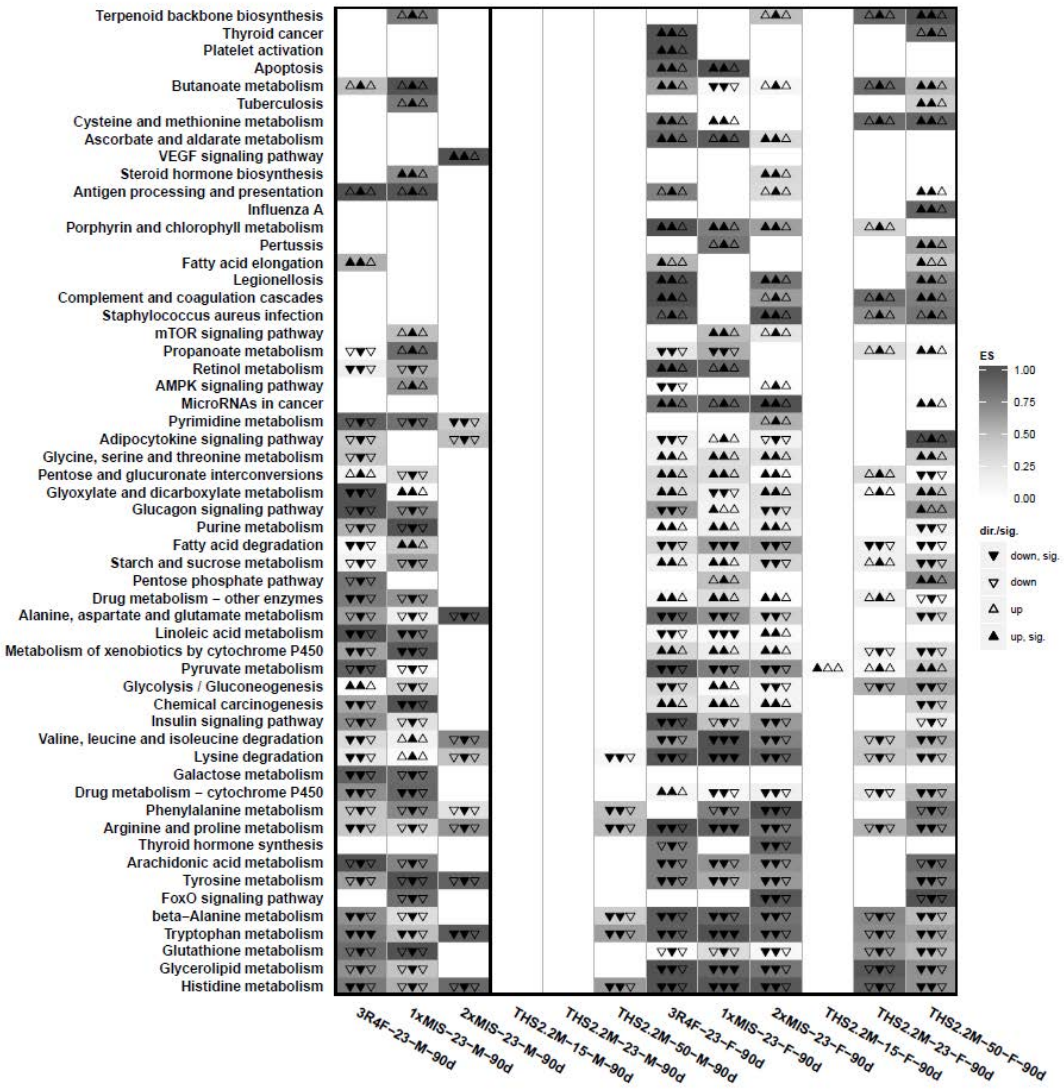


Figure 31: Set enrichment results for 90 days of exposure in liver (Set 1).

Set enrichment was assessed by over-representation analysis (ORA) and gene-set analysis (GSA). The fold change compared with sham exposure was used as the protein-level statistic, the mean as the set statistic, and sample permutation (Q2) to assess statistical significance. Enrichment results are normalized per pathway and the normalized GSA enrichment score (ES) is mapped to the grayscale (see key). Significance is indicated by a filled triangle (BH-adjusted p-value < 0.05), with the direction given by the orientation of the triangle (see key). The first triangle represents the overall adjusted Fisher *p*-value of the GSA and ORA analyses, the second triangle the GSA, and the third triangle the ORA results. Non-significant associations are left blank.

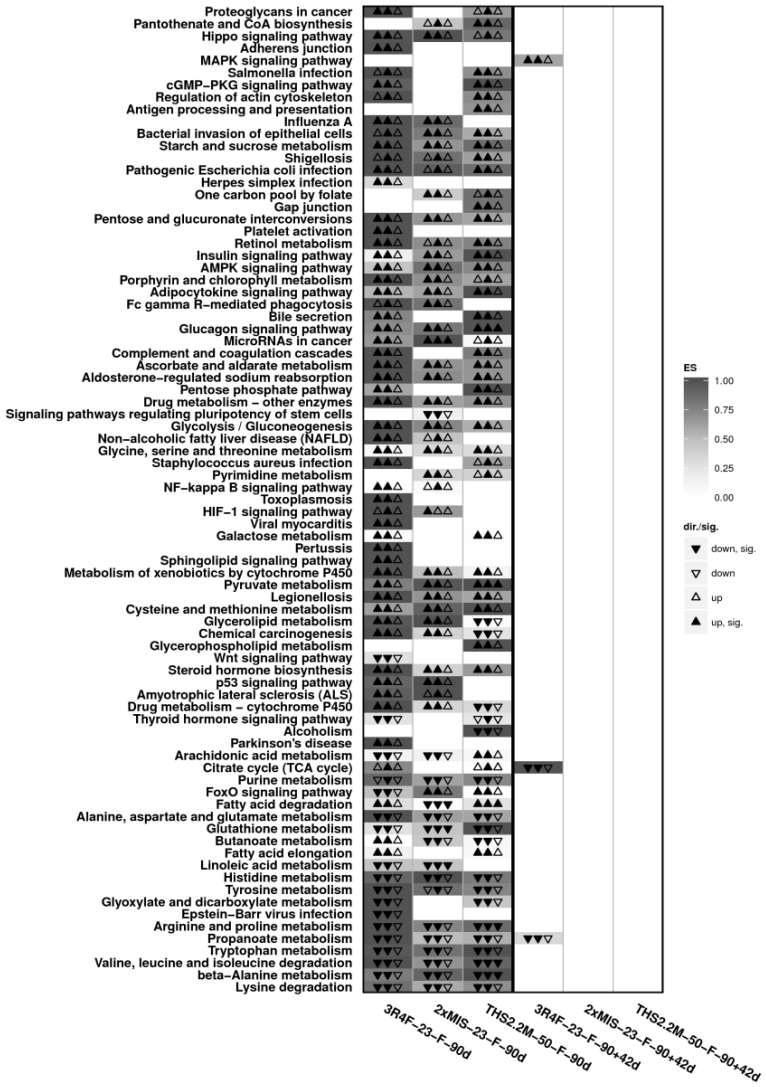


Figure 32: Set enrichment results for 90 days and 90+42-days of exposure in liver (Set 2).

Set enrichment was assessed by over-representation analysis (ORA) and gene-set analysis (GSA). For GSA, the fold change compared with sham exposure was used as the protein-level statistic, the mean as the set statistic, and sample permutation (Q2) to assess statistical significance. Enrichment results are normalized per pathway and the normalized GSA enrichment score (ES) is mapped to the grayscale (see key). Significance is indicated by a filled triangle (BH-adjusted p-value < 0.05), with the direction given by the orientation of the triangle (see key). The first triangle represents the overall adjusted Fisher p-value of the GSA and ORA analyses, the second triangle the GSA, and the third triangle the ORA results. Non-significant associations are left blank.

As for previous observations, the response in female rats was more pronounced than in male rats. However, THS2.2M at the lowest nicotine concentration (15 µg/L) only affected one gene set in female livers. In rats exposed to THS2.2M at 23 µg/L of nicotine, the system response was higher compared with THS2.2M at 15 µg/L, but still lower compared to reference cigarette smoke. Finally, female rats exposed to 50 µg/L nicotine-containing THS2.2M showed a similar system response to the reference cigarette smoke.

After the 42-day recovery period, almost all the gene sets analyzed returned to the sham condition, with the exception of three pathways still significantly regulated in the 3R4F group.

9.8 Lung Lipidome after 90 days of Exposure and after a 42-day Recovery Period in Male and Female Rats

Lipidomics analysis of the lung samples included a broad range of lipid classes and their associated lipids species. The lipid classes monitored on selected lipidomics platforms are presented in Table 8. In total, three platforms were used for lung lipidomics analysis (the Shotgun, Ceramide, and Eicosanoid platforms).

In lung, the 3R4F and DDA3 2xMIS references displayed similar behavior in general (not always significant in both cases, but showing the same fold change and the same directionality). THS2.2M groups (23 and 50 µg/L nicotine) showed less pronounced lipid changes than the reference groups when compared with the sham group.

The difference was especially notable for cholesterol esters, showing a decrease in the reference groups but no alterations in the THS2.2M groups in lungs from male rats, and showing a weak decrease in the reference groups but a strong increase in the lungs from female rats.

Ceramides displayed a steeper increase in the reference groups than in the THS2.2M groups; we observed the same in globotriaosylceramides. Several glucosyl/galactosylceramides in particular displayed a sharp increase in the reference groups, but no change in the THS2.2M groups.

For phospholipids as phosphatidylcholine and phosphatidylethanolamines, as well as for sphingomyelins and diacylglycerols, we did not observe alterations when comparing reference and THS2.2M groups (Figure 33).

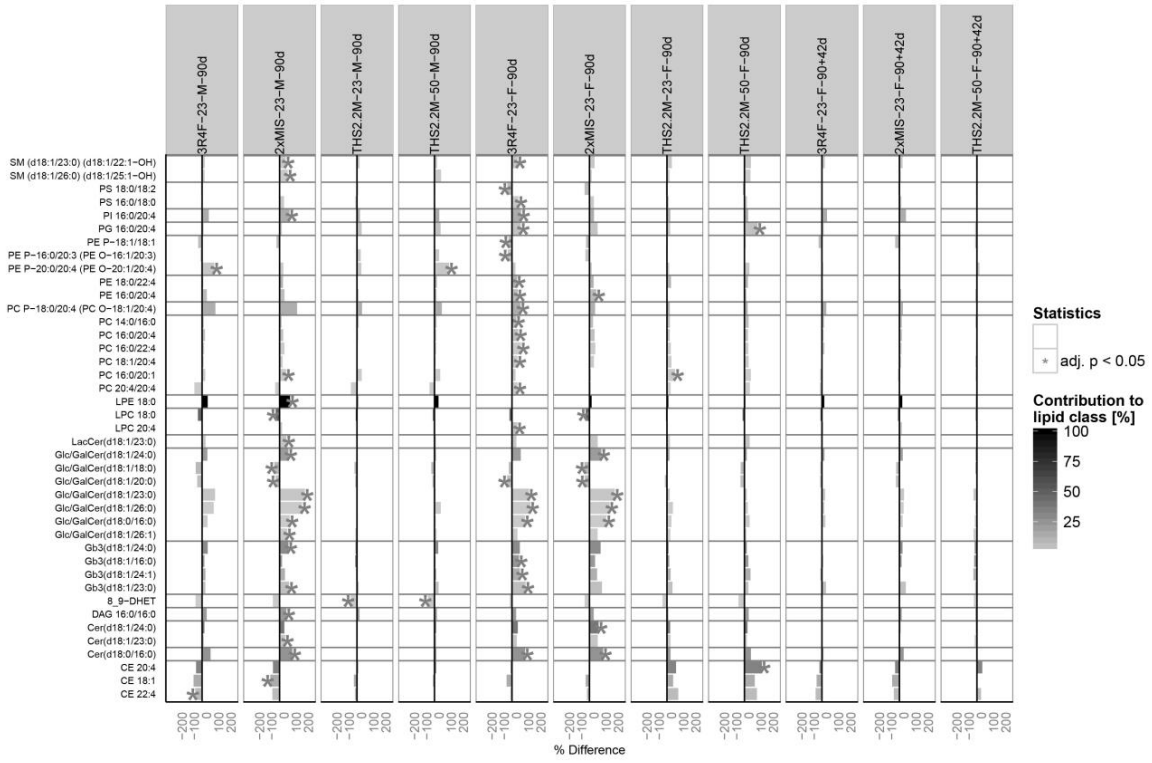


Figure 33: Effects on the lung lipidome.

Lipids with statistically significant relative percentage. Significance of values as (*) adjusted $p < 0.05$. Gb, Globotriaosylceramides; SM, Sphingomyelins; PS, Phosphatidylserines; PI, Phosphatidylinositols; PG, Phosphatidylglycerols; PE, Phosphatidylethanolamines; PC, Phosphatidylcholines; LPC, Lysophosphatidylcholines; LacCer, Lactosylceramides; LPE, lysophosphatidylethanolamine; Glc/GalCer, glucosyl/galactosylceramides; Cer, Ceramides; CE, Cholesteryl esters.

9.9 Liver Lipidome after 90 days of Exposure and after a 42-day Recovery Period in Male and Female Rats

Lipidomics analysis of the liver samples included a broad range of lipid classes and their associated lipids species. The lipid classes monitored on the selected lipidomics platforms are presented in Table 8. In total, two platforms were used for liver lipidomics analysis (the Shotgun and Ceramide platforms).

Figure 34 shows liver lipids in male and female rats. At an FDR adjusted *p*-value < 0.05 (see 7.14), only a few lipid species were significantly affected, and only for male rats exposed to THS2.2M at 23 and 50 µg/L of nicotine. Of note, these changes generally reflected the trends also observed for male rats exposed to DDA3 2xMIS. THS2.2M at 23 µg/L of nicotine resulted in an increase of phosphatidylethanolamines (PE) 16:0/20:4 and 16:0/22:5, and of phosphatidylcholine (PC) 16:0/18:1. PC 16:0/18:1 was also increased upon THS2.2M exposure at 50 µg/L of nicotine. This latter experimental condition also resulted in the decrease of several different lipid species: PE 18:1/20:4, PC 18:1/20:4 and 18:1/18:2, and a number of ceramide species (LacCer d18:1/22:0; d18:0/24:0; d18:0/22:0). The observed changes for all the other lipid species in the different experimental conditions did not reach statistical significance.

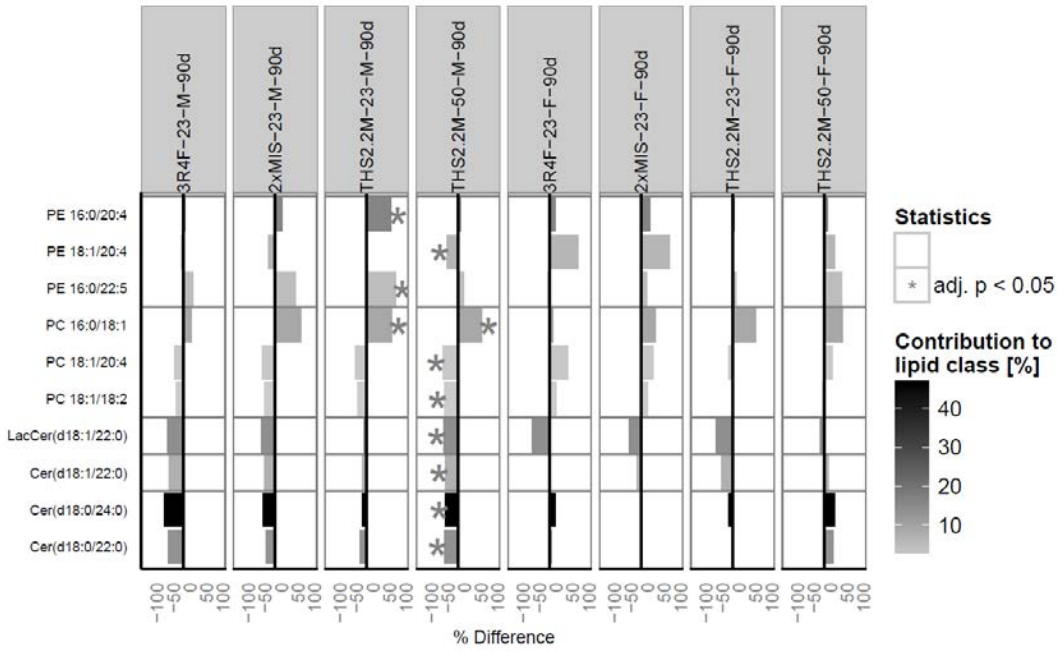


Figure 34: Effects on the liver lipidome.

Lipids with statistically significant relative percentage. Significance of values as (*) adjusted $p < 0.05$. PE, Phosphatidylethanolamines; PC, Phosphatidylcholines; LacCer, Lactosylceramides; Cer, Ceramides.

.

10 Discussion and Conclusion

The standard OECD study designs according to test guidelines 412 or 413 are providing information on the hazards from repeated exposures by the inhalation route. These reveal effects on pulmonary inflammation and other biological endpoints, including histopathological endpoints (e.g. (Kogel 2014, Werley 2008)). Because toxicological markers are often only detectable after substantial damage has already occurred, these can lack sensitivity (Ellinger-Ziegelbauer 2011). The OECD also promotes the regulatory use of alternative testing methods that reduce, refine, and replace traditional animal testing. As a foundation of alternative testing methods, the mechanisms and modes of toxicity need to be understood (OECD 2013).

To obtain additional insights into the molecular mechanisms underlying the potential toxicity of THS2.2M and to increase sensitivity, we have included an additional study arm (the "PLUS" arm) into the classical OECD inhalation study design. In addition to the classical endpoints, we also investigate –using omics approaches—how the exposures affect the transcriptome, proteome, and lipidome. Such combined approaches of omics and conventional toxicology are effective for mechanistic investigations and identification of putative biomarkers (Ellinger-Ziegelbauer 2011, Moffat 2015, Oberemm 2005). Here, we compared the exposure effects of THS2.2M aerosol with the effects of CS from 3R4F and two mentholated combustible cigarettes (DDA3 1xMIS and DDA3 2xMIS) with two different menthol concentrations.

In the **nasal respiratory epithelium** of 3R4F-, DDA3 1xMIS-, DDA3 2xMIS- (all 23 µg/L nicotine) exposed male and female rats after 90 days of exposure, more than 7,000 genes were differentially expressed. In contrast, after exposure to the high dose of THS2.2M (50 µg/L nicotine) for 90 days, only 9 genes were differentially expressed in the RNE of male rats and slightly more than 2,100 genes were differentially expressed in the RNE of female rats. After 42 days of recovery from THS2.2M exposure, most genes approached sham group levels: only 120 genes remained differentially expressed in the RNE of female rats. In addition, the fold change of the differentially expressed genes were generally much lower after THS2.2M exposure than after 3R4F or DDA3 1x or 2x MIS exposure.

To elucidate the affected biology, we analyzed the data with the help of computational causal biological networks. These are a collection of modular, evolving, manually curated, biological expression language (BEL)-scripted causal network models that describe signaling pathways relevant to diseased and non-diseased pulmonary and vascular tissues (Boué 2015). We evaluated network models in five categories describing mechanisms

related to cell fate, tissue repair and angiogenesis, inflammatory processes, cell stress, and cellular proliferation. All these biological processes are well-known from the literature to be perturbed by cigarette smoke exposure. Indeed, we found all these processes impacted in the RNE of male and female rats that had been exposed to CS from either of the three reference cigarettes. While these processes were also impacted in the RNE of female rats after THS2.2M exposure, the amplitude of this impact was lower than for the reference CS.

Consistently, analysis of the RNE proteome showed a strong reduction in the number of differentially expressed proteins for the THS2.2M compared with the DDA3 1xMIS, DDA3 2xMIS, and 3R4F exposure groups.

In the **lung tissue** after exposure to reference smoke, about 2,700 genes were differentially regulated for female rats and about 1,700 genes for male rats. In contrast, after exposure to the highest THS2.2M concentration (50 µg/L nicotine), 45 genes were differentially regulated for the lung tissue of female rats and only one gene for the lung tissue of male rats.

Causal network analysis showed that cell fate, tissue repair and angiogenesis, inflammatory processes, cell stress, and cellular proliferation were impacted by exposure to CS from the reference cigarettes in the lung. Exposure to the highest concentration of THS2.2M (50 µg/L nicotine) for 90 days perturbed cell stress and inflammatory processes in males and all five tested biological processes in females. However, the perturbation amplitudes were much lower after THS2.2M aerosol than after reference CS smoke exposure.

As for the RNE proteome, analysis of the lung proteome showed a strong reduction in the number of differentially expressed proteins for the THS2.2M compared with the DDA3 1xMIS, DDA3 2xMIS, and 3R4F exposure groups.

The **liver** proteome and transcriptome was affected by the different exposure similarly to RNE and lung tissues. Thus, THS2.2M showed a lower impact in the liver expression of genes and proteins compared to the reference cigarettes.

Overall, both the transcriptome and proteome response profiles supported an overall reduction of the THS2.2M aerosol induced molecular effects compared with reference cigarette smoke exposure in all the tissues analyzed (Table 15). In addition, the molecular changes induced by THS2.2M aerosol appeared for the most part to revert to their original levels after the 42-day recovery period. Taking into account the uncertainty inherent in inter-species extrapolation, the data suggest that human adults smoking THS2.2M would not be exposed to additional hazards beyond those presented by smoking conventional cigarettes.

Table 15: Overarching summary of results

	Tissue		RNE			Lung			Liver		
	Group		DEG	DEP	RBIF	DEG	DEP	RBIF	DEG	DEP	RBIF
90d	3R4F	male	3684 ↑ / 3304 ↓	675 ↑ / 676 ↓	70%	950 ↑ / 644 ↓	24 ↑ / 3 ↓	96%	110 ↑ / 46 ↓	6 ↑ / 11 ↓	NA
		female	4196 ↑ / 3476 ↓	677 ↑ / 623 ↓	82%	746 ↑ / 499 ↓	39 ↑ / 7 ↓	96%	89 ↑ / 96 ↓	21 ↑ / 6 ↓	NA
	1xMIS	male	3993 ↑ / 3559 ↓	708 ↑ / 659 ↓	100%	981 ↑ / 544 ↓	14 ↑ / 7 ↓	100%	144 ↑ / 83 ↓	14 ↑ / 14 ↓	NA
		female	4318 ↑ / 3736 ↓	677 ↑ / 657 ↓	100%	1591 ↑ / 1274 ↓	69 ↑ / 27 ↓	100%	154 ↑ / 133 ↓	17 ↑ / 9 ↓	NA
	2xMIS	male	4185 ↑ / 3544 ↓	723 ↑ / 677 ↓	53%	996 ↑ / 792 ↓	44 ↑ / 20 ↓	98%	45 ↑ / 23 ↓	0 ↑ / 1 ↓	NA
		female	4238 ↑ / 3725 ↓	615 ↑ / 593 ↓	99%	1031 ↑ / 941 ↓	66 ↑ / 22 ↓	73%	94 ↑ / 94 ↓	16 ↑ / 4 ↓	NA
	THS2.2M low	male	0 ↑ / 0 ↓	4 ↑ / 2 ↓	0%	0 ↑ / 0 ↓	0 ↑ / 0 ↓	0%	0 ↑ / 0 ↓	0 ↑ / 0 ↓	NA
		female	1 ↑ / 0 ↓	1 ↑ / 0 ↓	0%	0 ↑ / 0 ↓	0 ↑ / 0 ↓	5%	22 ↑ / 21 ↓	3 ↑ / 1 ↓	NA
	THS2.2M med	male	0 ↑ / 1 ↓	5 ↑ / 2 ↓	0%	0 ↑ / 0 ↓	0 ↑ / 0 ↓	1%	1 ↑ / 0 ↓	0 ↑ / 0 ↓	NA
		female	0 ↑ / 0 ↓	0 ↑ / 1 ↓	0%	4 ↑ / 2 ↓	0 ↑ / 0 ↓	7%	33 ↑ / 27 ↓	10 ↑ / 4 ↓	NA
	THS2.2M high	male	6 ↑ / 3 ↓	101 ↑ / 165 ↓	0%	1 ↑ / 0 ↓	0 ↑ / 0 ↓	3%	39 ↑ / 18 ↓	1 ↑ / 0 ↓	NA
		female	1198 ↑ / 920 ↓	212 ↑ / 266 ↓	9%	12 ↑ / 33 ↓	1 ↑ / 0 ↓	8%	103 ↑ / 92 ↓	11 ↑ / 7 ↓	NA
90+42d	3R4F	female	1308 ↑ / 1210 ↓	460 ↑ / 491 ↓	35%	691 ↑ / 443 ↓	16 ↑ / 2 ↓	71%	0 ↑ / 2 ↓	0 ↑ / 0 ↓	NA
	2xMIS	female	2877 ↑ / 2864 ↓	420 ↑ / 492 ↓	44%	592 ↑ / 312 ↓	11 ↑ / 0 ↓	61%	0 ↑ / 0 ↓	0 ↑ / 0 ↓	NA
	THS2.2M high	female	102 ↑ / 18 ↓	0 ↑ / 0 ↓	0%	1 ↑ / 0 ↓	0 ↑ / 0 ↓	1%	0 ↑ / 0 ↓	0 ↑ / 1 ↓	NA

The table summarizes the number of differential expressed genes (DEG), the number of diffential expressed proteins (DEP), and the value of the relative biological impact factor (RBIF). Then number of DEG and DEP were given in the bar charts in the respective tissue chapter. The RBIF was given on the top of the starplots indicating the level of network perturbation. The highest perturbation was set to 100%.

11 Archiving

After completion of the study, the study plan with any amendments, the test and reference item retention samples, all raw data, the report with any amendments and all further study-related records needed to reconstruct the study will be archived. They will be retained for at least 10 years according to the applicable archiving procedures. Paper records will be archived in the archive at Philip Morris Products S.A., Research & Development, PMI Product Testing, Neuchâtel, Switzerland; electronic records will be managed by a PMI Product Testing e-archivist on the central archiving server at Philip Morris S.A., Lausanne, Switzerland.

12 References

12.1 Literature

Ackermann M, Strimmer K. A general modular framework for gene set enrichment analysis. BMC bioinformatics. 2009;10(1):47.

Boué S, Talikka M, Westra JW, Hayes W, Di Fabio A, Park J, et al. Causal biological network database: a comprehensive platform of causal biological network models focused on the pulmonary and vascular systems. Database. 2015;2015:bav030.

Brettschneider J, Collins F, Bolstad BM. Quality Assessment for Short Oligonucleotide Microarray Data. Technometrics. 2008;50(3):241-64.

Cutler P, Bell DJ, Birrell HC, Connelly JC, Connor SC, Holmes E, et al. An integrated proteomic approach to studying glomerular nephrotoxicity. Electrophoresis. 1999;20(18):3647-58. Epub 1999/12/28. PubMed PMID: 10612292.

Deems R, Buczynski MW, Bowers-Gentry R, Harkewicz R, Dennis EA. Detection and quantitation of eicosanoids via high performance liquid chromatography-electrospray

ionization-mass spectrometry. Methods in enzymology. 2007;432:59-82. PubMed PMID: 17954213.

Ekroos K, Chernushevich IV, Simons K, Shevchenko A. Quantitative profiling of phospholipids by multiple precursor ion scanning on a hybrid quadrupole time-of-flight mass spectrometer. Analytical chemistry. 2002;74(5):941-9.

Ekroos K, Ejsing CS, Bahr U, Karas M, Simons K, Shevchenko A. Charting molecular composition of phosphatidylcholines by fatty acid scanning and ion trap MS3 fragmentation. Journal of lipid research. 2003;44(11):2181-92.

Ellinger-Ziegelbauer H, Adler M, Amberg A, Brandenburg A, Callanan JJ, Connor S, et al. The enhanced value of combining conventional and "omics" analyses in early assessment of drug-induced hepatobiliary injury. Toxicology and applied pharmacology. 2011;252(2):97-111. Epub 2010/10/05. PubMed PMID: 20888850.

Food and Drug Administration. FDA's guidance for industry ''modified risk tobacco products applications''request for comments docket No. FDA-2012-D-0071. Available from:http://www.fda.gov/TobaccoProducts/GuidanceComplianceRegulatoryInformation/ucm297750. htm>(accessed 23.05. 2012), 2012.

Gautier L, Cope L, Bolstad BM, Irizarry RA. affy---analysis of Affymetrix GeneChip data at the probe level. Bioinformatics. 2004;20:307-15.

Gaworski CL, Oldham MJ, Wagner KA, Coggins CR, Patskan GJ. An evaluation of the toxicity of 95 ingredients added individually to experimental cigarettes: approach and methods. Inhalation toxicology. 2011a;23 Suppl 1:1-12. PubMed PMID: 21417965.

Gaworski CL, Schramke H, Diekmann J, Meisgen TJ, Tewes FJ, Veltel DJ, et al. Effect of filtration by activated charcoal on the toxicological activity of cigarette mainstream smoke

from experimental cigarettes. Inhalation toxicology. 2009;21(8):688-704. PubMed PMID: 19555222.

Gaworski CL, Wagner KA, Morton MJ, Oldham MJ. Insights from a multi-year program designed to test the impact of ingredients on mainstream cigarette smoke toxicity. Inhalation toxicology. 2011b;23 Suppl 1:172-83. PubMed PMID: 21545299.

Gentleman RC, Carey VJ, Bates DM, Bolstad B, Dettling M, Dudoit S, et al. Bioconductor: open software development for computational biology and bioinformatics. Genome biology. 2004a;5(10):R80.

Gentleman RC, Carey VJ, Bates DM, Bolstad B, Dettling M, Dudoit S, et al. Bioconductor: open software development for computational biology and bioinformatics. Genome Biol. 2004b;5(10):R80. Epub 2004/10/06. PubMed PMID: 15461798; PubMed Central PMCID: PMC545600.

Health Canada. Official Method T-115, Determination of "Tar", Nicotine and Carbon Monoxide in Mainstream Tobacco Smoke. Ottawa: 1999.

Herbrich SM, Cole RN, West Jr KP, Schulze K, Yager JD, Groopman JD, et al. Statistical Inference from Multiple iTRAQ Experiments without Using Common Reference Standards. Journal of proteome research. 2013;12(2):594-604.

Hoeng J, Talikka M, Martin F, Sewer A, Yang X, Iskandar A, et al. Case study: the role of mechanistic network models in systems toxicology. Drug discovery today. 2014;19(2):183-92. Epub 2013/08/13. PubMed PMID: 23933191.

Huber W, Von Heydebreck A, Sültmann H, Poustka A, Vingron M. Variance stabilization applied to microarray data calibration and to the quantification of differential expression. Bioinformatics. 2002;18(suppl 1):S96-S104.

Hultin-Rosenberg L, Forshed J, Branca RM, Lehtio J, Johansson HJ. Defining, comparing, and improving iTRAQ quantification in mass spectrometry proteomics data. Molecular & cellular proteomics : MCP. 2013;12(7):2021-31. Epub 2013/03/09. PubMed PMID: 23471484; PubMed Central PMCID: PMCPMC3708183.

International Organization for Standardization. ISO 3308:2000 - Routine analytical cigarette-smoking machine -- Definitions and standard conditions. 2000.

Irizarry RA, Hobbs B, Collin F, Beazer-Barclay YD, Antonellis KJ, Scherf U, et al. Exploration, normalization, and summaries of high density oligonucleotide array probe level data. Biostatistics. 2003;4(2):249-64. Epub 2003/08/20. PubMed PMID: 12925520.

Jung HR, Sylvänne T, Koistinen KM, Tarasov K, Kauhanen D, Ekroos K. High throughput quantitative molecular lipidomics. Biochimica et Biophysica Acta (BBA)-Molecular and Cell Biology of Lipids. 2011;1811(11):925-34.

Kanehisa M, Goto S, Sato Y, Kawashima M, Furumichi M, Tanabe M. Data, information, knowledge and principle: back to metabolism in KEGG. Nucleic acids research. 2014a;42(Database issue):D199-205. Epub 2013/11/12. PubMed PMID: 24214961; PubMed Central PMCID: PMCPMC3965122.

Kanehisa M, Goto S, Sato Y, Kawashima M, Furumichi M, Tanabe M. Data, information, knowledge and principle: back to metabolism in KEGG. Nucleic acids research. 2014b;42(D1):D199-D205.

Kelstrup CD, Young C, Lavallee R, Nielsen ML, Olsen JV. Optimized fast and sensitive acquisition methods for shotgun proteomics on a quadrupole orbitrap mass spectrometer. Journal of proteome research. 2012;11(6):3487-97.

Kogel U, Schlage WK, Martin F, Xiang Y, Ansari S, Leroy P, et al. A 28-day rat inhalation study with an integrated molecular toxicology endpoint demonstrates reduced exposure effects for a prototypic modified risk tobacco product compared with conventional cigarettes. Food and Chemical Toxicology. 2014;68:204-17.

Martin F, Sewer A, Talikka M, Xiang Y, Hoeng J, Peitsch M. Quantification of biological network perturbations for mechanistic insight and diagnostics using two-layer causal models. BMC Bioinformatics. 2014;15(1):238. PubMed PMID: doi:10.1186/1471-2105-15-238.

Martin F, Thomson T, Sewer A, Drubin D, Mathis C, Weisensee D, et al. Assessment of network perturbation amplitudes by applying high-throughput data to causal biological networks. BMC Systems Biology. 2012;6(1):54. PubMed PMID: doi:10.1186/1752-0509-6-54.

McAnoy AM, Wu CC, Murphy RC. Direct qualitative analysis of triacylglycerols by electrospray mass spectrometry using a linear ion trap. Journal of the American Society for Mass Spectrometry. 2005;16(9):1498-509.

Merrill AH, Sullards MC, Allegood JC, Kelly S, Wang E. Sphingolipidomics: high-throughput, structure-specific, and quantitative analysis of sphingolipids by liquid chromatography tandem mass spectrometry. Methods. 2005;36(2):207-24.

Moennikes O, Vanscheeuwijck PM, Friedrichs B, Anskeit E, Patskan GJ. Reduced toxicological activity of cigarette smoke by the addition of ammonia magnesium phosphate to the paper of an electrically heated cigarette: subchronic inhalation toxicology. Inhalation toxicology. 2008;20(7):647-63. PubMed PMID: 18464053; PubMed Central PMCID: PMC2442902.

Moffat I, Chepelev NL, Labib S, Bourdon-Lacombe J, Kuo B, Buick JK, et al. Comparison of toxicogenomics and traditional approaches to inform mode of action and points of

departure in human health risk assessment of benzo [a] pyrene in drinking water. Critical reviews in toxicology. 2015.

Oberemm A, Onyon L, Gundert-Remy U. How can toxicogenomics inform risk assessment? Toxicology and applied pharmacology. 2005;207(2):592-8.

OECD. Guidance document on developing and assessing adverse outcome pathways. Series on Testing and Assessment No. 184. OECD Environment, Health and Safety Publications. 2013;ENV/JM/MONO(2013)6.

OECD OfEC-oaD. Test No. 413. Subchronic Inhalation Toxicity: 90-day Study. http://iccvam.niehs.nih.gov/SuppDocs/FedDocs/OECD/OECD-TG413.pdf2009.

Patskan G, Reininghaus W. Toxicological evaluation of an electrically heated cigarette. Part 1: Overview of technical concepts and summary of findings. Journal of applied toxicology : JAT. 2003;23(5):323-8. PubMed PMID: 12975771.

R Development Core Team. R: A Language and Environment for Statistical Computing. 2007.

Renne RA, Yoshimura H, Yoshino K, Lulham G, Minamisawa S, Tribukait A, et al. Effects of flavoring and casing ingredients on the toxicity of mainstream cigarette smoke in rats. Inhalation toxicology. 2006;18(9):685-706. PubMed PMID: 16864559.

Sales G, Calura E, Cavalieri D, Romualdi C. graphite - a Bioconductor package to convert pathway topology to gene network. BMC Bioinformatics. 2012;13(1):20. PubMed PMID: doi:10.1186/1471-2105-13-20.

Smyth GK. Linear models and empirical bayes methods for assessing differential expression in microarray experiments. Statistical applications in genetics and molecular biology. 2004;3:Article3. Epub 2006/05/02. PubMed PMID: 16646809.

Ståhlman M, Ejsing CS, Tarasov K, Perman J, Borén J, Ekroos K. High-throughput shotgun lipidomics by quadrupole time-of-flight mass spectrometry. Journal of Chromatography B. 2009;877(26):2664-72.

Stavanja MS, Curtin GM, Ayres PH, Bombick ER, Borgerding MF, Morgan WT, et al. Safety assessment of diammonium phosphate and urea used in the manufacture of cigarettes. Experimental and toxicologic pathology : official journal of the Gesellschaft fur Toxikologische Pathologie. 2008;59(6):339-53. PubMed PMID: 18272354.

Terpstra PM, Teredesai A, Vanscheeuwijck PM, Verbeeck J, Schepers G, Radtke F, et al. Toxicological evaluation of an electrically heated cigarette. Part 4: Subchronic inhalation toxicology. Journal of applied toxicology. 2003;23(5):349-62. Epub 2003/09/17. PubMed PMID: 12975774.

Theophilus EH, Keith Shreve W, Ayres PH, Garner CD, Pence DH, Swauger JE. Comparative 13-week cigarette smoke inhalation study in Sprague-Dawley rats: evaluation of cigarettes with two banded cigarette paper technologies. Food and chemical toxicology: an international journal published for the British Industrial Biological Research Association. 2007;45(6):1076-90. PubMed PMID: 17306918.

Vanscheeuwijck PM, Teredesai A, Terpstra PM, Verbeeck J, Kuhl P, Gerstenberg B, et al. Evaluation of the potential effects of ingredients added to cigarettes. Part 4: subchronic inhalation toxicity. Food and chemical toxicology : an international journal published for the British Industrial Biological Research Association. 2002;40(1):113-31. PubMed PMID: 11731041.

Varemo L, Nielsen J, Nookaew I. Enriching the gene set analysis of genome-wide data by incorporating directionality of gene expression and combining statistical hypotheses and

methods. Nucleic acids research. 2013;41(8):4378-91. Epub 2013/02/28. PubMed PMID: 23444143; PubMed Central PMCID: PMCPMC3632109.

Werley MS, Freelin SA, Wrenn SE, Gerstenberg B, Roemer E, Schramke H, et al. Smoke chemistry, in vitro and in vivo toxicology evaluations of the Electrically Heated Cigarette Smoking System Series K. Regul Toxicol Pharmacol. 2008;52(2):122-39. Epub 2008/07/02. PubMed PMID: 18590791.

12.2 Philip Morris International's List of Standard Operating Procedures (SOP) and Work Instructions (WKI)

The procedures and instructions followed to perform the study are listed below:

Protein extraction from murine liver samples and acetone precipitation: PMI_RD_WKI_001211

Protein extraction from murine nasal epithelium and colon tissues and acetone precipitation: PMI_RD_WKI_001297

Normalization Macro Prior to IVT Protocol: PMI_RD_WKI_001118
Tissue_IVT_Worksheet: PMI_RD_FOR_000763

Affymetrix IVT PLUS Protocol: PMI_RD_WKI_001109

Affymetrix-3'array-Cartridge-Hybridization: PMI_RD_WKI_000816

Tissue_AGCC_Upload: PMI_RD_FOR_000761

Isolation of total RNA including miRNA in lung tissue slices using RNeasy mini kit RLT protocol: PMI_RD_WKI_001115

Proteins Extraction from Lung Tissues and Acetone Precipitaion: PMI_RD_WKI_001043

Isolation of total RNA including microRNAs from Tissue and Organotypic tissue inserts using miRNeasy mini kit protocol: PMI_RD_WKI_001117

Determination of Protein Concentration by using Bradford Assay: PMI_RD_WKI_001103

Quality Control of Protein samples using LabChip instrument: PMI_RD_WKI_001131

12.3 Philip Morris International's Internal Documents.

15025 THS SP: Philip Morris International. Unpublished on file data. Internal Study Plan; "90-Day OECD Inhalation Study On Sprague-Dawley Rats To Characterize Toxicity Of Mainstream Aerosol From THS2.2 Menthol Sticks And Comparison To Mainstream Smoke Toxicity From 3R4F And DDA3 1XMIS And DDA3 2XMIS Mentholated Combustible Cigarettes". Study Number 15025. 2015.

15025_176500 THS SP: Philip Morris International. Unpublished on file data. Internal Study Plan; "90 Days OECD (+) THS2.2 M, Omics Endpoints". Study Number 176500. 2014.

15025 THS SR Part 1: Philip Morris International. Unpublished on file data. Internal Study Report; "Study Report 90-Day OECD Inhalation Study On Sprague-Dawley Rats To Characterize Toxicity Of Mainstream Aerosol From THS2.2 Menthol Sticks And Comparison To Mainstream Smoke Toxicity From 3R4F And DDA3 1XMIS And DDA3 2XMIS Mentholated Combustible Cigarettes. Study Number 15025. Part 1 – Summary Of Results For OECD Group Animals". 2015

15025 THS SR Part 9: Philip Morris International. Unpublished on file data. Internal Study Report; "90-Day OECD Inhalation Study On Sprague-Dawley Rats To Characterize Toxicity Of Mainstream Aerosol From THS2.2 Menthol Sticks And Comparison To Mainstream Smoke Toxicity From 3r4f And Dda3 1XMIS And DDA3 2XMIS Mentholated Combustible Cigarettes". Study Number 15025. 2015

15006 THS SR Part 1: Philip Morris International. Unpublished on file data. Internal Study Report; "Study report 90 day OECD reg inhalation study – Part 1: Summary of results for OECD group animals". Study Number 15006. 2014.

Philip Morris International. Unpublished on file data. Internal Study Report; "Repeated Dose Inhalation Toxicity Assay with the PMI Smoking Articles SMAR-1841, SMAR-1844, and SMAR-1845, and the Reference Cigarette 3R4F, 28-Day Inhalation Study on Rats, Project: SMAR Flavor MIX III, Summary of Results". 12694 SR Part 1. Study Number 12694. 2010

Philip Morris International. Unpublished on file data. Internal Study Report; "Dose range finding study on Sprague Dawley rats to determine maximum tolerable exposure concentration for mainstream smoke/aerosol from mentholated THS 2.2 sticks and DDA3 2xMIS mentholated combustible cigarettes". 15024 SR. Study Number 15024. 2014.

13 Abbreviations

BALF	bronchoalveolar lavage fluid
BIF	biological impact factor
CC	conventional cigarettes
CFA	cell fate
CST	cell stress
CPR	cellular proliferation
DEG	differential expressed gene
FDA	Food and Drug Administration
FDR	false discovery rate
HCI	Health Canada Intense (smoking regimen)
IPN	inflammatory processes network
ISO	International Organization for Standardization
MIS	menthol in smoke
MMAD	mass median aerodynamic diameter
MS	mainstream smoke
MRTP	modified risk tobacco product
NACLAR	National Advisory Committee for Laboratory Animal Research
NPA	network perturbation amplitude
OECD	Organisation for Economic Co-operation and Development
RNE	respiratory nasal epithelium
THS	tobacco heating system
TRA	tissue repair and angiogenesis
TG	test guideline
TPM	total particulate matter

14 Supplementary Tables and Figures

14.1 Tables

N/A

14.2 Figures

N/A